MECHANISM OF ACTOMYOSIN ATPASE REACTION AND MUSCLE CONTRACTION

MITSUKUNI YASUI

DEPARTMENT OF BIOLOGY, FACULTY OF SCIENCE, OSAKA UNIVERSITY

September 1987

CONTENTS

GENERAL INTRODUCTION

Muscles have transducers of the chemical energy of ATP hydrolysis into mechanical work. The mechanism of muscle contraction has been studied by many workers in various fields. Most important of the progress in this field has been the establishment of the so-called "sliding theory" in which muscle contraction is viewed as occurring as a result of the sliding of two kinds of filaments in relation to each other. The sliding theory was proposed from the studies on the structure of muscle fibers (see review articles (1-5)).

A muscle cell has several hundreds of contractile filaments called myofibrils, which are composed of repeating units called sarcomere (Fig. 1). Each sarcomere is separated by Z-lines. The middle, optically dense portion of a sarcomere is called the A-band, while each side of the Z-line is light and is called the I-band. The center of the A-band, which is rather light, is called the H-zone. It is now known that there are two kinds of filaments in a sarcomere: a thick filament located in the A-band and a thin filament from the Z-line to the end of the H-zone (I-band and A-band except the H-zone).

In 1954, A. F. Huxley and Niedergerke (6) and H. E. Huxley and Hanson (7) showed that A-bands maintain a constant width during shortening of muscle fibers, whereas the I-band and the H-zone become narrower. They therefore proposed that the shortening is brought about by the sliding of these filaments relative to each other. Later, Gordon et al. (8) showed that the development of tension in a muscle fiber is related to the

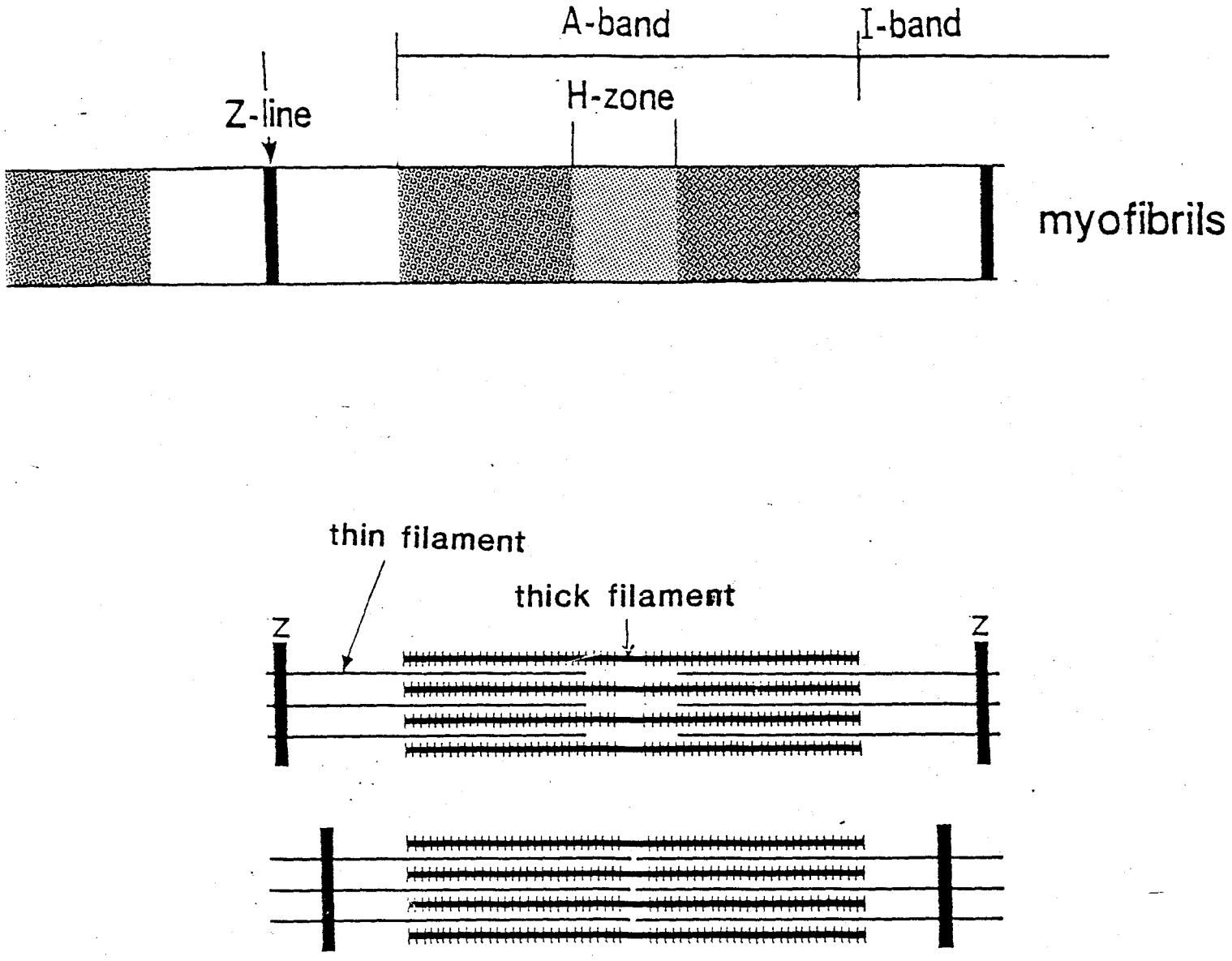

Fig. 1. Structure of sarcomere and contraction of muscle fiber by sliding of thick and thin filaments.

overlap between thick and thin filaments.

The A-band disappears after cold 0.6 M KCl extraction of myosin from the myofibrils (9), and the optical density of the I-band decreases markedly after extraction of actin with KI (10). Quantitative comparison between the decrease in optical density and the quantity of the extracted proteins demonstrated that the main component of thick filaments is myosin while that of thin filaments is actin.

Before the establishment of the 'sliding theory' of muscle contraction, Szent-Gyorgyi (11, 12) showed that the ATPase reaction of myosin is greatly accelerated by actin and that when ATP is added to the complex of actin and myosin (actomyosin) under low ionic strength, actomyosin precipitates very rapidly, and this phenomenon is called superprecipitation. He also showed that ATP induces contraction of actomyosin gel, which is called actomyosin thread. These findings agree well with the sliding theory in which contraction occurs in the overlap between myosin and actin filaments.

Myosin plays a very important role in muscle contraction. The myosin molecule aggregates under low ionic strength and forms a thick filament. ATP is hydrolyzed by myosin and the energy liberated by ATP hydrolysis undergoes transduction into mechanical work through interaction between myosin and actin. Myosin can be purified by cycles of precipitation by dilution and dissolution by addition of 0.5 M KCl. The structure of the myosin molecule has been studied by biochemical analysis and electron microscopy (Fig. 2). Myosin has a molecular weight of about 480 000 (13). It is a long ($\backsim$160 nm) asymmetric molecule

with two globular heads on one side of the molecule (14). The myosin molecule decomposes into polypeptide chains upon treatment with denaturating reagents. The myosin molecule consists of two heavy chains (HC) of molecular weight of 200 000 and four light chains (LC), two of which are identical with a molecular weight of about 18 000 and two of which have molecular weights of 16 000 or 21 000 (13, 15).

To find which part of the myosin molecule is responsible for the function of myosin, various subfragments were obtained by proteolytic digestion of myosin (16). Tryptic digestion of myosin yields a heavy meromyosin (HMM) with a molecular weight of 340 000 and a light meromyosin (LMM) with a molecular weight of 120 000 (16). HMM is soluble even at low ionic strength and retains the ATPase activity and the actin binding ability. On the other hand, LMM has neither ATPase activity nor actin binding ability, but assembles into filaments at low ionic strength. When HMM is further digested with trypsin, chymotrypsin or papain, one mol of HMM yields two mol of subfragment-1 (S-1) and one mol of subfragment-2 (S-2). S-1, with a molecular weight of 120 000 and a length of 10-20 nm, corresponds to the head portion of the myosin molecule. Both ATPase activity and actin binding ability are retained in S-1. S-2, with a molecular weight of 60 000 and a length of 50 nm, and correspond to the neck region of the molecule. When myosin is digested with chymotrypsin or papain, a tail devoid of heads (a rod) and S-1 are obtained. The rod has a molecular weight of 220 000 and a length of 140 nm, and it assembles into filaments at low ionic strength. It was also shown that the bonds between S-1 and S-2 and between

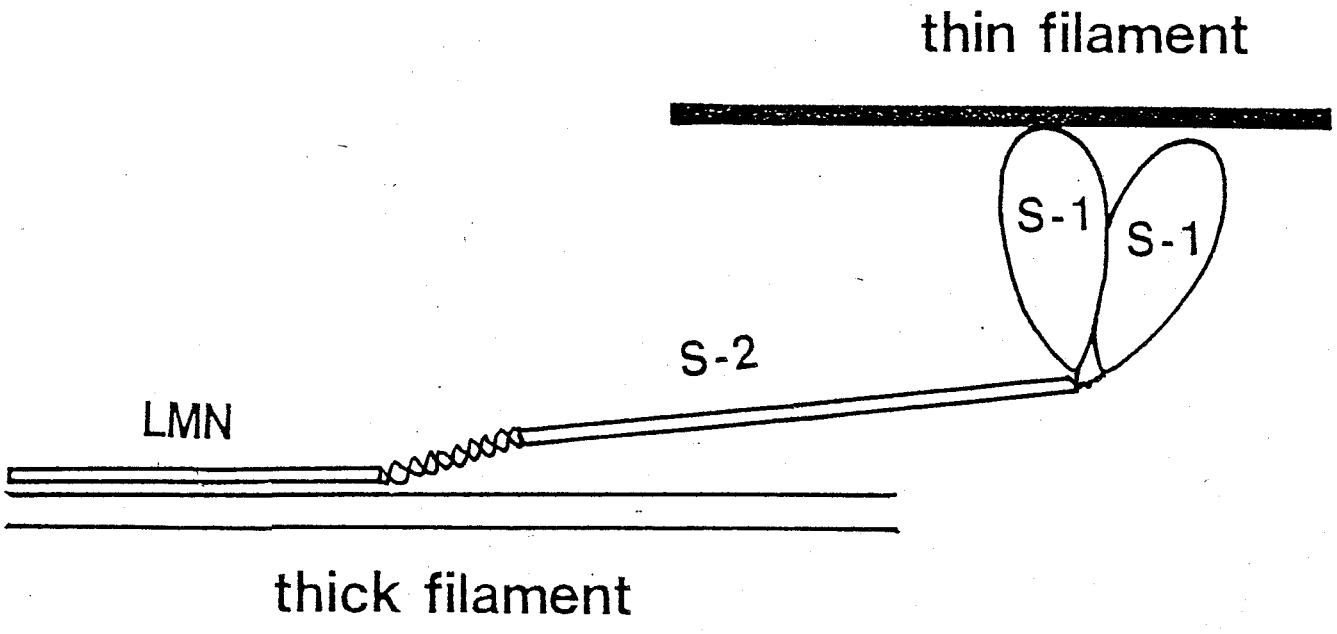

Fig. 2. Schematic diagram for the structure of the myosin molecule. See text for details.

S-2 and LMM are flexible, with S-2 playing the role of a crankshaft (17).

The head portions of myosin have been identified in muscle fiber as projections from the thick filament by electron microscopy and X-diffraction analysis (18, 19). The projections bind with thin filament and form crossbridges, and contraction is believed to be induced as a result of a change in the structure of crossbridges.

To understand the molecular mechanism of contraction, it is important to clarify the mechanism of the reaction of the myosin head (crossbridges) with actin and ATP. However, this is difficult as the muscle is an extremely organized organ, and the diffusion of substrate is rather slow. Furthermore, actomyosin (the complex of myosin and F-actin) shows superprecipitation upon addition of ATP, and the rate of the actomyosin ATPase reaction varies during the time course of superprecipitation; it is not easy to analyze the binding of myosin heads with F-actin during superprecipitation. Therefore, analyse of the ATPase reaction have been carried out mainly with proteolytic fragments of myosin, HMM or S-1, which are soluble even at low ionic strength.

When the myosin ATPase reaction is measured based on the time course of Pi liberation after the reaction is stopped with trichloroacetic acid (TCA), 1 mol of Pi/mol of myosin is rapidly released during the initial phase of the reaction (20). This shows that when myosin reacts with ATP, the complex of myosin with ADP and Pi, called the myosin-phosphate-ADP complex, M_P^{ADP}, is rapidly formed and that the rate of release of ADP and Pi from this intermediate is slow (see Fig. 3).

Head B

$$M + ATP \rightleftharpoons MATP \rightarrow M_a^*ATP \rightarrow M_b^*ATP \rightleftharpoons M\begin{matrix}ADP\\P\end{matrix} \rightarrow M + ADP + Pi$$

(loose complex) (tight complex) (spectral change)

Head A

$$M + ATP \rightleftharpoons MATP \rightarrow M + ADP + Pi$$

Fig. 3. Mechanism of myosin Mg^{2+}ATPase reaction by two heads of the myosin molecule.

Inoue et al. (21-23) showed that the ATPase reaction of the two heads of myosin are different from each other and M_P^{ADP} is formed only by one of the two heads (head B). The other head (head A) forms the myosin-ATP complex, MATP, as a stable intermediate. Also, the ATPase reaction of head B is highly accelerated by F-actin and this head plays an important role in energy transduction in muscle, while head A is considered to play a role in the regulation of contraction and the support of a smooth movement of heads on the thin filament (21).

The mechanism of the actomyosin ATPase reaction was studied based on the mechanisms of the myosin ATPase reaction and the dissociation of actomyosin by ATP and its analogs (13, 21, 24, 25). Since the rate-limiting step of the myosin ATPase reaction is the release of products from M_P^{ADP}, the acceleration of the myosin ATPase reaction by F-actin relies on the acceleration of this step.

The rate of the actomyosin ATPase reaction depends greatly on ionic strength and temperature. At relatively high concentrations (0.05 - 0.2 M) of KCl and low temperatures, most of the myosin heads are dissociated from F-actin during the act-HMM or acto-S-1 ATPase reaction. Lymn and Taylor (26) found that at a high concentration of ATP, the rate of dissociation of acto-S-1 or acto-HMM is much higher than the rate of M_P^{ADP} formation. Therefore, actomyosin dissociates as follows:

$$AM + ATP \rightleftharpoons AMATP \rightleftharpoons A + MATP \rightleftharpoons A + M_P^{ADP}$$

Under these conditions the rate of the overall reaction is

limited by the rate of recombination of HMM_P^{ADP} or $S\text{-}1_P^{ADP}$ with F-actin. However, the rate of the actomyosin-type ATPase reaction and that of recombination of M_P^{ADP} with F-actin do not show a linear relationship with F-actin concentration; they approach a maximal level as the F-actin concentration increases. Chock et al. (27) explained this result by postulating that M_P^{ADP} in a refractory state which cannot react with F-actin is formed by the reaction of actomyosin with ATP, and that conversion of M_P^{ADP} in the refractory state (R) to that in the non-refractory state (N) is slow:

$$M_P^{ADP}(R) \rightleftharpoons M_P^{ADP}(N) \xrightarrow{FA} AM_P^{ADP} \longrightarrow AM + ADP + P.$$

Inoue et al. (28) found that at low KCl concentrations and at room temperature, the myosin head is bound to F-actin even during the ATPase reaction in the steady state. Under these conditions, the rate of the ATPase reaction is proportional to the amount of the complex of F-actin with HMM or S-1, AM_P^{ADP}. In addition, the rate of the ATPase reaction is much faster than the rate of binding of HMM_P^{ADP} or $S\text{-}1_P^{ADP}$ with F-actin (28, 29). Therefore, under these conditions, the main route of the actomyosin ATPase reaction is the hydrolysis of ATP without the accompanying dissociation of actomyosin as given by the following mechanism:

$$AM + ATP \rightleftharpoons AMATP \rightleftharpoons AM_P^{ADP} \longrightarrow AM + ADP + Pi$$

Under these general conditions, the two routes co-exist (28). ATP is hydrolyzed via both routes, one without dissociation of

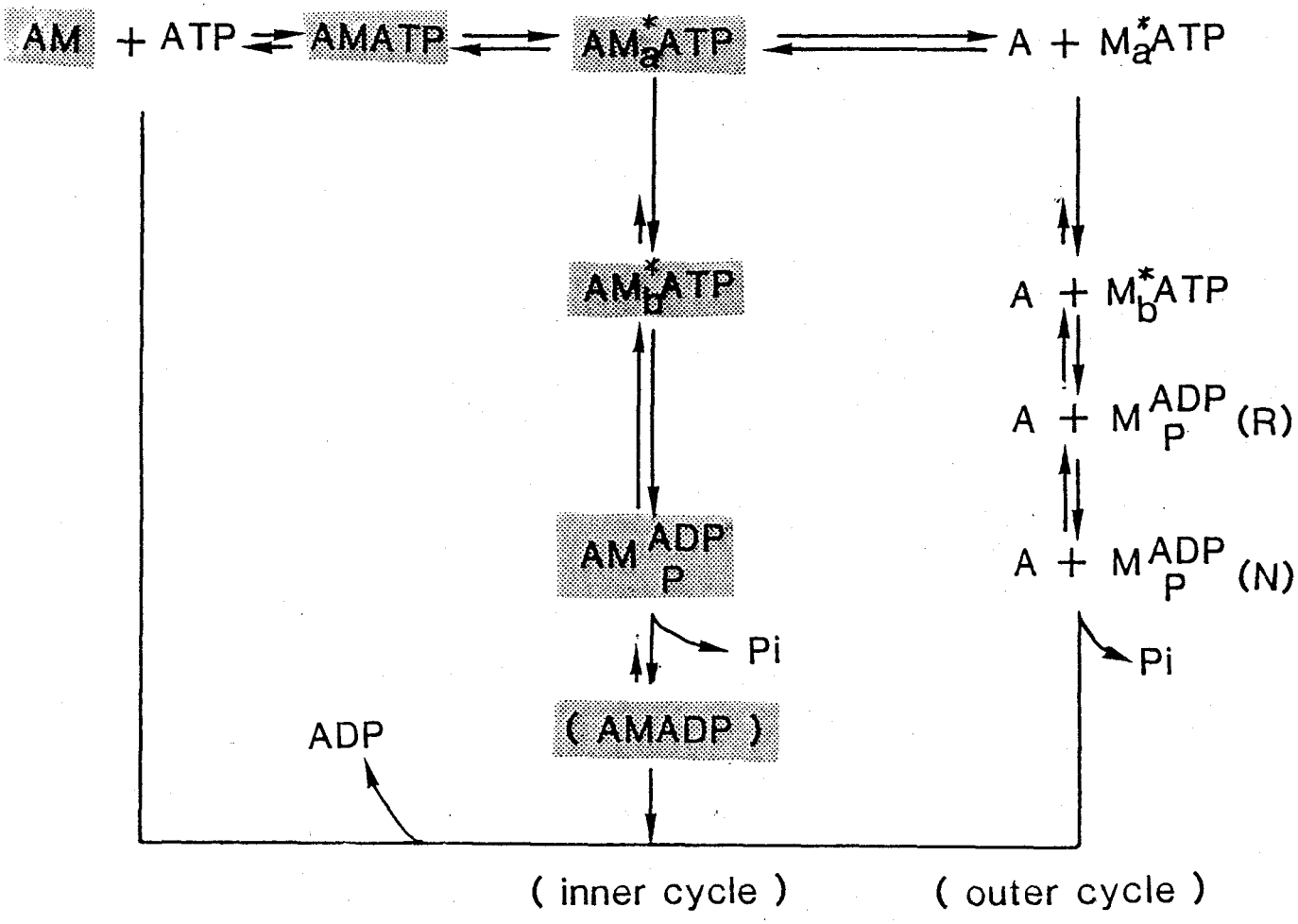

Fig. 4. Mechanism of the actomyosin-ATPase reaction.

actomyosin and the other with dissociation and recombination of actomyosin. Figure 4 shows the mechanism of the actomyosin ATPase reaction proposed by Inoue et al. (28). There is rapid equilibrium between AM_a^*ATP and $A + M_a^*ATP$.

One of the major quetions concerning the crossbridge function is how transduction of chemical energy into mechanical energy occurs. A.F. Huxley (1) postulated the sliding of two filaments by a cycle of three reactions: formation of the crossbridge by binding of the myosin head with thin filament, movement of the myosin head relative to the thin filament, and detachment of the myosin head from the thin filament. A. F. Huxley and Simmons (4, 5, 30) showed evidence for on elastic component in the cross-bridges. Therefore, tension might develop by the lengthening of this elastic component when myosin heads move along the thin filament. Figure 5 shows a mechanism of muscle contraction proposed from a structural study of muscle. In the relaxed state, myosin heads are separated from F-actin. a) Myosin heads move to an adjacent thin filament; this movement occurs by diffusion since there are flexible hinge regions in the myosin molecule. b) In the power stroke, the myosin heads undergo a change in shape or crossbridge angle causing lengthening of the elastic component and thus the development of tension. c) Sliding of thick filament past the thin filament is induced by the elastic component. d) Myosin heads dissociate from the thin filament.

There are diverse of opinions among researchers as to the mechanism of the actomyosin ATPase reaction. The cycle of crossbridges described above is generated by the hydrolysis of

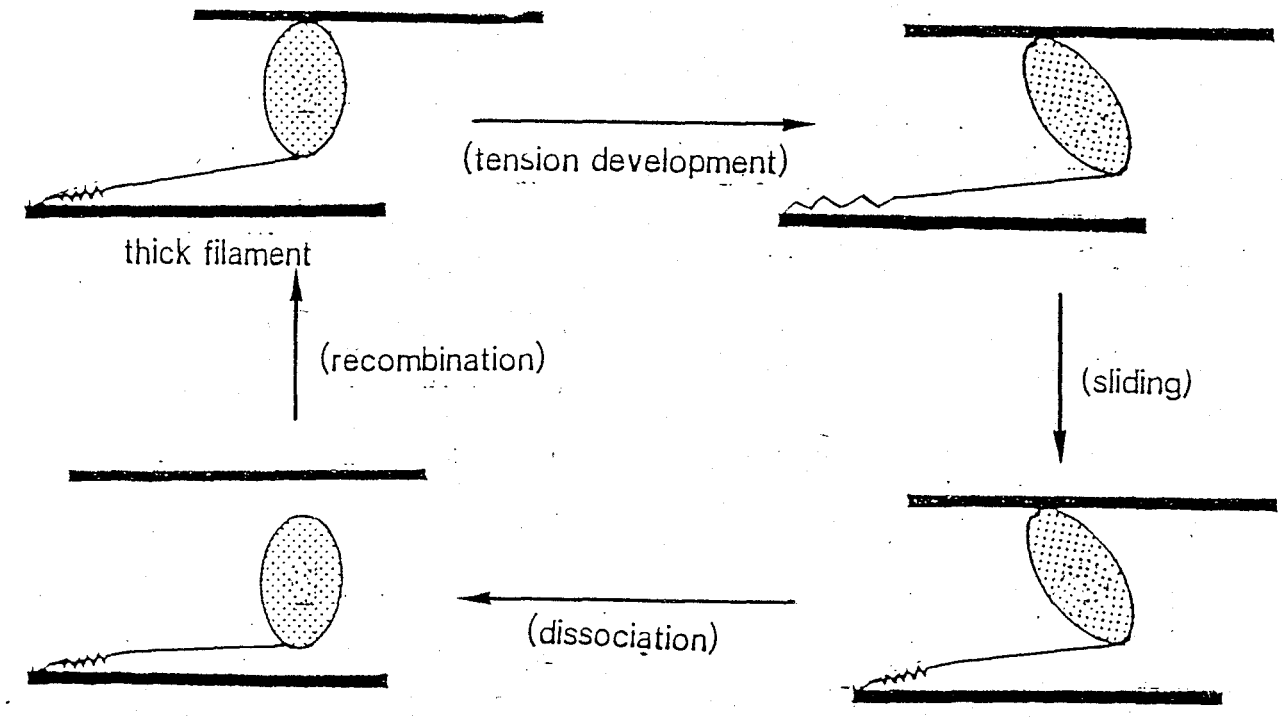

Fig. 5. Mechanism of muscle contraction proposed from structural study of muscles.

ATP, but it remains difficult to determine which step of the ATPase reaction is coupled with this cycle. Tonomura (13) proposed that the two routes of the actomyosin ATPase reaction occur alternately and tension is induced by the formation of AM_P^{ADP} from AMATP. On the other hand, Lymn and Taylor (25, 26) proposed that contraction is coupled with the dissociated cycle of the actomyosin ATPase reaction and tension is developed by the decomposition of AM_P^{ADP} into AM + ADP + Pi.

The present study was focused at determining which route of the actomyosin ATPase is coupled with contraction. The mechanism of the actomyosin ATPase reaction was studied using the ^{18}O exchange reaction, because it was difficult to examine the mechanism when the reaction was in progress in muscle fiber.

When ATP is hydrolyzed in ^{18}O water, ^{18}O is incorporated into Pi as follows:

$$ATP + H_2{}^{18}O \rightleftharpoons ADP + {}^{18}O\text{-}P\text{-}O_3$$

However, if there is a backward reaction from the enzyme-product complex into the enzyme-ATP complex, the number of ^{18}O atoms in Pi increases:

$$M + ATP + H_2{}^{18}O \rightarrow M\text{-}ATP + H_2{}^{18}O \underset{k_{-3}}{\overset{k_3}{\rightleftharpoons}} M\text{-}{}^{18}O\text{-}P\text{-}ADP \xrightarrow{k_4} M + ADP + {}^{18}O\text{-}\overset{{}^{18}O}{\overset{|}{P}}\text{-}{}^{18}O$$

In the present study, ATP enriched with ^{18}O at γ-P position was synthesized from ^{18}O water and ATPase reaction was carried out using ^{18}O ATP as substrate. The Pi produced was trimethylsilylated and then analyzed using a gas chromato-mass spectrometer. The myosin ATPase reaction in the absence of divalent cations (EDTA(K^+)ATPase) was found to include no ^{18}O exchange

reaction between the intermediate Pi and the medium $H_2{}^{18}O$ (32). The distribution of ^{18}O in the γ-P-position of the starting ATP was estimated from the distribution of $3^{18}O/Pi$, $2^{18}O/Pi$, $1^{18}O/Pi$, and $0^{18}O/Pi$ produced by the EDTA(K^+)ATPase reaction.

The amount of exchange can be determined from the value of the exchange ratio, $R(= k_{-3}/k_4)$. When ATP is hydrolyzed into M-P-ADP, the fraction (X) which hydrolyzed into M + ADP + Pi is given by $X = k_4/(k_{-3} + k_4)$, which is equal to $1/(R + 1)$. The remaining fraction, $R/(R + 1)$, is converted into M-ATP. However, in the 1/4 fraction, the incorporated ^{16}O atom is liberated as $H_2{}^{16}O$. The expected distribution of $3^{18}O/Pi$ for a given value of R can be found from:

$$a = \sum_{y=1}^{y=\infty} a_0 \left(\frac{1}{R+1}\right)^y \left(\frac{1}{4}\,\frac{R}{R+1}\right)^{y-1}$$

$$= a_0 \frac{4}{3R+4}$$

in which a_0 indicates how many original oxygens per Pi have been retained. In considering the individual phosphate species, $n^{18}O/Pi$, similar logic leads to the following equation:

$$2^{18}O/Pi: \; b = (a_0 + b_0 - a)\frac{2}{R+2}$$

$$1^{18}O/Pi: \; c = (a_0 + b_0 + c_0 - a - b)\frac{4}{R+4}$$

$$0^{18}O/Pi: \; d = 100 - (a + b + c)$$

Therefore, we can determine the ratio of k_{-3}/k_4 from the distributions of $3^{18}O$, $2^{18}O$, $1^{18}O$ and $0^{18}O/Pi$.

In the case of the myosin Mg^{2+}-ATPase reaction, there is a rapid equilibrium between M^*ATP and M_P^{ADP} and k_3 has a currently accepted value of 10 - 30 sec^{-1}, whereas k_4 has a value of 0.01 - 0.03 sec^{-1}. Most of the O atom in Pi produced by the myosin Mg^{2+}-ATPase reaction is derived from water. On the other hand, in the actomyosin ATPase reaction via the direct decomposition of AM_P^{ADP}, k_4 is extremely high and the amount of exchange is expected to be low. Furthermore, if ATP is hydrolyzed via two different routes the number of ^{18}O in the product Pi may show two R values.

This paper is composed of five sections. Part 1 describes the determination of the affinity of S-1 with F-actin in the absence of nucleotide. This value is essential for estimating the free energy change in the actomyosin ATPase reaction. Part 2 discusses the rate constant for elementary steps of actomyosin ATPase reaction without the accompanying dissociation of actomyosin using transient kinetics and the ^{18}O exchange reaction. The overall reaction of actomyosin ATPase could be determined by the transition from AMATP into M_P^{ADP}. Part 3 concerns the free energy change in the elementary steps of the actomyosin ATPase reaction. Most of the free energy obtained by ATP hydrolysis is liberated by the step from AM_P^{ADP} into AMADP. Part 4 offers evidence using the ^{18}O exchange reaction in which the actomyosin ATPase reaction ATP is hydrolyzed via two routes, one via direct decomposition of AM_P^{ADP} and the other via dissociation and recombination of $A + M_P^{ADP}$. The ratio of the two

routes to ^{18}O exchange was equal to that estimated by the kinetic method. The last part describes the ATPase reaction of myofibrils and muscle fibers studied by oxygen exchange. We found that the fraction of ATP hydrolysis without accompanying the dissociation of actomyosin was high in low ionic strength where the tension development is large. Therefore, ATP hydrolysis via this route may coupled with muscle contraction. Based on these studies, a mechanism of muscle contraction is proposed in which power stroke is coupled with the step of converting AM_P^{ADP} into AMADP.

REFERENCES

1. Huxley, A. F. (1957) Prog. Biophys. Biophys. Chem. 78, 255-318
2. Huxley, H. E. (1960) The Cell (J. Brandet & E. A. Mirsky eds.) vol. 4, 99. 365-481, New York : Academic Press
3. Huxley, H. E. (1969) Science 164, 1356-1366
4. Huxley, A. F. (1974) J. Physiol. 243, 1-43
5. Huxley, A. F. (1973) Cold Spring Harb. Symo. Quant. Biol. 37, 669-680
6. Huxley, A. F. & Niedergerke, R. (1954) Nature 173, 971-973
7. Huxley, A. F. & Hanson, J. (1954) Nature 173, 973-976
8. Gordon, A. M., Huxley, A. F., & Julian, F. S. (1966) J. Physiol. 184, 170-192
9. Hasselbach, W. (1953) Z. Naturforch. 86, 449-454
10. Huxley, H. E. & Hanson, J. (1957) Biochem. Biophys. Acta. 23, 229-249
11. Szent-Gyorgyi, A. (1942) Stud. Inst. Med. Chem. Univ. Szeged. 1, 17
12. Szent-Gyorgyi, A. (1951) Chemistry of Muscle Contraction 2nd ed. Academic Press, New York.
13. Tonomura, Y. (1972) Muscle Protein, Muscle Contraction and Cation Transport Tokyo and Baltimore, Japan Scientific Society Press & University Park Press.
14. Slayter, H. & Lowey, S. (1967) Proc. Natl. Acad. Sci. U.S.A. 58, 1611-1618
15. Squire, J. (1981) The Structural Basis of Muscle Contraction Plenum Press, New York.

16. Lowey, S. (1971) in Subunits in Biological System (S. N. Timasheff & G. C. Fasman eds.) part A, pp. 201-259, New York : Academic Press

17. Morales, M. F., Borejdo, J., Botts, J., Cook, R., Mendelson, R. A., & Takashi, R. (1983) Ann. Rev. Phys. Chem. 33, 340-351

18. Huxley, H. E. (1957) J. Biophys. Biochem. Cytol. 3, 631-648

19. Huxley, H. E. & Brown, W. (1967) J. Mol. Biol. 30, 383-434

20. Kanazawa, T. & Tonomura, Y. (1965) J. Biochem., 57, 604-615

21. Inoue, A. Takenaka, H. Arata, H. & Tonomura, Y. (1979) Adv. Biophys. 13, 1-194

22. Tonomura, Y. & Inoue, A. (1975) Mol. Cell. Biochem. 5,127-143

23. Tonomura, Y. & Inoue, A. (1975) in MTP International Review of Science (E. Racker eds.) vol. 3, pp. 121-161, London : Butter Worths

24. Trentham, D. R., Eccleston, J. F., & Bagshaw, C. R. (1976) Q. Rev. Biophys. 9, 217-281

25. Taylor, E. W. (1979) CRC Crit. Rev. Biochem. 6, 103-164 26.

26. Lymn, R. W. & Taylor, E. W. (1971) Biochemistry 10, 4617-4624

27. Chock, S. P., Chock, P. B., & Eisenberg, E. (1976) Biochemistry 15, 3244-3253

28. Inoue, A., Ikebe, M., & Tonomura, Y. (1980) J. Biochem. 88, 1663-1677

29. Inoue, A. Shigekawa, M., & Tonomura, Y. (1979) J. Biochem. 74, 923-934

30. Huxley, A. F. & Simmons, R. M. (1971) Nature 233, 533-538

31. Koshland, D. E. & Clark, E. (1953) J. Biol. Chem. 205, 917-924

32. Yount, R.C., & Koshland Jr., D.E. (1963) J. Biol. Chem. 238,1708-1713.

Abbreviations

HMM	heavy meromyosin
S-1	subfragment-1 of myosin
A	monomer in F-actin
M	myosin head
AMPPNP	adenyl-5'-yl imidodiphosphate
pyr	N-(1-prenyl) iodoacetoamide
PEP	phosphoenolpyruvate
Ap_5A	diadenosine pentaphosphate
DTT	dithiothreitol
SDS	sodium dodecyl sulfate
Hepes	N-2-(hydroxyethyl)-piperazine-N'-2-ethanesulfate
EDC	1-ethyl-3-[3-(dimethylamino)propyl]-carbodiimido
TCA	trichloroacetic acid
PCA	perchloric acid

PART 1

Kinetic Properties of Binding of S-1 with F-actin in the Absence of Nucleotide

SUMMARY

The rate constant for the binding of myosin subfragment-1 (S-1) with F-actin in the absence of nucleotide, k_1, and that for dissociation of the F-actin-myosin subfragment-1 complex (acto-S-1), k_{-1}, were measured independently. The rate of S-1 binding with F-actin was measured from the time course of the change in the light scattering intensity after mixing S-1 with various concentrations of F-actin, and k_1 was found to be 2.55 x 10^6 $M^{-1} \cdot s^{-1}$ at 20 ℃. The dissociation rate of acto-S-1 was determined using F-actin labeled with pyrenyl iodoacetoamide (Pyr-FA). Pyr-FA, with its fluorescence decreased by binding with S-1, was mixed with acto-S-1 complex and the rate of displacement of F-actin by Pyr-FA was measured from the decrease in the Pyr-FA fluorescence intensity. The k_{-1} value was calculated to be 8.5 x 10^{-3} s^{-1} (or 0.51 min^{-1}). The value of dissociation constant of S-1 from acto-S-1 complex, K_d, was calculated from $K_d = k_{-1}/k_1$ to be 3.3 x 10^{-9} M at 20 ℃. K_d was also measured at various temperatures (0 - 30 ℃), and the thermodynamic parameters, $\Delta G°$, $\Delta H°$, and $\Delta S°$, were estimated from the temperature dependence of K_d to be -11.3 Kcal/mol, +2.5 Kcal/mol, and +47 cal/deg·mol, respectively. Thus, the binding of the myosin head with F-actin was shown to be endothermic and entropy-driven.

INTRODUCTION

Muscle contraction is driven by a cyclic interaction of myosin heads with F-actin coupled with ATP hydrolysis. In the absence of ATP, a muscle becomes rigid and inextensible (rigor state), and myosin heads bind very strongly with F-actin. In order to understand the interaction during muscle contraction, it is important to know about the binding of myosin head (S-1) with F-actin in the absence of ATP as well as about the binding of various S-1-nucleotide complexes with F-actin during ATP hydrolysis. However, accurately measuring the binding constant of S-1 with F-actin is difficult because the binding is so strong that very low concentrations of S-1 and F-actin must be used. Many studies (1-4) have been done on the binding of S-1 with F-actin in the absence of ATP, and the dissociation constant of acto-S-1 complex has been reported to be about 10^{-7} M. However, most of these studies used fluorescent or radioisotope-labeled S-1 which have different binding properties from intact S-1.

In this study, the rate constant of the binding of S-1 with F-actin, k_1, and that of the dissociation of S-1 from acto-S-1, k_{-1}, were measured independently and the dissociation constant for the binding of S-1 with F-actin, K_d, was calculated as $K_d = k_{-1}/k_1$. The changes in entropy and enthalpy accompanying the binding of S-1 with F-actin were estimated from the temperature dependence of the dissociation constant.

EXPERIMENTAL PROCEDURE

Materials —— Myosin was prepared from rabbit white skeletal muscle by the method of Perry (5). S-1 was prepared by chymotryptic digestion of myosin, as described by Weeds and Taylor (6). G-actin was prepared from an acetone powder of rabbit white skeletal muscle by the method of Spudich and Watt (7). The concentration of free ATP in G-actin solution was reduced to 2 μM by dialysis against 2 mM Tris-HCl at pH 7.8. Therefore, the molar concentration of nucleotide in the reaction mixture was less than 1/60 that of S-1. G-actin was polymerized by adding KCl to 0.1 M. Protein concentrations were determined by the biuret reaction calibrated by nitrogen determination. The molecular weights adopted for S-1 and the actin monomer were 1.2×10^5 and 4.2×10^4, respectively (8). N-(1-Pyrenyl)iodoacetamide and N-(iodoacetyl)-N'-(5-sulfo-1-naphtyl)ethylenediamine (IAEDANS) were purchased from Molecular Probes, Inc., TX. All other reagents were of analytical grade.

Fluorescent labeling of F-actin —— F-Actin (50 μM actin monomer) was incubated with 1.2-fold molar excess of N-(1-pyrenyl)iodoacetamide overnight in 0.1 M KCl, 2 mM $MgCl_2$, 2 mM $CaCl_2$, 0.2 mM ATP, and 20 mM Tris-HCl at pH 7.8 and 20 °C. The reaction was quenched by adding a 10-fold molar excess (600 μM) of β-mercaptoethanol over the dye and the resulting mixture was dialyzed against the solution of 0.2 mM ATP at pH 8.3 and 0 °C to remove the unreacted dye and to depolymerize F-actin into G-actin. The resulting solution was centrifuged at 1.0×10^5 g for 3 h to remove F-actin and denaturated actin, and then G-actin

in the clear supernatant was polymerized by adding KCl (final 0.1 M). After the non-polymerized G-actin had been removed by centrifugation at 1.0×10^5 g for 3 h, the F-actin pellet was gently homogenized, and used as "pyrene labeled F-actin (Pyr-FA)". The degree of labeling was determined using the molar extinction coefficient of 2.2×10^4 $M^{-1} \cdot cm^{-1}$ at 344 nm for the pyrenyl group (9). The molar ratio of dye to actin monomer was about 0.9.

S-1 was labeled with IAEDANS by essentially the same method as Takashi et al. (10). S-1 (50 μM) was mixed with 500 μM IAEDANS in 0.15 M KCl, 1 mM EDTA, and 50 mM Tris-HCl at pH 7.8 and 0 ℃ in darkness. After 2 h the reaction was quenched with 2.5 mM β-mercaptoethanol. S-1 was precipitated by adding 60% saturated ammonium sulfate, and after centrifugation at 10^5 g for 20 min, the pellet was dialyzed against 5 mM Tris-HCl at pH 7.8 and 0 ℃. More than 0.95 mol of label was incorporated per mol of S-1. The fluorescence intensity of the AEDANS group was measured at 360 nm excitation and 475 nm emission using a Hitachi-Perkin Elmer MPF-4 fluorescence spectrometer.

Optical measurements —— The rate of binding of S-1 with Pyr-FA and that of dissociation of S-1 from the Pyr-FA-S-1 complex were measured from the change in fluorescence intensity excited at 366 nm and emitted at 406 nm. The time course of the change was measured using a stopped-flow apparatus combined with a Hitachi-Perkin Elmer MPF-2A fluorescence spectrometer (11) and was recorded using a San-ei FR-301 visigraph recorder. The rate of binding of F-actin with S-1 was measured from the light scattering intensity at 360 nm using a stopped-flow apparatus as

described above. The rate of dissociation of acto-S-1 was measured by adding Pyr-FA to the acto-S-1 complex. All experiments were performed in 0.1 M KCl, 2 mM $MgCl_2$, and 20 mM Tris-HCl at pH 7.8 and 20 °C.

The value of the dissociation constant of S-1 from acto-S-1 complex, K_d, was calculated from $K_d = k_{-1}/k_1$. The standard free energy change (ΔG°) for the binding of S-1 with F-actin in 0.1 M KCl at pH 7.8 and 20 °C was estimated to be $\Delta G^\circ = RT\ln K_d$. Since $\Delta G^\circ = \Delta H^\circ - T\Delta S^\circ$, the values of ΔH° and ΔS° were calculated from a plot of $RT\ln K_d$ *vs.* T, by assuming that both ΔH° and ΔS° were constant and independent of temperature.

RESULTS

Binding of Pyr-FA to S-1 —— The fluorescence intensity of Pyr-FA excited at 366 nm and emitted at 406 nm was markedly reduced to about 30% by the binding of S-1 (9). Therefore, the binding of S-1 to Pyr-FA was monitored by both the change in fluorescence intensity of the pyrenyl group and that in the light scattering intensity (*cf.* refs. 1, 12, 13). Figure 1 shows the dependence on S-1 concentration of the changes in fluorescence intensity at 406 nm with 366 nm excitation and that in light scattering intensity at 360 nm when S-1 at various concentrations was added to 4 μM Pyr-FA in 0.1 M KCl, 2 mM $MgCl_2$, and 20 mM Tris-HCl at pH 7.8 and 20 °C. The light scattering intensity increased linearly with an increase in the S-1/Pyr-FA molar ratio

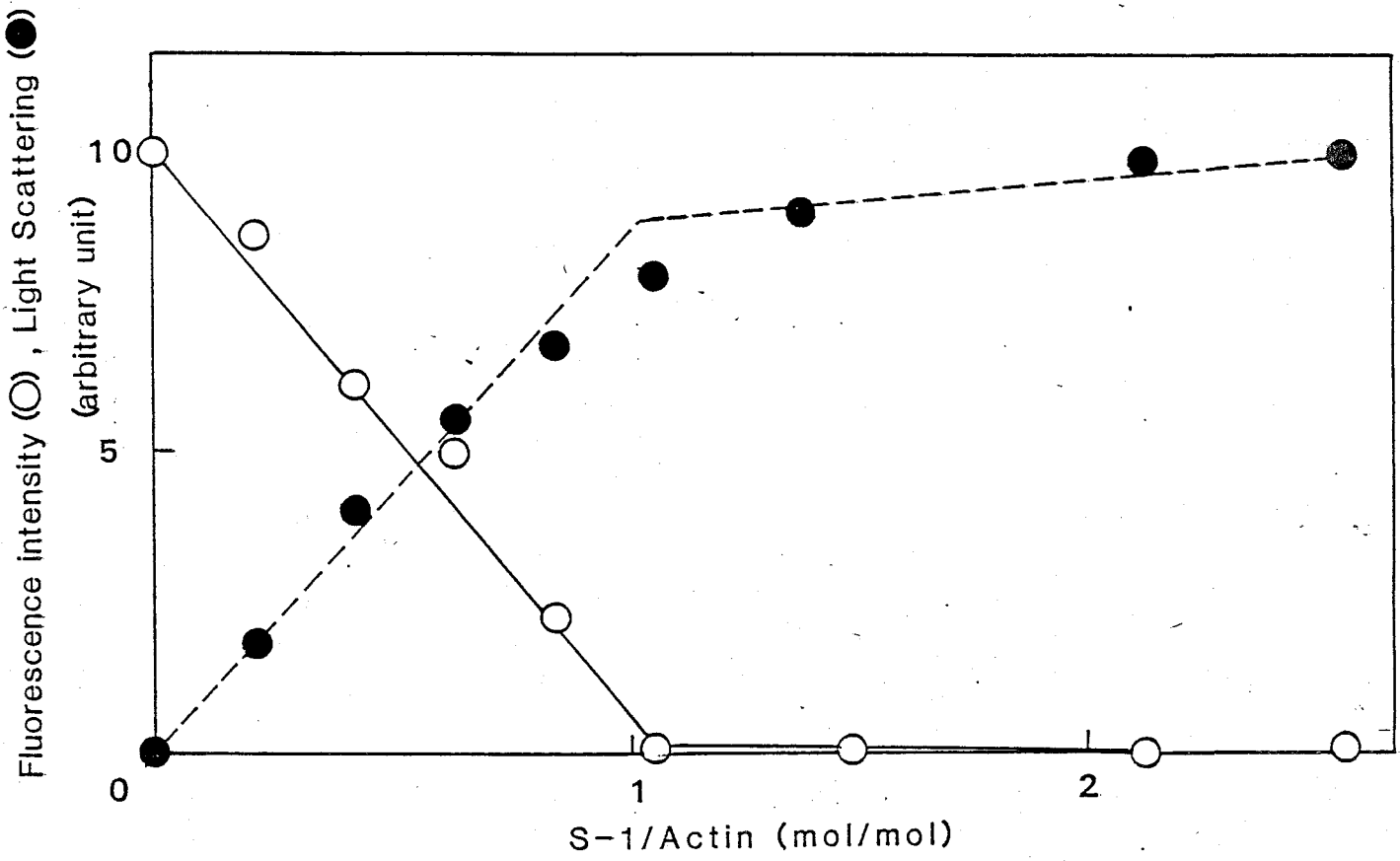

Fig. 1. Changes in the fluorescence intensity and light scattering intensity as a function of the molar ratio of S-1 added to Pyr-FA. Pyr-FA (4 μM) was mixed with various concentrations of S-1 and the fluorescence intensity at 406 nm emission with 366 nm excitation and the light scattering intensity at 406 nm were measured. 0.1 μM KCl, 2 mM $MgCl_2$, and 20 mM Tris-HCl at pH 7.8 and 20 °C. ○, fluorescence intensity; ●, light scattering intensity.

and was saturated at the molar ratio of about 1. The fluorescence intensity decreased linearly with an increase in the S-1/Pyr-FA molar ratio and was also saturated at the molar ratio of about 1. Since the binding stoichiometry of S-1 to monomeric actin in F-actin is known to be 1:1 (8), the fluorescence of Pyr-FA is also an excellent measure of the binding of S-1 with F-actin.

Binding Rate Constant of S-1 with Pyr-FA —— To accurately obtain the dissociation constant of S-1 from Pyr-FA-S-1 complex, the rate constant for the binding of S-1 with Pyr-FA and that for the dissociation of Pyr-FA-S-1 complex were measured independently. The binding rate constant, k_1', of S-1 with Pyr-FA was determined from the time course of the decrease in the fluorescence intensity after adding 0.3-0.9 μM of S-1 to Pyr-FA (0.1 μM actin monomer). The time course followed approximately first order kinetics and the apparent binding rate constant (v') was obtained as a slope of the initial phase of a semilogarithmic plot of decrease in the fluorescence intensity. If the binding of S-1 with F-actin (FA) is represented by FA + S-1 $\rightleftharpoons$ FA-S-1, the apparent rate constant (v') is given by $v' = k_{-1}' + k_1'(S\text{-}1)$, where (S-1) is the concentration of added S-1, and k_1' and k_{-1}' are the rate constants of the forward and the backward reaction, respectively. The value of k_1' is obtained from the slope of v' *vs.* (S-1) plot. As shown in Fig. 2, the apparent binding rate constant increased linearly with an increase in S-1 concentration, and the binding rate constants, k_1', were estimated to be 0.45, 0.78, 1.46, and 2.30×10^9 $M^{-1} \cdot s^{-1}$, respectively, at 0, 10, 20, and 30 °C.

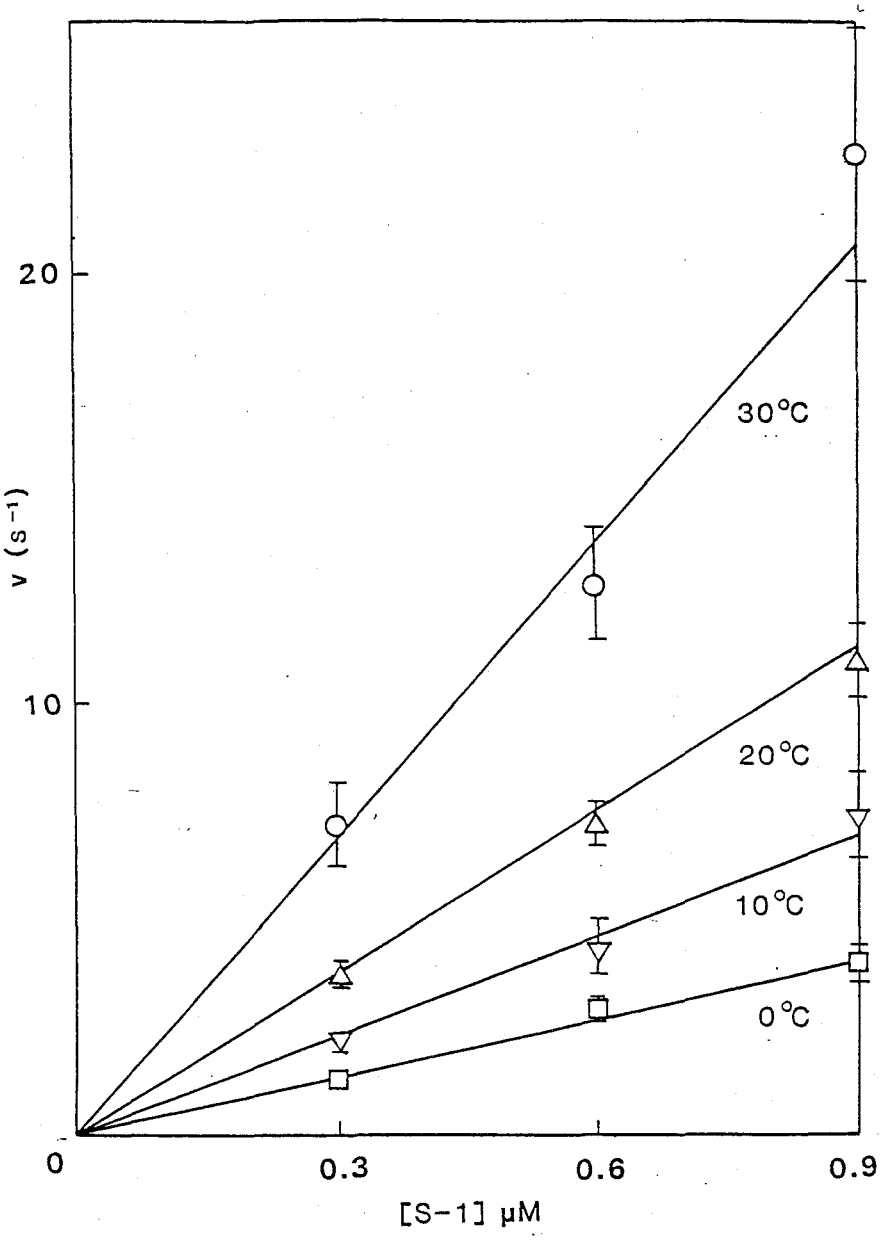

Fig. 2. Dependence on F-actin concentration of the apparent rate constant for the binding of S-1 with Pyr-FA. The apparent rate constant (v') for the binding of S-1 with Pyr-FA was determined from a semilogarithmic plot of the decrease in the fluorescence intensity excited at 366 nm and emitted at 406 nm after the mixing with 0.1 μM Pyr-FA and various concentrations of S-1, 0.1 M KCl, 2 mM $MgCl_2$, and 20 mM Tris-HCl at pH 7.8. Other conditions were the same as for Fig. 1. Bars indicate the standard deviations.

Dissociation Rate Constant of S-1 from Pyr-FA —— The fluorescence intensity of the Pyr group after addition of an excess of unlabeled F-actin (46 μM) to the Pyr-FA-S-1 complex (0.2 μM Pyr-FA and 0.4 μM S-1) was measured. The dissociation rate constant, k_{-1}', of Pyr-FA from S-1 was determined from the rate of increase in the fluorescence intensity of Pyr-FA due to its displacement by unlabeled F-actin. As shown in Fig. 3, the increase in fluorescence intensity followed approximately first order kinetics, and values of k_{-1}' were estimated from the slope of semilogarithmic plots of the increase in fluorescence intensity to be 0.063, 0.093, 0.151, and 0.221 s^{-1}, respectively, at 0, 10, 20, and 30 °C.

Dissociation Constant for Binding of Pyr-FA with S-1 —— The dissociation constant of S-1 from the Pyr-FA-S-1 complex, K_d', was calculated from the binding rate constant, k_1', and the dissociation rate constant, k_{-1}', as $K_d = k_{-1}'/k_1'$ (Table I). The value of K_d' was 1.40×10^{-8} M at 0 °C. It decreased to 1.19, 1.03 and 0.96×10^{-8} M, respectively, on raising temperature from 0 to 10, 20, and 30 °C. The ratio of the dissociation constant of S-1 from acto-S-1 complex, K_d, to that of S-1 from Pyr-FA-S-1 complex, K_d', was obtained by mixing a solution of 2 μM Pyr-FA and 2 μM unlabeled F-actin with 1.8 μM S-1 and measuring the fluorescence and light scattering intensities. Since K_d = (free FA) x (free S-1)/(acto-S-1) and K_d' = (free Pyr-FA) x (free S-1)/(Pyr-FA-S-1), K_d/K_d' = (free FA) x (Pyr-FA-S-1) / (acto-S-1) x (free Pyr-FA) = $(0.1-\Delta F/\Delta F_{max}) \times \Delta F/\Delta F_{max}$ / $(0.9-\Delta F/\Delta F_{max}) \times (1-\Delta F/\Delta F_{max})$, where ΔF and ΔF_{max} are the decreases in fluorescence intensity at 1.8 μM S-1 and at an

Table I. Binding of S-1 with pyrene-labeled F-actin. The rate constant of binding of S-1 with Pyr-FA, k_1', was obtained from Fig. 1. The rate constant of dissociation of S-1 from Pyr-FA-S-1 complex, k_{-1}', was obtained from Fig. 2. The dissociation constant of S-1 from Pyr-FA-S-1 complex, K_d', was calculated as k_{-1}'/k_1'. The conditions were as described for Fig. 1.

Temp. (°C)	k_1' ($\times 10^7$ $M^{-1}s^{-1}$)	k_{-1}' (s^{-1})	$K_{d(Pyr-FA)}'$ ($\times 10^{-8}$ M)	$K_{d(FA)}/K_{d(Pyr-FA)}'$ [a]	$K_{d(FA)}$ [b] ($\times 10^8$ M)
0	0.45	0.063	1.40	0.38	5.29
10	0.78	0.093	1.19	0.36	4.29
20	1.46	0.151	1.03	0.30	3.10
30	2.30	0.221	0.96	0.25	2.40

[a] The ratio of dissociation of S-1 from acto-S-1 to that of S-1from Pyr-FA-S-1 complex was estimated as described in RESULTS.

[b] The dissociation constant S-1 from acto-S-1 was calculated as the product of $K_{d(Pyr-FA)}'$ and $K_{d(FA)}/K_{d(Pyr-FA)}'$.

infinite concentration of S-1. As shown in the fifth column of Table I, K_d/K_d' was estimated to be about 0.3 at 0-30 °C. The dissociation constant of S-1 from acto-S-1 complex, K_d, was estimated as the product of K_d' and K_d/K_d' and listed in the last column of Table II. The values of K_d thus obtained decreased from 5.3×10^{-9} M to 2.4×10^{-9} M on raising the temperature from 0 to 30 °C.

Effect of SH_1 Modification on the Dissociation Constant of Acto-S-1 —— Many studies have been done using myosin of which the SH_1 thiol residue was modified. We examined the effect of modification of the SH_1 thiol residue with IAEDANS on the dissociation constant of S-1 from acto-S-1. S-1 (10 μM) and 0.91, 2.07 or 4.08 uM S-1 labelled with IAEDANS was mixed with 10 uM F-actin in 0.1 M KCl, 2 mM $MgCl_2$, and 20 mM Tris-HCl at pH 7.8 and 20 °C, and the mixture was centrifuged at 1.6×10^5 g for 60 min to precipitate F-actin. The amount of free S-1s, (free AEDANS-S-1) + (free S-1), and that of free AEDANS-S-1 were estimated from the concentration of protein and the fluorescence intensity, respectively, of the supernatant. The amount of free S-1 was estimated as the difference between them. The amounts of bound AEDANS-S-1 and bound S-1 were calculated by subtracting (free AEDANS-S-1) and (free S-1), respectively, from (added AEDANS-S-1) and (added S-1) (data not shown). The ratio of the dissociation constants, $K_{d(AEDANS\text{-}S\text{-}1)}/K_{d(S\text{-}1)}$ calculated as (free AEDANS-S-1)/(free S-1) / (bound AEDANS-S-1)/(bound S-1) , was found to be 2.1 for all AEDANS-S-1 concentrations.

The Binding Rate of S-1 to Intact F-actin —— The dissociation constant of S-1 from acto-S-1 complex was estimated

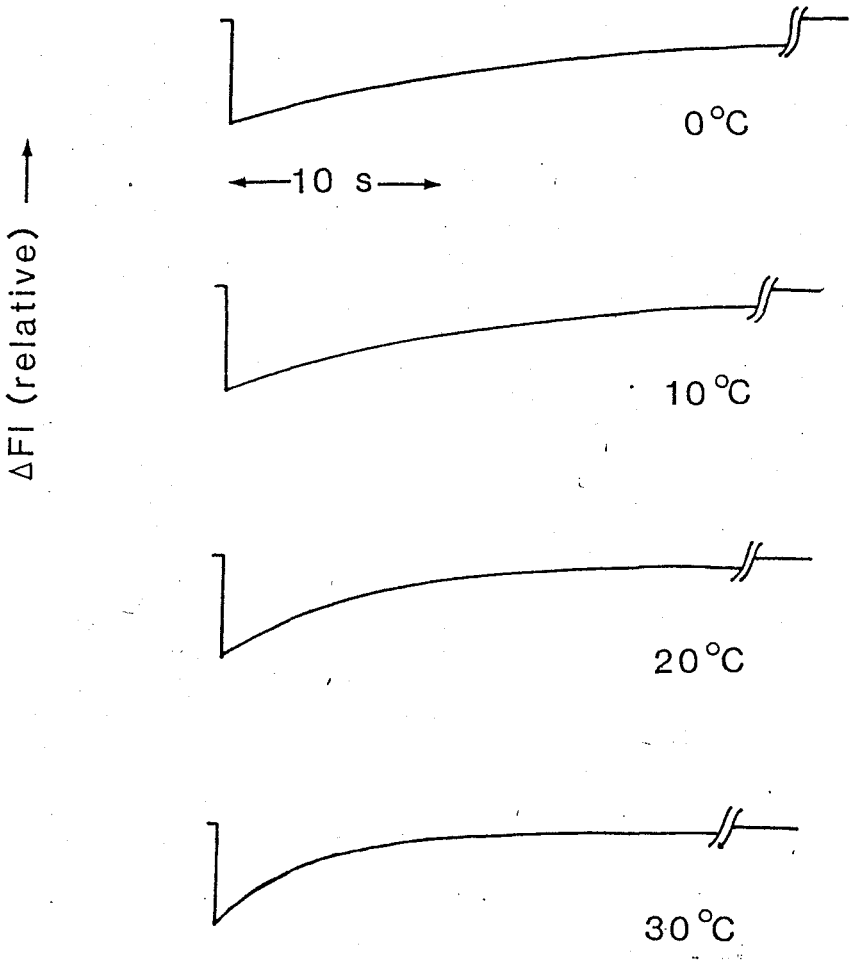

Fig. 3. Time course of increase in the fluorescence intensity of Pyr-FA after mixing F-actin with Pyr-FA-S-1 complex. Pyr-FA-S-1 complex was formed by adding 0.4 μM S-1 with 0.2 μM Pyr-FA was mixed with an excess (46 μM) of F-actin and the fluorescence intensity excited at 366 nm and emitted at 406 nm after the mixing of F-actin was followed using a stopped flow apparatus. Conditions were the same as for Fig. 1.

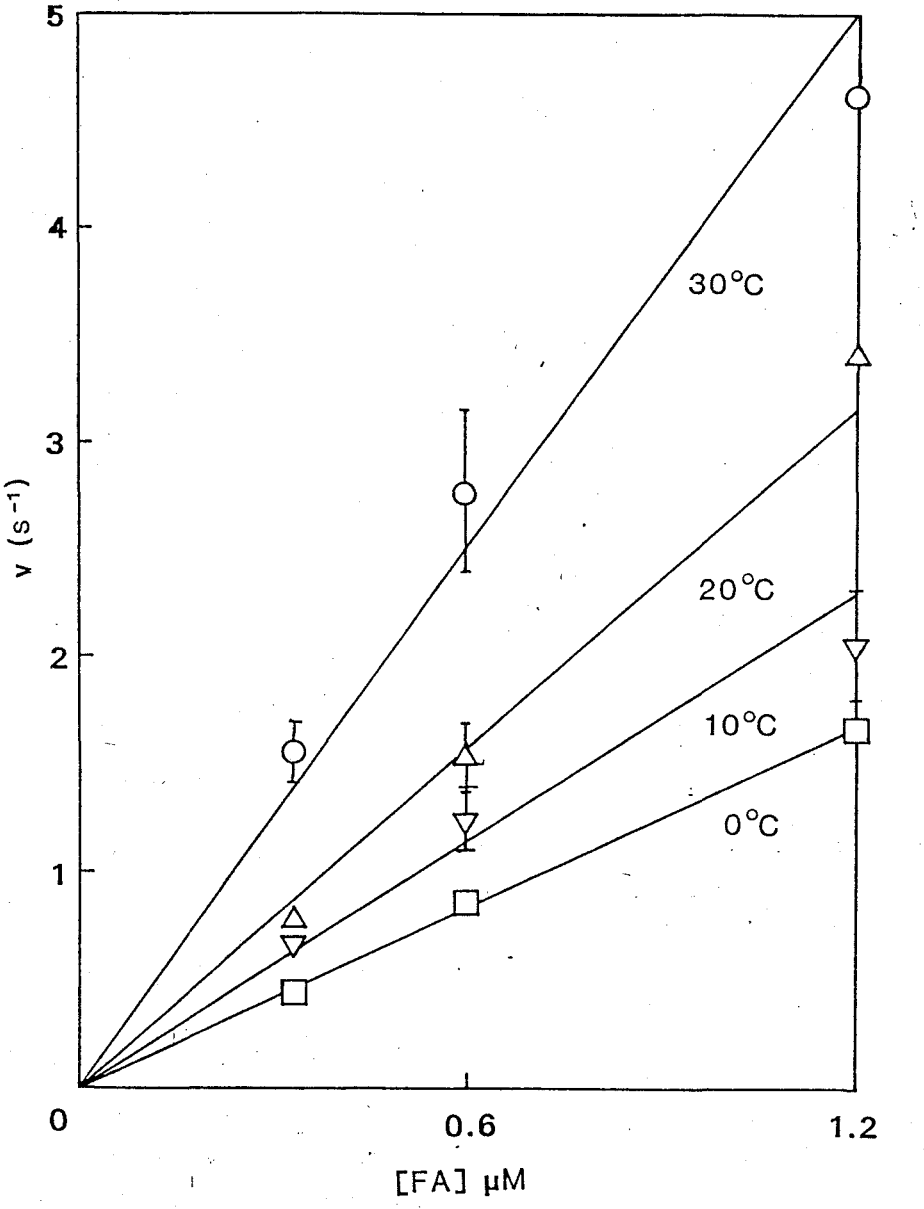

Fig. 4. F-actin concentration dependence of the apparent rate constant for the binding of S-1 with F-actin. The apparent rate constant, v, for the binding of S-1 with F-actin was determined from a semilogarithmic plot of the increase in the light scattering intensity at 360 nm after mixing 0.1 μM S-1 with various concentrations of F-actin. Other conditions were as described for Fig. 1. Bars indicate standard deviations of the means.

from the binding rate constant of S-1 with F-actin and the dissociation rate constant of acto-S-1 complex. The rate constant for the binding of S-1 with intact F-actin, k_1, was measured from the increase in the light scattering intensity using a stopped flow apparatus. S-1 (0.3 μM) was mixed with 0.3-1.2 μM F-actin in 0.1 M KCl, 2 mM $MgCl_2$, and 20 mM Tris-HCl at pH 7.8. The time course of the increase in the light scattering intensity followed second order kinetics. The apparent binding rate constant (v) was determined from the initial velocity of the time course. Figure 4 shows the plot of the apparent binding rate constant (v) against F-actin concentration. The value of v increased linearly with an increase in F-actin concentration, and the values of k_1 were determined from the slope of the plot to be 1.4, 1.94, 2.55, and 4.2×10^6 $M^{-1} \cdot s^{-1}$, respectively, at 0, 10, 20, and 30 °C.

Dissociation Rate Constant of S-1 from F-actin —— To determine the dissociation rate constant, k_{-1}, of acto-S-1, Pyr-FA (3 μM) was mixed with acto-S-1 complex (6 μM F-actin + 3 μM S-1). The rate of dissociation of acto-S-1 was monitored from displacement of F-ctin by Pyr-FA. The formation of Pyr-FA-S-1 complex was monitored from the decrease in the fluorescence intensity of the pyrenyl group. The values of the initial rate, v, of the decrease in the fluorescence intensity, $\Delta F/\Delta F_{max}$, were 0.0137, 0.0166, 0.0217, and 0.0317 s^{-1}, respectively, at 0, 10, 20, and 30 °C.

The Pyr-FA-S-1 complex seems to be formed via two steps: A-S-1 $\rightleftharpoons$ A + S-1 (1) and S-1 + Pyr-FA $\rightleftharpoons$ Pyr-FA-S-1 (2). We denote the rate constants for the forward and backward reactions

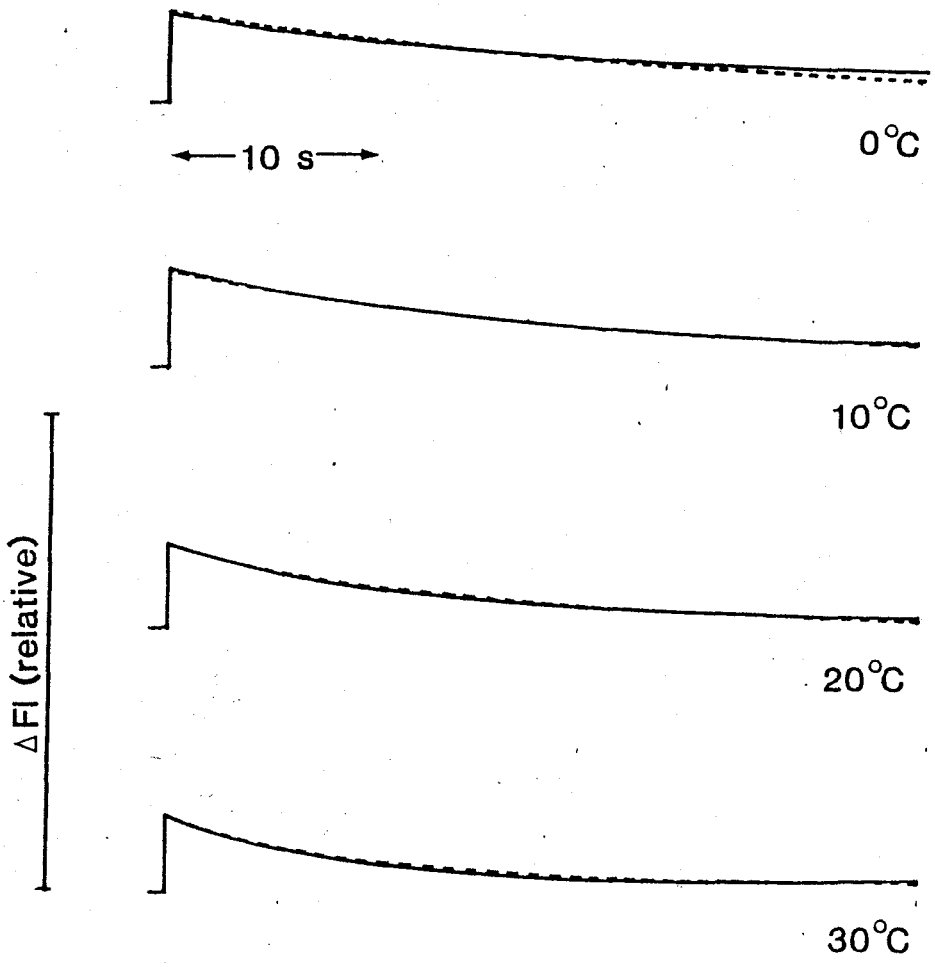

Fig. 5. Time course of decrease in the fluorescence intensity of pyrene-labeled F-actin excited at 366 nm and emitted at 406 nm after mixing with acto-S-1 complex. 3 μM Pyr-FA was mixed with a mixture of 6 μM F-actin and 3 μM S-1, and the decrease in fluorescence intensity of Pyr-FA (excited at 366 nm and emitted at 406 nm) due to the binding with S-1 was followed using a stopped flow apparatus. The rate constant for the dissociation of acto-S-1 was estimated from the initial rate of the decrease in the fluorescence intensity as described in RESULTS. The bar indicates the maximal decrease in the fluorescence intensity of Pyr-FA due to binding with S-1. Other conditions were as described for Fig. 1.

of step (1) to be k_{-1} and k_1, respectively, and those of step (2) to be k_1' and k_{-1}', respectively. Since the concentrations of free FA, free Pyr-FA, and acto-S-1 complex in the initial phase were all 3 μM, the initial rate of Pyr-FA-S-1 complex formation, v, is approximated by $v = k_1'(\text{Pyr-FA})\, k_{-1}/(k_1 + k_1')$. The values of k_1 and k_1', given in Figs. 4 and 2, were used to calculate the k_1 value. From the value of v shown in Fig. 5, the values of the rate constant of dissociation of acto-S-1, k_1, were calculated to be 0.0060 s^{-1} (or 0.36 min^{-1}), 0.0069 s^{-1} (or 0.41 min^{-1}), 0.0085 s^{-1} (or 0.51 min^{-1}), and 0.0125 s^{-1} (or 0.75 min^{-1}), respectively, at 0, 10, 20, and 30 °C.

Thermodynamic Properties of the Binding of S-1 with F-actin —— The temperature dependences of the values of k_1 and k_{-1}, which were obtained from Fig. 4 and 5, are summarized in Table II. The dissociation constants, K_d, calculated as k_{-1}/k_1 were 4.3, 3.6, 3.3, and 3.0 x 10^{-9} M, respectively at 0, 10, 20, and 30 °C. The standard free energy change ΔG° was calculated from K_d as $\Delta G^\circ = RT\ln K_d$, and was -11.3 Kcal/mol (20 °C). Figure 6 shows the dependence on temperature of the free energy change, ΔG°. Enthalpy change, ΔH°, and entropy change, ΔS°, calculated from this plot were +42.5 Kcal/mol and +47 cal/deg·mol, respectively.

DISCUSSION

Since myosin head (S-1) binds very strongly with F-actin in the absence of nucleotide, it is not easy to accurately measure the

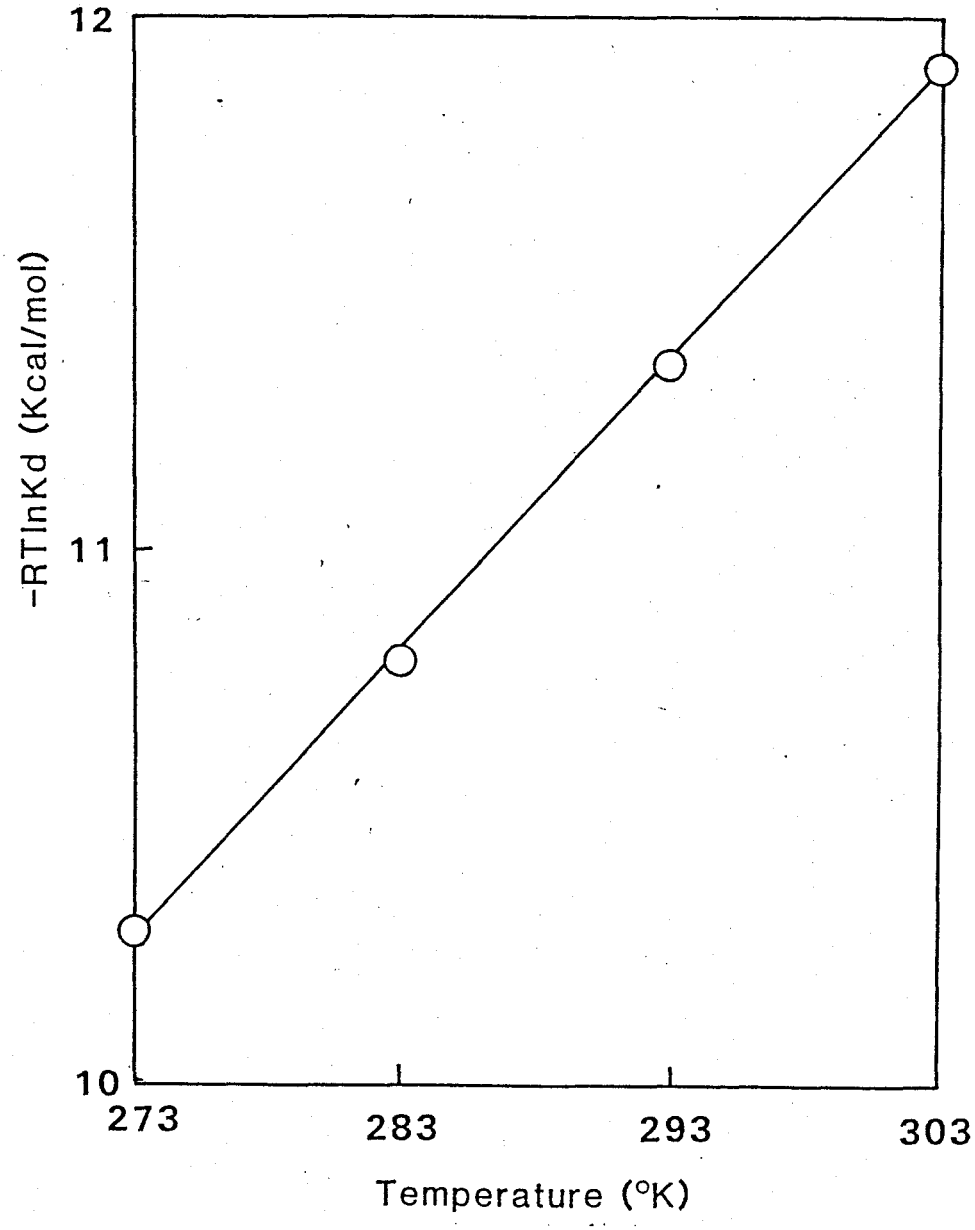

Fig. 6. Dependence on temperature of change in the free energy, ΔG°, for the binding of S-1 with F-actin. The free energy change, ΔG°, was calculated as $\Delta G^{\circ} = RT\ln K_d$ using the data presented in Table II.

Table II. Binding of S-1 with F-actin. The rate constant for the binding of S-1 with F-actin, k_1, was obtained from Fig. 3. The rate constant for the dissociation of S-1 from acto-S-1 was estimated from Fig. 4. The dissiociation constant of S-1 from acto-S-1, K_d, was calculated as $K_d = k_{-1}/k_1$. The conditions were as described for Fig. 1.

Temperature (°C)	k_1 ($\times 10^6$ M^{-1} s^{-1})	k_{-1} (s^{-1})	K_d ($\times 10^{-9}$ M)
0	1.40	0.0060	4.3
10	1.94	0.0069	3.6
20	2.55	0.0085	3.3
30	4.20	0.0125	3.0

value of the dissociation constant for the binding of S-1 with F-actin. In this study, we measured the dissociation constant as the ratio of the dissociation rate constant, k_{-1}, of acto-S-1 complex to the binding rate constant, k_1, of S-1 with F-actin. The binding rate constant was found to be very large (2.55×10^6 $M^{-1} \cdot s^{-1}$ at 20 °C) and higher than that measured at higher ionic strength by Tonomura et al. (14) (10^5 $M^{-1} \cdot s^{-1}$). The rate constant of dissociation was very small, about 0.5 min^{-1} (Fig. 5). This value was of the same order of magnitude as that of the slow decay in tension when the muscle fiber is stretched in the absence of ATP, ($t_{1/2}$ = 100 - 400 s) (Ref. 15 and Arata and Podolsky, personal communication).

The dissociation constant of S-1 from acto-S-1, K_d, was calculated from k_1 and k_{-1} to be 3.3×10^{-9} M. This value was higher than the previous report of Takeuchi and Tonomura (1), (10^{-6} M). Marston and Weber (2), Margossian and Lowey (3), and Highsmith (4) also reported a value of 10^{-6} - 10^{-7} M. However, they used S-1 of which the specific thiol residue (SH_1) was modified with radioactive reagent or fluorescent label. Greene and Eisenberg (16) and Inoue and Tonomura (13) calculated the dissociation constant of S-1 from acto-S-1 using the dissociation constants of steps, S-1-AMPPNP $\rightleftharpoons$ acto-S-1-AMPPNP, AMPPNP $\rightleftharpoons$ S-1-AMPPNP and AMPPNP $\rightleftharpoons$ acto-S-1-AMPPNP complex, to be 10^{-7} M and 10^{-9} M, respectively. The value of K_d obtained in the present study is of the same order of magnitude as that of Inoue and Tonomura (13).

When F-actin was labeled with pyrene iodoacetamide, the rate of binding of S-1 to F-actin increased about 3-fold (Tables I and

II). However, the rate of dissociation of acto-S-1 increased about 10-fold. Therefore, the affinity of S-1 for F-actin decreased about 3-fold by the modification of F-actin. The value of the dissociation constant of S-1 from acto-S-1, K_d, was calculated from the value of the dissociation constant of S-1 from Pyr-FA-S-1, $K_{d(Pyr-FA)} = k_{-1}'/k_1'$, and the ratio of the dissociation constants, $K_{d(FA)}/K_d'_{(Pyr-FA)}$ (Table I). This value agreed well with that calculated from $K_d = k_{-1}/k_1$ (Table II).

Many studies have been conducted using S-1 with a modified SH_1 thiol residue. We examined the effect of modification of the SH_1 thiol residue with IAEDANS on the dissociation constant of S-1 from acto-S-1 and found that it caused about a 2-fold increase in the dissociation constant in 0.1 M KCl at pH 7.8 and 20 °C (see RESULTS).

The standard free energy change ΔG° was calculated as $RT\ln K_d$ (20 °C) to be -11.3 Kcal/mol. The thermodynamic parameters, ΔH° and ΔS°, for the binding of S-1 with F-actin were calculated from the temperature dependence of the $RT\ln K_d$ value (Fig. 5). The enthalpy change (ΔH°) and the entropy change (ΔS°) were found to be +2.5 Kcal/mol and +43 cal/deg mol, respectively, in 0.1 M KCl at pH 7.8 and 20 °C. The positive enthalpy change shows that the binding of S-1 and F-actin is endothermic. The large entropy change indicates that the binding of S-1 to F-actin is driven strongly by an entropy increase. Therefore, a structural change including helix-to-coil transition may occur in the S-1 and/or F-actin structure. Alternatively, highly ordered protein-bound water and ions may be displaced into the bulk solvent upon the binding of S-1 with F-actin.

REFERENCES

1. Takeuchi, K. & Tonomura, Y. (1971) J. Biochem. 70, 1011-1026
2. Marston, S. & Weber, A. (1975) Biochemistry 14, 3868-3873
3. Margossian, S.S. & Lowey, S. (1978) Biochemistry 17, 5431-5439
4. Highsmith, S. (1978) Biochemistry 17, 22-26
5. Perry, S.V. (1952) in Methods in Enzymology (Colowick, S.P. & Kaplan, N.O., eds.) Vol. 2, pp.582-588, Academic Press, New York
6. Weeds, A.V. & Taylor, R.S. (1975) Nature 257, 54-56
7. Spudich, J.A. & Watt, S. (1971) J. Biol. Chem. 246, 4866-4871
8. Tonomura, Y. (1972) Muscle Protein, Muscle Contraction and Cation Transport, Univ. Tokyo Press and Univ. Park Press, Tokyo and Baltimore
9. Kouyama, T. & Mihashi, K. (1981) Eur. J. Biochem. 114, 33-38
10. Takashi, R., Duke, J., Ue, K., & Morales, M.F. (1976) Arch. Biochem. Biophys. 175, 279-283
11. Takemori, S., Nakamura, M., Suzuki, K., Katagiri, M. & Nakamura, T. (1972) Biochem. Biophys. Acta 284, 382-393
12. Morita, F. & Tonomura, Y. (1960) J. Am. Chem. Soc. 82, 5172-5177
13. Inoue, A. & Tonomura, Y. (1980) J. Biochem. 88, 1643-1651
14. Tonomura, Y., Watanabe, S., & Morales, M.F. (1969) Biochemistry 8, 2171-2176
15. Kuhn, H.J. (1978) Biophys. Struct. Mechanism 4, 159-168
16. Green, L.E. & Eisenberg, E. (1980) J. Biol. Chem. 255, 549-554

PART 2

Elementary Steps of the Actomyosin ATPase Reaction Without Accompanying the Dissociation of Actomyosin: Studies by Transient Kinetics and Oxygen Exchange

SUMMARY

The elementary steps of the actomyosin ATPase reaction without accompanying the dissociation of actomyosin were studied using crosslinked acto-subfragment-1 (acto-S-1) or non-cross-linked acto-S-1 at low ionic strength and at high concentrations of F-actin by a transient kinetics and an oxygen exchange. The data obtained were adjusted to the following scheme (Inoue, Takenaka, Arata and Tonomura, Adv. Biophys. 13, 1-194, 1979):

$$AM + ATP \underset{}{\overset{K_1}{\rightleftharpoons}} AMATP \underset{k_{-2}}{\overset{k_2}{\rightleftharpoons}} AM^*ATP \underset{k_{-3}}{\overset{k_3}{\rightleftharpoons}} AM_P^{ADP} \xrightarrow{k_4} AM + ADP + Pi$$

where AMATP, AM^*ATP, and AM_P^{ADP} are the loosely bound actomyosin-ATP complex, the tightly bound complex and the actomyosin-P-ADP complex, respectively.

The values of Km and Vmax of the overall ATPase reaction of crosslinked acto-S-1 ATPase at 20 °C in 0.1 M KCl were 12 μM and 13 s^{-1}, respectively. The amount of AM_P^{ADP} during the steady state of the crosslinked acto-S-1 ATPase reaction was estimated from the Pi-burst size to be 0.1 mole/mole·S-1. The value of k_4 was estimated as $Vmax/AM_P^{ADP}$ to be 130 s^{-1}. During the hydrolysis of (γ-^{18}O)ATP by acto-S-1 there is an oxygen exchange of between water and Pi, and the exchange ratio ($R = k_{-3}/k_4$) was estimated from the distribution of (^{18}O)Pi species formed by acto-S-1 ATPase to be 0.52. Then, the value of k_{-3} was estimated to be 68 s^{-1}. The amount of tightly bound ATP (AM^*ATP) in crosslinked acto-S-1 ATPase reaction measured by quenching the ATPase either with large amount of cold ATP or TCA was 0.4

mole/mole S-1, and the amount of (AM^*ATP) + (AM_P^{ADP}) is close to the amount of active site estimated from the Pi-burst size in S-1 ATPase reaction. Since the net rate of step 3, $k_3(AM^*ATP) - k_{-3}(AM_P^{ADP})$, is equal to Vmax, the value of k_3 was calculated to be 49.5 s^{-1}. It was suggested from the existence of tightly bound ATP in acto-S-1 ATPase reaction that the value of k_{-2} is much smaller than that of k_3 ($k_{-2} < 5\ s^{-1}$). The second order rate constant of AM^*ATP formation at various ATP concentrations (k_2/K_1) which is equal to Vmax/Km is $2 \times 10^6\ s^{-1}M^{-1}$ (active site = 0.5 mole/mole S-1). Since the amount of loosely bound ATP (AMATP) during the steady-state of the ATPase reaction is low. the value of k_2 is assumed to be extremely high (if k_2 = 1000 s^{-1}, K_1 = 0.5 mM). The rate constants of the elementary steps of acto-S-1 ATPase reaction at extremely high F-actin concentration were almost same as those for crosslinked acto-S-1. On the other hand, with S-1 K_1 = 0.5 mM, k_2 = 1000 s^{-1}, k_{-2} = 0.05 s^{-1}, k_3 = 100 s^{-1}, k_{-3} = 10 s^{-1}, and k_4 = 0.05 s^{-1}. (Inoue, Takenaka, Arata and Tonomura, Adv. Biophys. 13, 1-194, 1979). Thus, in the acto-S-1 ATPase reaction k_4 is 2600 times higher than that in the S-1 ATPase reaction and the rate of acto-S-1 ATPase reaction is determined by the formation of M_P^{ADP}.

INTRODUCTION

Muscle contraction is driven by the cyclic interaction of myosin head with actin coupled with ATP hydrolysis. Myosin itself has a low activity of ATPase reaction. At low ionic strength, F-actin greatly accelerate the ATP hydrolysis by myosin and actomyosin ATPase thus appeared is coupled with contraction.

The mechanism of actomyosin ATPase reaction was studied using soluble subfragments of myosin, heavy-meromyosin (HMM) and subfragment-1 (S-1) (1-4). The actomyosin-ATPase reaction is catalyzed via the myosin-phosphate-ADP complex, M_P^{ADP}, a key intermediate of the myosin ATPase reaction (5-7). Inoue et al. (8,9) studied the relationship between the elementary steps of ATP hydrolysis and the dissociation and recombination of actin and myosin head, and proposed that ATP is hydrolyzed via two routes one with and the other without accompanying the dissociation of actomyosin:

$$\begin{array}{l} AM + ATP \rightleftharpoons AMATP \rightleftharpoons AM_a^*ATP \rightleftharpoons AM_b^*ATP \rightleftharpoons AM_P^{ADP} \longrightarrow AM + ADP + Pi \\ \qquad\qquad\qquad\qquad\qquad\qquad\qquad\qquad\qquad\qquad\qquad\quad (AM_P^{ADP}) \\ \qquad\qquad\qquad\qquad\qquad\qquad\qquad\qquad\qquad\qquad\qquad\quad \text{(inner cycle)} \\ A + M_a^*ATP \rightleftharpoons A + M_b^*ATP \rightleftharpoons A + M_P^{ADP}(R) \rightleftharpoons A + M_P^{ADP}(N) \\ \qquad\qquad\qquad\qquad\qquad\qquad\qquad\qquad\qquad\qquad\qquad\quad \text{(outer cycle)} \end{array}$$

Where M_a^*ATP and M_b^*ATP are the tightly bound ATP complex with different fluorescent spectrum.

The ATPase reaction of the outer cycle is determined by the transition from M_P^{ADP} in the refractory state (R) to that in the non-refractory state (N)(9,10). Since the rate of this process is slow in acto-S-1 ATPase reaction it was suggested that ATP hydrolysis in the inner cycle is coupled with contraction. Arata

(11,12) and Trayer and Trayer (13) reported the structural change in acto-S-1 by formation of acto-S-1-nucleotide complex. However, the Km and Vmax of overall ATPase reaction and the rate of each elementary steps in the actomyosin ATPase reaction of this route was not sufficiently examined. Especially, the Pi burst size is differently reported by Inoue et al. (9), Rosenfeld and Taylor (14), Bioska et al. (15) and Stein et al. (16). It has not been clarified which step is the rate limiting of the ATPase reaction and how the eqquilibrium between AM_b^*ATP and AM_P^{ADP} shifts.

Inoue et al. (9) showed that at infinite concentrations of F-actin ATP is mainly hydrolyzed via inner route of the ATPase reaction. However, it succeeded only at low ionic strength and at room temperature. In this paper, we study the mechanism of actomyosin ATPase reaction using crosslinked acto-S-1, since the ATPase activity of crosslinked acto-S-1 is as high as Vmax of acto-S-1 ATPase at infinite F-actin concentration (11,17). We measured the amount of AM_P^{ADP} and tightly bound ATP complex from the Pi-burst size and Pi-release after cold ATP chase, as described by Biosca et al. (15). We also measured the ^{18}O exchange reaction which is induced by the step, $AM_b^*ATP \rightleftharpoons AM_P^{ADP}$ (18-20). The rates of each elementary steps are assumed from these results and the values of Vmax and Km of the overall reaction. We found that the rate limiting step of the actomyosin ATPase reaction without accompanying the dissociation of actomyosin is the transition from AM^*ATP to AM_P^{ADP}, and the decomposition of AM_P^{ADP} is more than 3000 times accelerated by F-actin.

EXPERIMENTAL PROCEDURES

Materials—Myosin was prepared from rabbit white skeletal muscle by the method of Perry (21). S-1 was prepared by chymotryptic digestion of myosin, as described by Weeds and Taylor (22). G-actin was prepared from an acetone powder of rabbit white skeletal muscle by the method of Spudich and Watt (23). G-actin was polymerized into F-actin by adding 50 mM KCl KCl. Free ATP in the F-actin solution was removed by ultracentrifugation at 1 x 10^5g for 90 min and the pellet was homogenized in the buffer. Pyruvate kinase was prepared from rabbit skeletal muscle as described by Tiez and Ochoa (24). Acetate kinase and myokinase were purchased from Boehlinger Mannheim, GMBH. The proteins were analyzed by SDS gel electrophoresis (25). Protein concentrations were determined by means of the Biuret reaction calibrated by nitrogen determination. The molecular weight of S-1 and actin monomer were adopted to be 1.2 x 10^5 and 4.2 x 10^4, respectively (1).

Reagents—EDC (1-ethyl-3-(3-dimethyl aminopropyl) carbodiimide) was purchased from Nakarai Chemical Co. Ltd, Kyoto. ATP and ADP were purchased from Kohjin Co. Ltd, Tokyo. AMP was purchased from Yamasa Co. Ltd. PEP was purchased from Sigma Co. (^{18}O)H_2O (98 atom % of ^{18}O) was purchased from Amersham International plc. or CEA oris. (γ-^{32}P)ATP was synthesized enzymatically by the method of Glynn and Chappel (26). All other reagents were of analytical grade.

Crosslinking of acto-S-1—Acto-S-1 was crosslinked essentially as described by Mornet et al. (17) and Arata (11).

S-1 (5 μM) was mixed with F-actin (20 μM) in 50 mM KCl, 2 mM $MgCl_2$, and 10 mM HEPES at pH 7.0 and 20 °C. The crosslinking reaction was started by adding 4 mM EDC, which had been dissolved to 40 mM immediately prior to use. The reaction was allowed to proceed for 90 min and terminated by adding 20 mM 2-mercapto-ethanol. About 90 % of added S-1 was crosslinked under this condition. After adding 0.5 M KCl, 6 mM $MgCl_2$, and 5 mM ATP at 4 °C, non-crosslinked S-1 was removed by centrifugation at 1.6 x 10^5 g for 60 min. The pellet was washed with cold distilled water and then gently homogenized in 2 mM $MgCl_2$, 10 mM Imidazole at pH 7.0 and 0 °C. The mixture was centrifuged again at 1.6 x 10^5 g for 60 min and the pellet was homogenized as described above. The amounts of crosslinked S-1 were determined by subtracting the free S-1 eliminated by the washing procedures from the initial concentration of S-1. Amount of non-crosslinked S-1 in the preparation was determined by SDS/polyacrylamide gel electrophoresis to be less than 5 % of total S-1.

ATPase activity—The rate of acto-S-1 ATPase reaction in the steady state was measured by coupling ATPase reaction with pyruvate kinase system. The reaction mixture contained 0.5 mg/ml pyruvate kinase, 0.1 mM ATP, 2 mM PEP, 0.1 M KCl, 2 mM $MgCl_2$, and 10 mM Imidazole at pH 7.0 and 20 °C. The amount of pyruvate liberated was determined as described by Reynard et al. (27).

Quenching flow experiment—The initial phase of ATP hydrolysis was measured from ^{32}Pi liberation from (γ-^{32}P)ATP by employing Durrum rapid-flow apparatus. The reaction was started by mixing crosslinked acto-S-1 (5 μM S-1) with 100 μM (γ-^{32}P)ATP in 0.1 M KCl, 2 mM $MgCl_2$, and 10 mM Imidazole at pH

7.0 and 20 °C, and the reaction was terminated with 0.1 N HCl containing 0.1 mM Pi as a carrier. After adding 1 ml of 10 % TCA the denatured proteins were removed by centrifugation at 1 x 10^3 g for 10 min. The amount of ^{32}Pi liberated was measured as described previously (28). In the ATP chase experiments, the reaction was quenched with 10 mM unlabeled ATP. After incubation for exactly 5 s at 20 °C, the reaction was terminated by mixing 10 % TCA, and the ^{32}Pi liberated was determined as described above. Zero time points were obtained by mixing γ-^{32}P -ATP with the unlabeled ATP, adding S-1 or crosslinked acto-S-1, and quenching in 10 % TCA after an incubation for 5 s.

(γ-^{18}O)ATP — (γ-^{18}O)ATP was synthesized based on the methods of Hackney et al. (29) and Ikeuchi and Miderfort (30) with slight modifications. ^{18}O- Enriched inorganic phosphate was prepared by hydrolysis of PCl_5 with 50 % molar excess (^{18}O)H_2O. The reaction was run for 24 hrs in a drybox under nitrogen atmosphere. The temperature was kept at 35-40 °C in heat block. The mixture was neutralized with imidazole, and after mixing KOH and water, the ^{18}O-phosphate was isolated as $K_2HP^{18}O_4$ (29). $K_2HP^{18}O_4$ was acetylated by the method of Stadman (31). ^{18}O-Enriched ATP was synthesized enzymatically using acetate kinase (30). (^{18}O)-Acetyl phosphate lithium salt (15 mM) was mixed with 8 mM $MgCl_2$, 7 mM AMP and small amount of ADP (0.02 mM) in the solution of 20 mM triethylamine-HCl buffer at pH 7.2. The reaction was started by adding 2 unit/ml acetate kinase and 1.8 unit/ml myokinase at 20 °C for 20 min. By this method O atoms in β and γ positions were replaced with ^{18}O. The reaction was terminated with 10 % PCA, then denatured proteins were removed by centrifugation at 1

x 10^3g for 10 min. The pH of the supernatant was adjusted by 5 N KOH to 8.0. After standing for 60 min at 0 °C, precipitate of K-PCA removed by centrifugation at 1 x 10^4g for 20 min. The ^{18}O-ATP was fractionated on DE-52 (HCO_3^-form) eluted with a linear gradient of triethylammonium bicarbonate (0.1 - 0.5 M) according to Wehrli et al. (32). The (^{18}O)ATP preparation was checked on a polyethyleneimine-cellulose thin-layer chromatography according to the method of Randerath and Randerath (33). ATP concentration was determined from the absorption at 259 nm.

^{18}O exchange reaction—— The ATPase reaction was carried out using (^{18}O)ATP as substrate. About 50 % of ATP added (0.1 μmoles) was hydrolyzed by the ATPase reaction. The product Pi was separated on Dowex 1 X2 (H^+) column (1 x 3 cm) eluted with 50 mM HCl. The Pi fraction was lyophilized and converted into trimethylsilyl phosphate (29). The fraction of each labeled Pi species were determined by a gas chromatograph that is directly coupled to the mass spectrometer (Shimadzu-LKB 9000 or Shimadzu QP-1000). The fragments of product gave higher peaks at m/e = 299, 301, 303 and 305, respectively. The amount of Pi which contained 0, 1, 2 and 3 ^{18}O atoms were determined from the signal intensities at m/e = 314, 316, 318 and 320, respectively. The natural abundance of ^{29}Si and ^{30}Si was corrected as described Hackney and Boyer (34). The amount of ^{18}O in the γ-position of ATP was determined from the distribution of Pi which is produced by the myosin EDTA ATPase reaction, since Levy et al. (35) reported that there was no oxygen exchange reaction in the myosin EDTA ATPase reaction.

The distribution of Pi produced by ATPase reaction was

calculated from the given value of R (= k_{-3}/k_4) and the distribution of Pi produced by the EDTA ATPase reaction (36). Oxygen atom is incorporated by the step from EATP to E_P^{ADP}, and $k_4/k_{-3} + k_4$ or $1/(1 + R)$ of E_P^{ADP} is decomposed into E + ADP + Pi. The remaining $R/(1 + R)$ was converted into EATP. However, 1/4 of O atom liberated by this step is that incorporated by the forward reaction. Then, if we denote the ratio of ATP with 3, 2, 1, and 0 ^{18}O atoms in the γ-P position as $a_o : b_o : c_o : d_o$ ($a_o + b_o + c_o + d_o = 100$), and those of product Pi with 3, 2, 1, and 0 ^{18}O atoms as $a : b : c : d$ ($a + b + c + d = 100$), the values of a, b, c, and d are given as:

$$a = a_o\,(4/3R + 4)$$

$$b = (a_0 + b_o - a)(2/R + 2)$$

$$c = (a_o + b_o + c_o - a - b)(4/R + 4)$$

$$d = 100 - (a + b + c)$$

RESULTS

Km and Vmax of Crosslinked Acto-S-1 ATPase Reaction——The rate of crosslinked acto-S-1 ATPase reaction in the steady state was measured using pyruvate kinase system. The rate of crosslinked acto-S-1 ATPase activity was dependent on the ratio of F-actin to S-1 in the crosslinked complex (Fig. 1). The rate of crosslinked acto-S-1 ATPase activity is 6.8 s^{-1} at actin monomer/S-1 of 1.75. S-1/FA. The rate of ATPase increased with increase in the ratio of actin to S-1, and it reached a maximal level of about 13 s^{-1} at F-actin/S-1 ratio of more than 5. Then, in the following experiments the ratio of F-actin/S-1 was chosen to be more than 5.

Figure 2 shows the double reciprocal plot dependence on ATP concentration of the rate of crosslinked acto-S-1 ATPase reaction in the steady state. Concentration of ATP was varied from 10 to 1000 μM. Km and Vmax of the crosslinked acto-S-1 ATPase reaction was given to be 11.4 μM and 13.3 s^{-1}, respectively. The rate of S-1 ATPase reaction under same condition was found to be 0.06 s^{-1}.

The rate of crosslinked acto-S-1 ATPase reaction was measured in various KCl concentrations. The activity in the absence KCl was 10.2 s^{-1}, which was slightly lower than that in 0.1 M KCl (13,2 s^{-1}). The ATPase activity decreased when KCl concentration was increased to more than 0.2 M. At 0.5 M KCl the activity was 7.5 s^{-1}.

Initial Stage of Crosslinked Acto-S-1 ATPase Reaction——The time course of Pi liberation in the initial phase of crosslinked

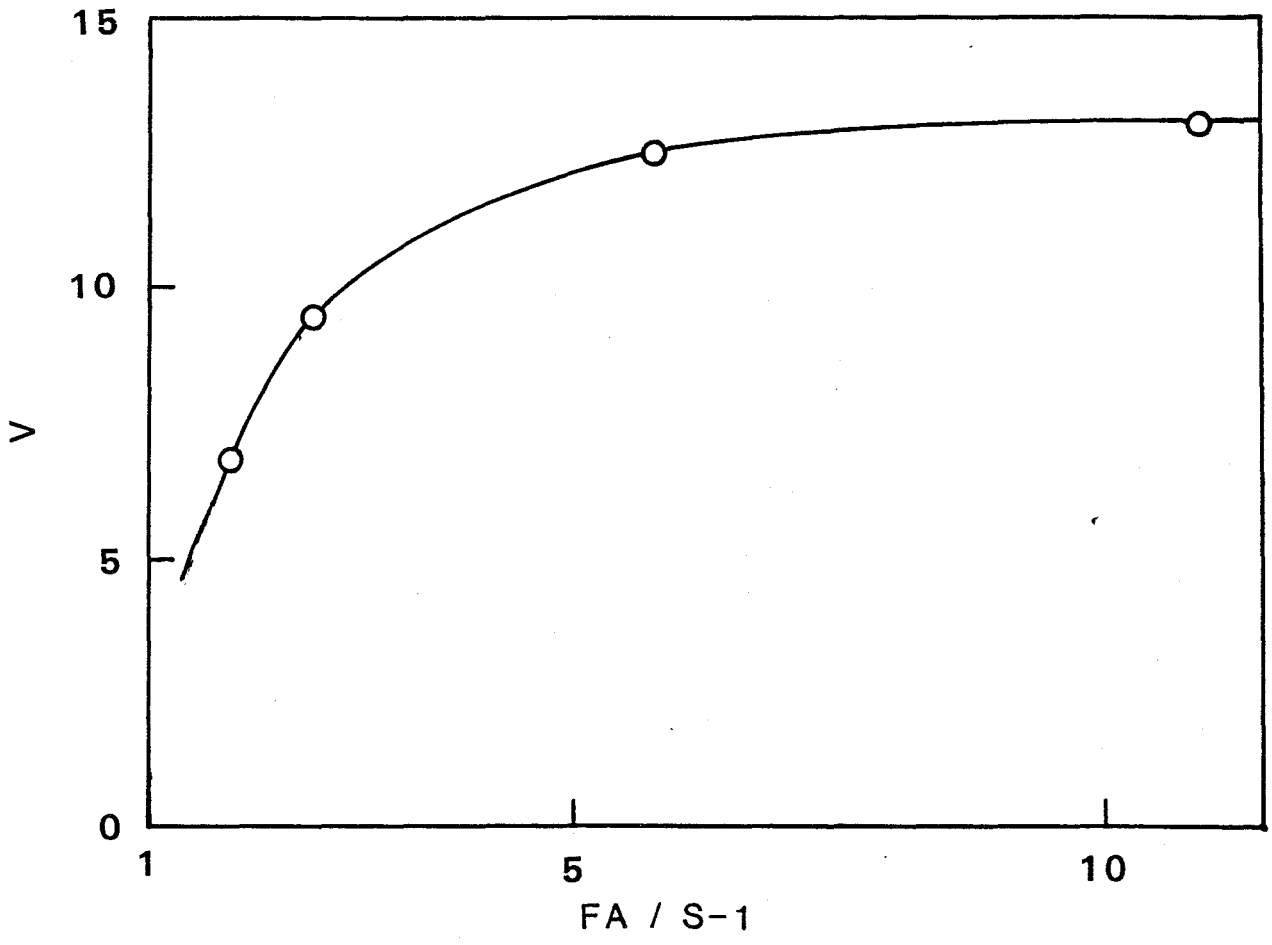

Fig. 1 Dependence on the ratio of F-actin to S-1 in crosslinked acto-S-1 of the rate of ATPase activity. Acto-S-1 (5 μM S-1, 5-50 μM F-actin) was crosslinked in 2 mM EDC, 0.1 M KCl, 2 mM $MgCl_2$, and 10 mM Imidazole-HCl at pH 7.0 and 20 °C for 90 min. The ATPase activity was measured in crosslinked acto-S-1 (0.05 μM S-1) 0.5 mg/ml pyruvate kinase, 0.1 mM ATP, 2 mM PEP, 0.1 M KCl, 2 mM $MgCl_2$, and 10 mM imidazole at pH 7.0 and 20°C. The rate of crosslinked acto-S-1 ATPase reaction was plotted against the molar ratio of actin and S-1 in the crosslinked complex.

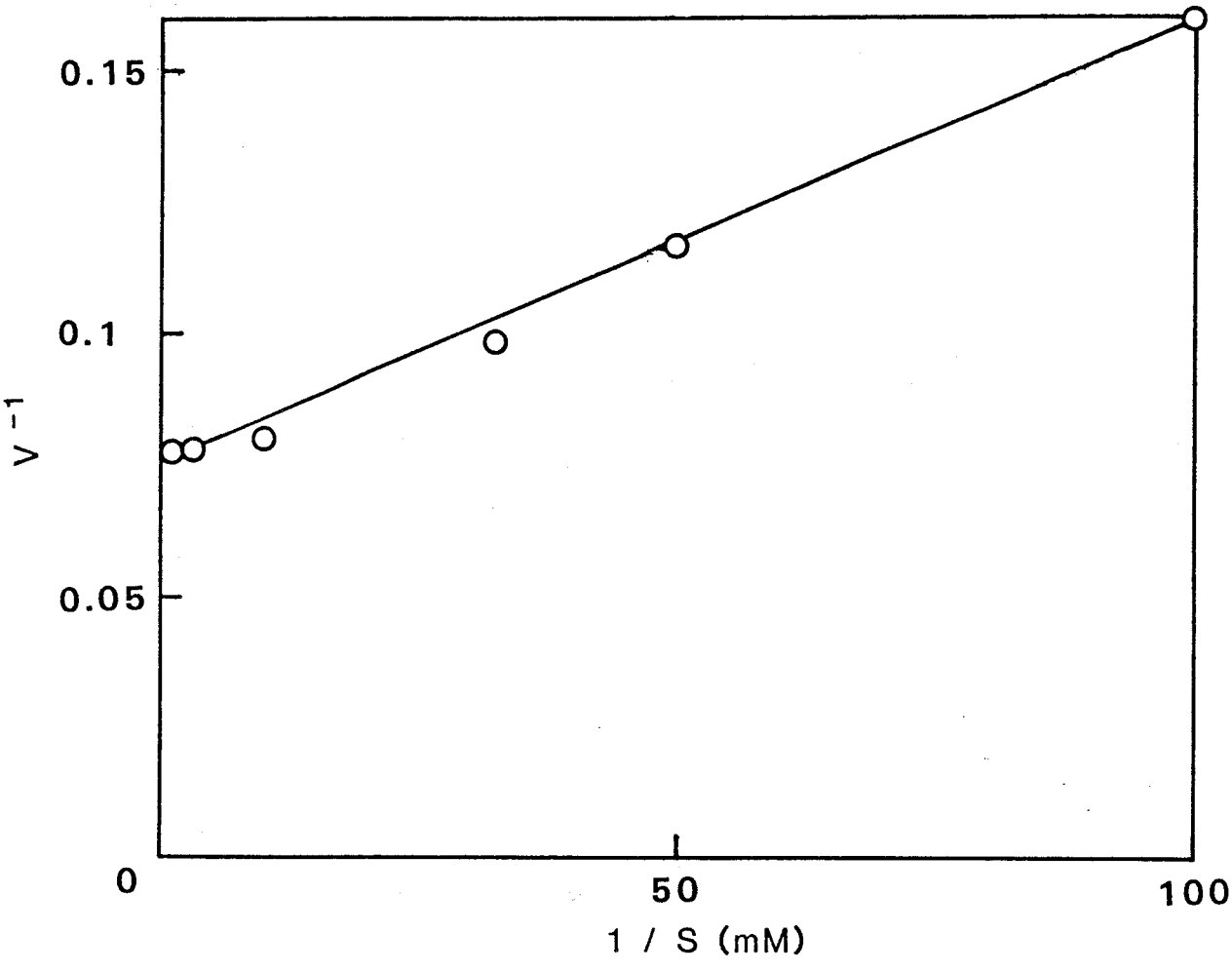

Fig. 2 The double reciprocal plot of the rate of crosslinked acto-S-1 ATPase reaction against ATP concentration. Crosslinked acto-S-1 (0.05 μM S-1), 10-1000 μM ATP. The other conditions are the same as for Fig. 1.

acto-S-1 ATPase reaction was measured with that of tightly bound ATP formation. Figure 3 shows the initial stage of S-1 ATPase reaction in 0.1 M KCl, 2 mM $MgCl_2$, 0.1 mM EDTA and 10 mM Imidazole-HCl at pH 7.0 and 20 °C. ATP (50 μM) was mixed with 10 μM non-crosslinked S-1 and the amount of Pi was determined after quenching the reaction with HCl. There was initial rapid liberation of Pi followed by the steady state hydrolysis of ATP. The Pi burst size was 0.52 mole/mole·S-1, and the rate of ATP hydrolysis in the steady state was 0.03 s^{-1}. The time course of Pi liberation was also measured after quenching the ATPase reaction with 5 mM cold ATP. The amount of initial rapid Pi-liberation was 0.56 mole/mole·S-1.

In figs 3 and 4, the time course of Pi-liberation was measured after mixing (γ-^{32}P)-labelled ATP (100 μM) with crosslinked acto-s-1 (5 μM S-1) in 0 or 0.1 M KCl, 2 mM $MgCl_2$, and 10 mM Imidazole at pH 7.0 and 20 °C (Figs. 3 and 4). The Pi burst size of crosslinked acto-S-1 was small 0.1 and 0.16 mole/mole S-1, respectively, in 0 and 0.1 M KCl. The amount of initial rapid Pi liberation after ATP quenching was 0.5 mole/mole·S-1 either 0 or 0.1 M KCl. The amount of tightly bound ATP was calculated as Pi liberation after ATP quenching minus Pi burst after acid quenching to be 0.34 and 0.40 mole/mole·S-1, respectively, in 0 or 0.1 M KCl.

Oxygen Exchange during Acto-S-1 ATPase——Oxygen exchange reaction in the crosslinked acto-S-1 ATPase was analyzed using (γ-^{18}O)ATP as substrate. Distribution of Oxygen in γ-P position of ATP was measured from the distribution of Pi produced by S-1 EDTA-ATPase reaction. As shown in Fig. 6-a, about 72 % of total

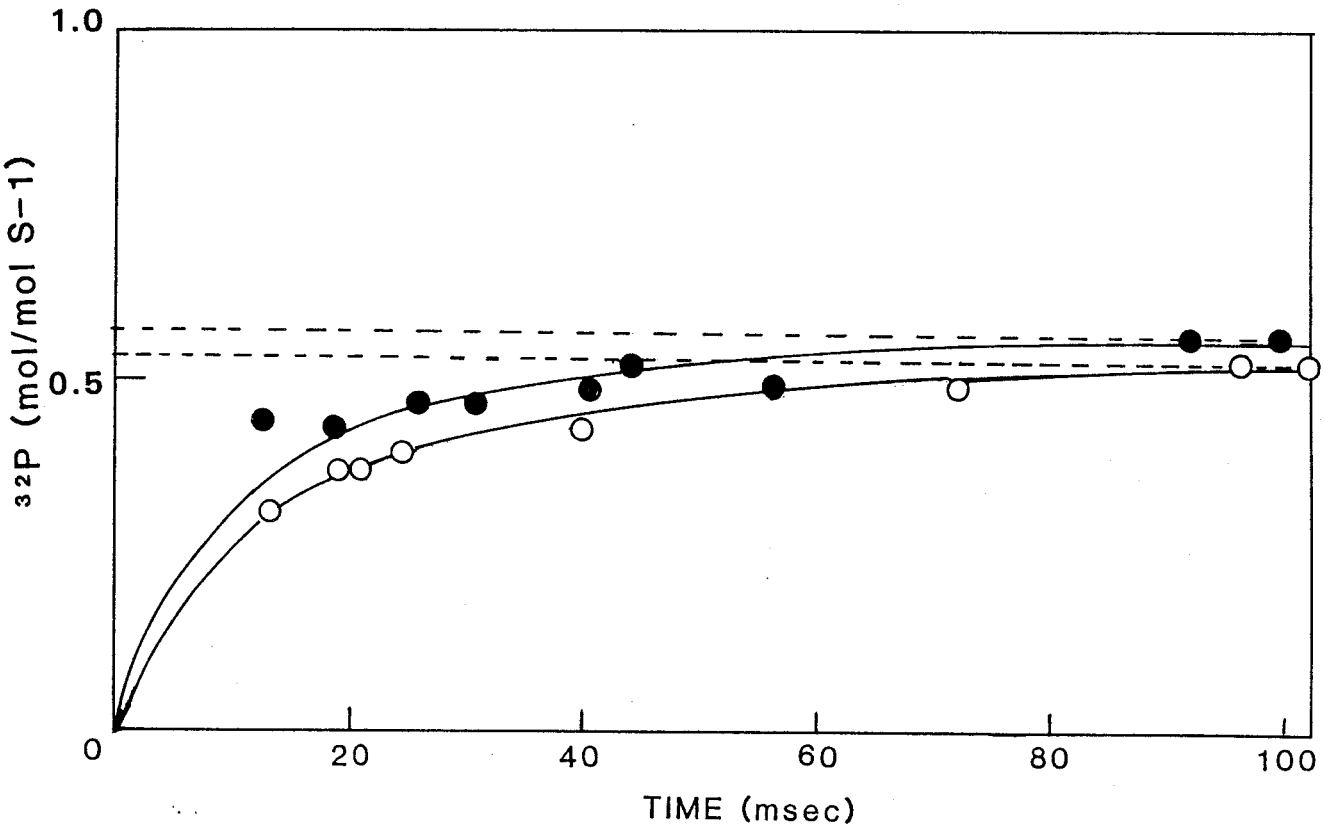

Fig. 3 The initial time course of S-1 ATPase reaction in 0.1 M KCl. 10 μM S-1, 50 μM (γ-^{32}P)ATP, 0.1 M KCl, 2 mM $MgCl_2$, 10 mM imidazole at pH 7.0 and 20 °C. ○, Pi liberation after quenching by HCl; ●, the tightly bound ATP after quenching by ATP.

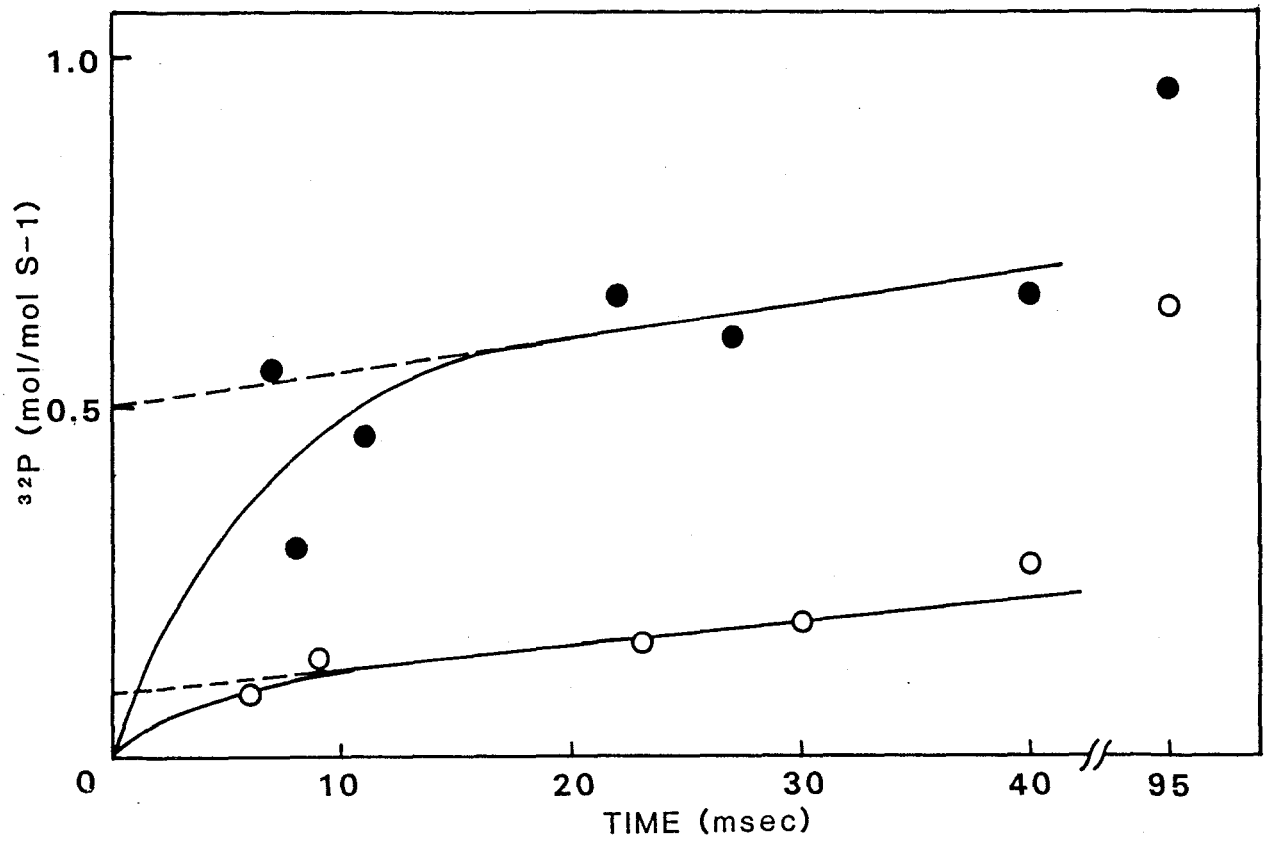

Fig. 4 The time course of Pi liberation in the initial phase of crosslinked acto-S-1 ATPase reaction in 0.1 M KCl. Crosslinked acto-S-1 (5 μM S-1), 100 μM (γ-^{32}P)ATP, 0.1 M KCl, 2 mM $MgCl_2$, 10 mM imidazole at pH 7.0 and 20 °C. ○, Pi liberation after quenching by HCl; ●, the tightly bound ATP after quenching with ATP.

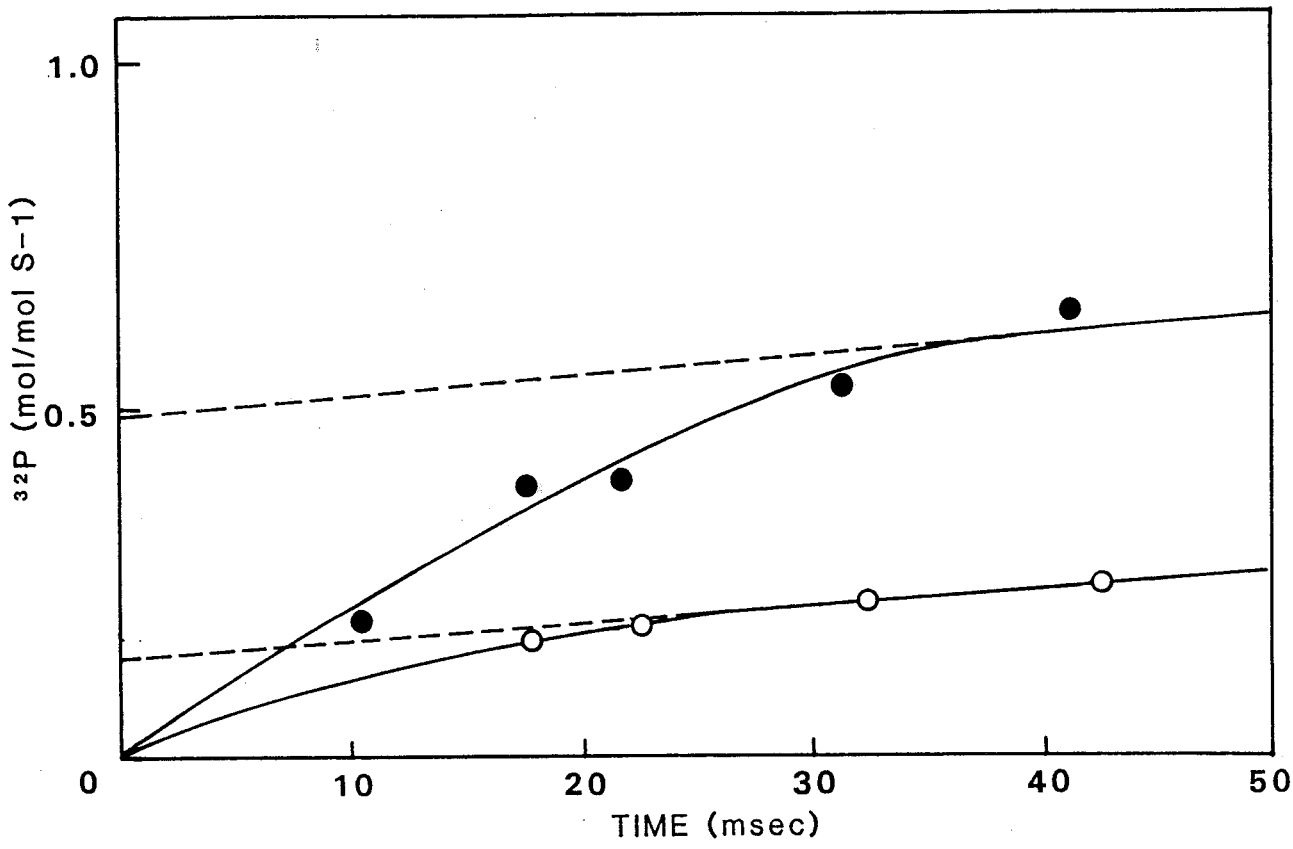

Fig. 5.The time course of Pi liberation in the initial phase of crosslinked acto-S-1 ATPase reaction in 0 M KCl. Crosslinked acto-S-1(5 μM S-1), 100 uM (γ-^{32}P)ATP, 0 M KCl, 2 mM $MgCl_2$, 10 mM imidazole at pH 7.0 and 20 °C. ○, Pi liberation after quenching with HCl; ●, the tightly bound ATP after quenching with cold ATP.

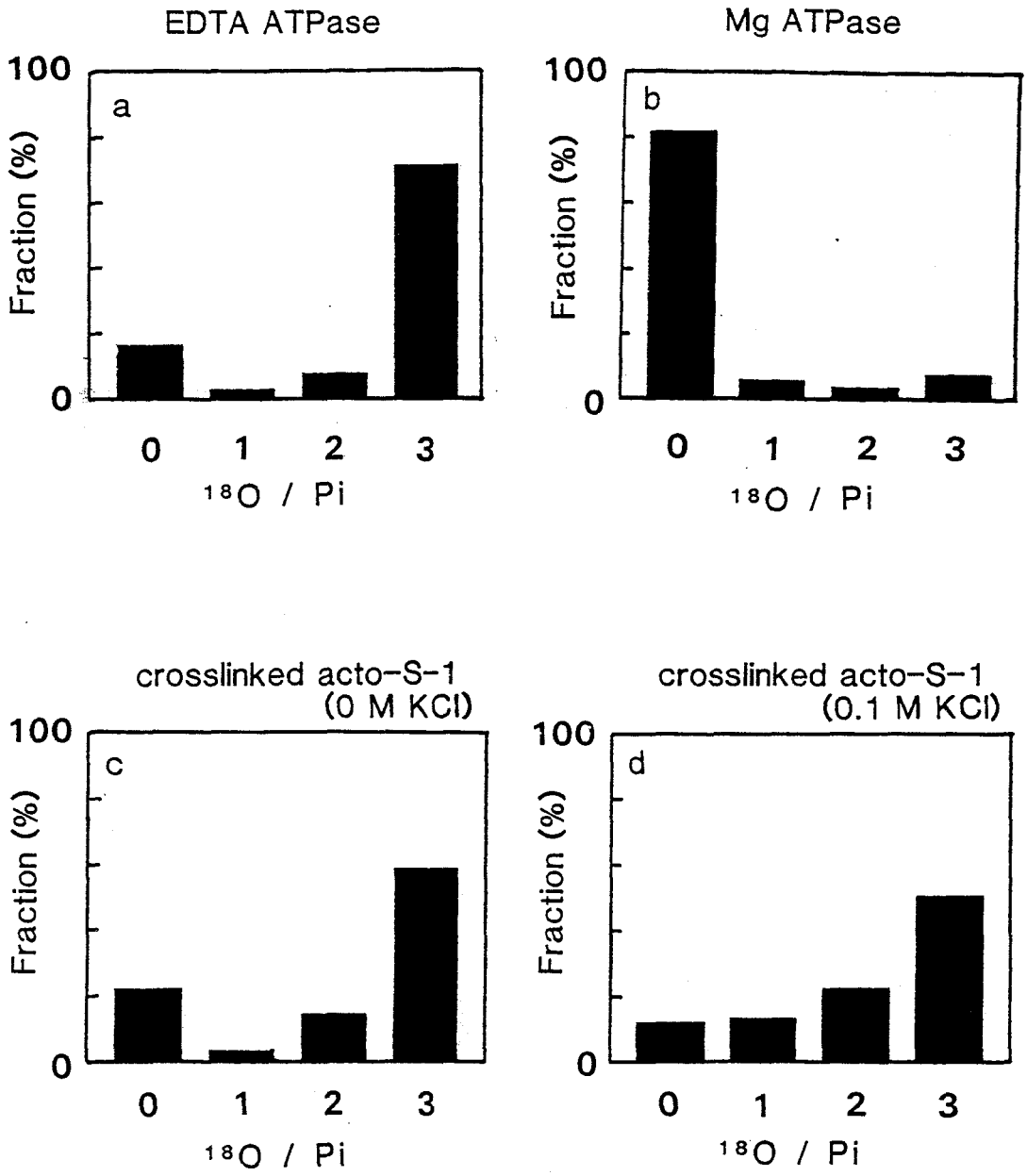

Fig. 6 Distribution patterns of (^{18}O)Pi species produced by S-1 EDTA- and Mg-ATPase and crosslinked acto-S-1 ATPase reactions. S-1-EDTA ATPase: 1 mM (γ-^{18}O)ATP, 10 μM S-1, 0.5 M KCl, 10 mM EDTA, 50 mM Tris-HCl at pH 7.8, 20°C for 5 min., S-1 Mg-ATPase: 1 mM (γ-^{18}O)ATP, 10 μM S-1, 50 mM KCl, 2 mM $MgCl_2$, 50 mM imidazole-HCl at pH 7.0, 20°C for 60 min., crosslinked acto-S-1 ATPase in 0 or 0.1 M KCl: 1 mM (γ-^{18}O)ATP, crosslinked acto-S-1(5 μM S-1), 0 or 0.1 M KCl, 2 mM $MgCl_2$, 50 mM imidazole-HCl at pH 7.0, 20°C for 1 min.

Pi contained 3 ^{18}O atoms. The amount of Pi with 0, 1, 2, and 3 ^{18}O atoms were 16.8, 3.4, 8.2 and 72.0 %, respectively. The same distribution pattern of Pi was obtained when Pi was produced by S-1 Ca-ATPase. The exchange ratio in the crosslinked acto-S-1 ATPase reaction was calculated using the distribution of Pi produced by the EDTA-ATPase reaction. In the S-1 Mg-ATPase reaction, most of ^{18}O atoms in (γ-^{18}O)ATP was subtracted with ^{16}O atoms (Fig. 6-b). The value of exchange ratio ($R = k_{-3}/k_4$) was estimated to be more than 20 (see Table I).

The extent of oxygen exchange in the crosslinked acto-S-1 ATPase reaction was much lower than that of S-1 ATPase reaction. When the ATPase reaction was carried out in the absence of KCl, the number of Pi with 3 ^{18}O atoms decreased from 72 to 59 %. The number of Pi with 0, 1, 2, and 3 ^{18}O atoms were 23.0, 3.8 and 15.4, and 59.0 %, respectively. The value of R was assumed to be 0.3. Distribution of Pi with 0, 1, 2 and 3 ^{18}O atom was calculated from the distribution of original (γ-^{18}O)ATP and R value (0.3) to be 17.2, 5.7, 18.6, and 58.5 %, respectively. When the ATPase reaction was carried out in 0.1 M KCl, the number of Pi with three ^{18}O atoms decreased from 72 to 51 %. The number of Pi with 0, 1 and 2 ^{18}O atoms were 12.5, 13.5 and 23.0 %, respectively. The value of R was assumed to be 0.52 (calculated distribution Pi with 0, 1, 2 and 3 atoms were 17.9, 8.2, 22.4, and 51,5 %, respectively).

Inoue et al. (9) showed that at low ionic strength and in the presence of high concentrations of F-actin, ATP is mainly hydrolyzed without accompanying the dissociation of actomyosin. Then, we analyzed the distribution of Pi hydrolyzed by acto-S-1

TABLE I. Oxygen exchange during crosslinked acto-S-1 ATPase reaction and non-crosslinked acto-S-1 ATPase at high F-actin concentrations. Experimental conditions were as described for Figs. 6 and 7. Values in parenthesis shows the distribution of Pi calculated from R values and original distribution of Pi as described in "EXPERIMENTAL").

		Pi with ^{18}O atoms			
ATPase	R	0	1	2	3
EDTA-ATPase	0	16.8	3.4	8.2	72.0
Mg-ATPase	20	82.0 (76.6)	5.8 (12.1)	4.3 (6.9)	7.9 (4.5)
crosslinked acto-S-1 (-KCl)	0.3	22.5 (17.2)	3.8 (5.7)	15.4 (18.6)	59.0 (58.5)
crosslinked acto-S-1 (0.1 M KCl)	0.52	12.5 (17.9)	13.5 (8.2)	23.0 (22.4)	51.0 (51.5)
non-crosslinked acto-S-1 (-KCl, high conc. FA)	0.65	26.2 (18.4)	7.2 (9.6)	18.5 (23.9)	48.2 (48.1)

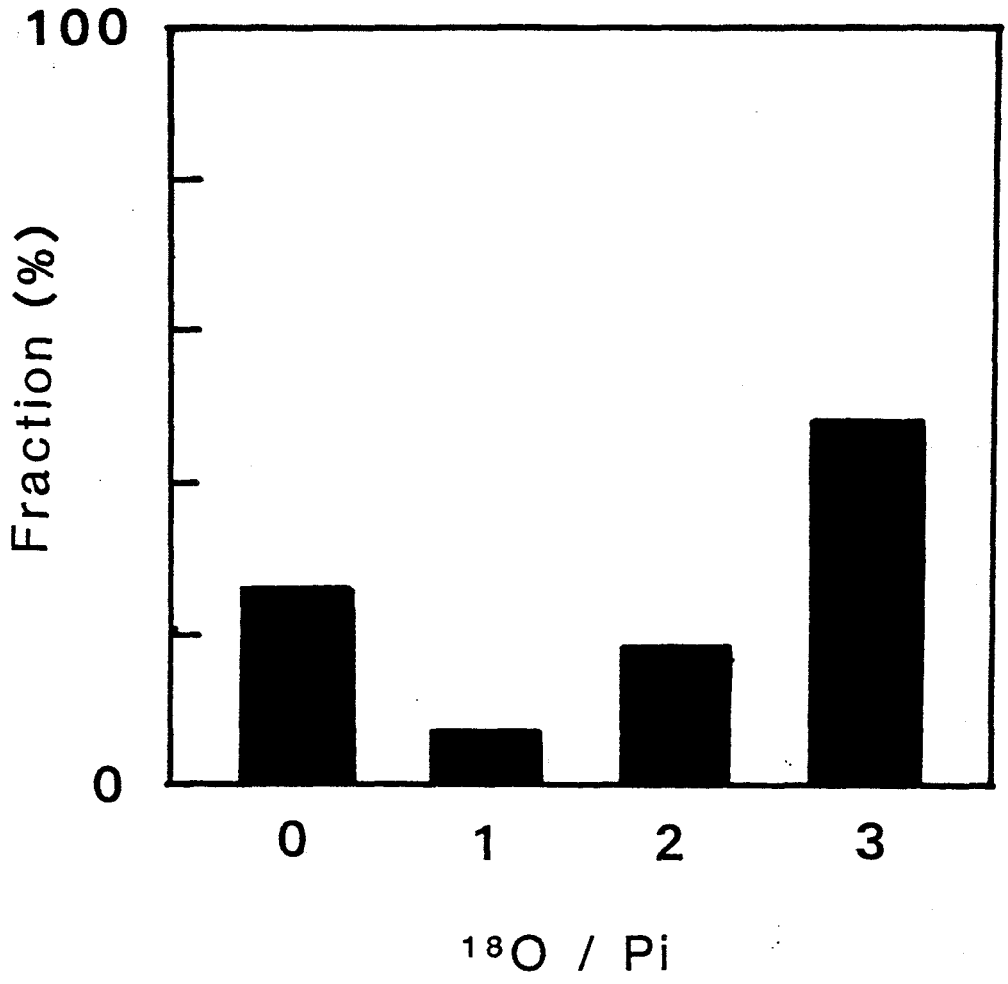

Fig. 7. Distribution pattern of (^{18}O)Pi species produced by non-crosslinked acto-S-1 ATPase at high concentrations of F-actin. 5.8 mg/ml F-actin, 5 μM S-1, 1 mM (γ-^{18}O)ATP, 2 mM $MgCl_2$, 10 mM Tris-HCl at pH 7.8 and 25 °C.

(5.8 mg/ml F-actin, 5 μM S-1) in 1 mM (γ-^{18}O)ATP, 2 mM $MgCl_2$, 10 mM Tris-HCl at pH 7.8 and 25 ℃. Amount of Pi with 0, 1, 2 and 3 ^{18}O atoms were found to be 26.2, 7.2, 18.5 and 48.2 %, respectively (Fig. 7). The exchange ratio was estimated to be 0.65 (at R = 0.65 calculated distribution of Pi with 0, 1, 2, and 3 ^{18}O were 18.4, 9.6, 23.9 and 48.1 %, respectively). This value of R was slightly higher than that of crosslinked acto-S-1 (0.3) under the same condition.

DISCUSSION

We analyzed the elementary steps of actomyosin ATPase reaction without accompanying dissociation of actomyosin. Inoue et al.(4) proposed that ATP is hydrolyzed by actomyosin via the following steps :

$$\begin{array}{l} \overset{k_1}{\rightleftharpoons}\ \overset{k_2}{\rightleftharpoons}\ \overset{k_2'}{\rightharpoonup}\ \overset{k_3}{\rightleftharpoons}\ \overset{k_4}{\longrightarrow} \\ AM + ATP \rightleftharpoons AMATP \rightleftharpoons AM_a^*ATP \rightharpoonup AM_b^*ATP \rightleftharpoons AM_P^{ADP} \longrightarrow AM + ADP + Pi \\ \qquad\qquad\qquad\qquad\qquad\qquad\qquad\qquad\qquad\qquad\qquad\qquad\qquad\qquad\quad \text{(inner cycle)} \qquad \downarrow\uparrow \\ \qquad\qquad\qquad\qquad\qquad\qquad\qquad\qquad\qquad\qquad\qquad\qquad\qquad\qquad\quad (AM_P^{ADP}) \\ \qquad\qquad\qquad\qquad\qquad\qquad\qquad\qquad\qquad\qquad\qquad\qquad\qquad\qquad\quad \downarrow\uparrow \\ A + M_a^*ATP \rightleftharpoons A + M_b^*ATP \rightleftharpoons A + M_P^{ADP}(R) \rightleftharpoons A + M_P^{ADP}(N) \\ \qquad\qquad\qquad\qquad\qquad\qquad\qquad\qquad\qquad\qquad\qquad\qquad\qquad\qquad\quad \text{(outer cycle)} \end{array}$$

AT high concentration of F-actin and low ionic strength, ATP is hydrolyzed mainly via upper route (inner cycle) (9). It was considered that muscle contraction is coupled with this reaction (4,12). However, it is difficult to study the elementary steps of the ATPase reaction under physiological ionic strength, since S-1 is easily dissociated from F-actin in the presence of ATP. Then, in this paper we studied using chemically crosslinked

acto-S-1. It was shown that crosslinked acto-S-1 has the same ATPase activity as the acto-S-1 ATPase reaction at high F-actin concentrations (14,17).

The ATPase activity of crosslinked acto-S-1 is dependent on the F-actin/S-1 ratio. AT low ratio of F-actin to S-1 the rate of ATPase reaction is low (Fig. 1). The rate of ATPase activity increased to nearly maximal value of 13 s^{-1} when the ratio of actin monomer was more than 5 times that of S-1. Then, in this paper we used crosslinked acto-S-1 in which molar ratio of actin/S-1 is more than 5. When the ratio of F-actin was low the amount of Pi measured after ATP chase was not changed, but the Pi-burst size was slightly decreased (data not shown). The result of oxygen exchange was unaffected by F-actin/S-1 ratio.

Km and Vmax of crosslinked acto-S-1 ATPase reaction was determined to be 12 μM and 13 s^{-1}, respectively. The value of Vmax was more than 200 times higher than that of S-1 alone (0.06 s^{-1}). It was shown that the Km value of myosin ATPase reaction *via* M_P^{ADP} was in the order of 0.04 μM (37). Thus, Km value of crosslinked acto-S-1 was 300 times higher than that of myosin alone. therefore in the actomyosin ATPase reaction only the decomposition of the reaction intermediate is greatly accelerated by F-actin.

ATP chase reaction revealed that the amount of tightly bound ATP of crosslinked acto-S-1 was 0.5 mol/mol S-1. This value was same as that of Pi-burst size of S-1 alone. Therefore, S-1 in crosslinked acto-S-1 is not denatured by the crosslinking reaction. On the other hand, the Pi-burst size decreased from 0.5 to 0.16 or 0.10 mol/mol·S-1, respectively, in 0 or 0.1 M

KCl. This result agrees well with those of Inoue et al.(9) and Rosenfeld and Taylor (15) that Pi burst size of S-1 was reduced by the presence of high concentrations of F-actin. Using crosslinked acto-S-1 Biosca et al. (14) reported the same result.

It is well understood Pi burst size means the size of AM_P^{ADP}. The burst size was obtained to be 0.1 mol/mol·S-1. k_4 can be calculated as V_{max}/AM_P^{ADP} to be 130 s^{-1} which is about 2000 times higher than the rate of k_4 of S-1 ATPase (0.05-0.06 s^{-1}).

From the result on the ^{18}O exchange reaction, the value of R ($=k_{-3}/k_4$) of the cross-linked acto-S-1 ATPase reaction was calculated to be 0.3 and 0.52 at 0 and 0.1 M KCl, respectively. Table I). The value of R in non-crosslinked acto-S-1 (0.65) in the absence of KCl was slightly higher than that of crosslinked acto-S-1. The $n^{18}O/Pi$ species which are calculated were slightly different from those observed. This is not due to the contamination of S-1, since the amount of free S-1 was less than 5% of total S-1 and the ATPase activity of non-crosslinked acto-S-1 was much less than that of crosslinked acto-S-1. We considered that the cause of difference is due to the uniformity in the state of S-1 crosslinked with F-actin. For example, the rate of ATPase reaction depends on the ratio of F-actin to S-1 (Fig. 1). Arata (11) suggested that ATPase reaction rate of crosslinked acto-S-1 was dependent on the condition of crosslinking reaction.

In this paper we denote the tightly bound ATP as one species. Tightly bound ATP can be detected by the following methods, 1) ATP chase reaction, 2) dissociation of acto-S-1, 3) H^+liberation or the change of fluorescence and UV absorption and 4) the

intermediate which is equilibrium with M_P^{ADP}. It is not evident whether these phenomena are caused by the same intermediate. However, we can not detect the rate of transition between probable intermediates. In this paper, we deal all the tightly bound ATP complexes as species, and it should be noted that the conclusion was unaffected by this assumption.

From the value of R (k_{-3}/k_4 = 0.52) estimated by ^{18}O exchange reaction and that of k_4 (130 s^{-1}) k_{-3} was calculated to be 68 s^{-1}. The value of k_3 can be solved from V_{max}, amount of AM^*ATP, amount of AM_P^{ADP} and k_{-3}, using the equation that V_{max} = , $(AM^*ATP)k_3 - (AM_P^{ADP})k_{-3}$. The value of k_3 was found to be 49.5 s^{-1} at 0.1 M KCl for crosslinked acto-S-1. Therefore, the equilibrium constant of step 3 was calculated as 49.5/68 to be about 0.7. This value is about 1/14 that of S-1 ATPase reaction (9).

The amount of AM^*ATP plus AM_P^{ADP} measured by quenching the ATPase reaction with cold ATP was almost the same as Pi burst size, so the amount of loosely bound ATP, AMATP, is considered to be small. Since k_2(AMATP) is higher than Vmax, the value of k_2 is considered to be extremely large. On the other hand, the value of k_{-2} is expected to be smaller than k_3, since the amount of AM^*ATP can be detected by cold ATP chase (Figs. 3 and 4). Sleep et al.(40) showed the formation of ATP from AM_P^{ADP} by adding F-actin and they suggested that k_{-2} is accelerated by F-actin. Therefore, k_{-2} is considered to be around 5 s^{-1}

The rate constant of the formation of tightly bound ATP at various concentrations of ATP can be expected from Km and Vmax of overall actomyosin ATPase reaction. If the backward reaction from tightly bound ATP to loosely bound ATP is slow, the second

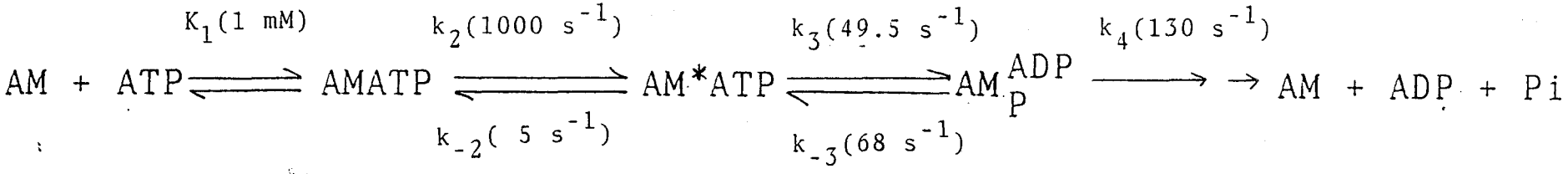

Fig. 8. The rate of elementary steps of acto-S-1 ATPase reaction without accompanying the dissociation of acto-S-1. See text for detail.

order rate constant for formation of tightly bound ATP, K_1k_2, can be calculated as V_{max}/Km to be 2. x 10^6 (active site 0.5 mol/mol·S-1). Therefore, if k_2 = 1000 s^{-1} (4), K_1 was assumed to be 0.5 mM. These values are the same order of magnitude as that of S-1 ATPase (4). Onishi et al. (41) showed that at high concentration of KCl, the rate of Pi burst for S-1 does not depend on F-actin concentration and that at low concentration of ATP the rate of dissociation of acto-S-1 is similar to the rate of Pi burst. Therefore, the formation for M^*ATP does not depend on F-actin concentration. The result presented here agrees with this result.

We consider that crosslinking of acto-S-1 does not affect the properties of the acto-S-1 ATPase reaction. In the absence of KCl, at 20 °C and at high concentration of F-actin, ATP is hydrolyzed without accompanying the dissociation of acto-S-1. Under these conditions Vmax, R and Pi-burst size were estimated to be 15 s^{-1} (data not shown), 0.65 (Fig. 7) and 0.1 mol/mol·S-1 (9). Then, the values of k_3, k_{-3}, and k_4 were calculated to be 61.8 s^{-1}, 97.5 s^{-1}, and 150 s^{-1}, respectively. These values are similar to those of crosslinked acto-S-1 in 0.1 M KCl. The rate of crosslinked acto-S-1 ATPase reaction depend on the concentration of KCl (see "RESULTS"). By decreasing KCl concentration from 0.1 to 0 M, Vmax, R, and Pi-burst size became 11 s^{-1}, 0.3, 0.16 mol/mol·S-1, respectively. Then the values of k_3, k_{-3}, and k_4 were found to be 42, 21, and 70 s^{-1}, respectively. Thus, at very low ionic strength the rate constants of these steps are suppressed slightly.

Figure 8 summarized the rate constants of actomyosin ATPase

reaction. For S-1 ATPase reaction it was reported that K_1 = 0.5 mM, k_2 = 1000 s^{-1}, k_{-2} = 0.05 s^{-1}, k_3 = 100 s^{-1}, k_{-3} = 10 s^{-1}, and k_4 = 0.05 s^{-1}. The large difference between S-1 and acto-S-1 ATPase reaction is that k_4 of acto-S-1 ATPase reaction is 2000 times higher than that of S-1 ATPase and that S-1 ATPase reaction is limited by the decomposition of AM_P^{ADP}, while acto-S-1 ATPase reaction is limited by the formation of AM_P^{ADP}.

REFERENCES

1. Tonomura, Y. (1972) Muscle Protein, Muscle Contraction and Cation Transport, Univ. Tokyo Press and Univ. Park Press, Tokyo and Baltimore
2. Taylor, E.W. (1979) CRC Crit. Rev. Biochem. 10, 102-164
3. Eisenberg, E. & Green, E. (1980) Ann. Rev. Physiol. 42, 293-309
4. Inoue, A., Takenaka, H., Arata, T. & Tonomura, Y. (1979) Adv. Biophys. 13, 1-194
5. Imamura, K., Kanazawa, T., Tada, M., & Tonomura, Y. (1965) J. Biochem. 57, 627-636
6. Lymn, R.W. & Taylor, E.W. (1971) Biochemistry 10, 4617-4624
7. Inoue, A., Shibata-Sekiya, K., & Tonomura, Y. (1972) J. Biochem. 71, 115-124
8. Inoue, A., Shigekawa, M., & Tonomura, Y. (1973) J. Biochem. 74, 923-934
9. Inoue, A. Ikebe, M. & Tonomura, Y. (1980) J. Biochem. 88, 1663-1677
10. Chock, S.P., Chock, P.B., & Eisenberg, E. (1976) Biochemistry 15, 3244-3253
11. Arata, T. (1984) J. Biochem. 96, 337-347
12. Arata, T. (1986) J. Mol. Biol. 191, 107-116
13. Trayer, H.R. & Trayer, I.P. (1983) Eur. J. Biochem. 135, 47-59
14. Biosca, J.A., Travers, F., Barman, T.E., Bertrand, R., Audemand, E., & Kassab, R. (1985) Biochemistry 24, 3813-3820
15. Rosenfeld, S.S.& Taylor, E.W. (1984) J. Biol. Chem. 259,

11908-11919

16. Stein, L.A., Chock, P.B., & Eisenberg, E. (1984) Biochemistry 23, 1555-1563
17. Mornet, D., Bertland, R., Pantel, P., Audemard, E., & Kassab, R. (1981) Nature 292, 301-306
18. Yount, R.C., & Koshland Jr., D.E. (1963) J. Biol. Chem. 238,1708-1713.
19. Sartoreli, L., From, H.J., Benson, R.W. & Boyer, P.D. (1966) Biochemistry 5, 2877-2884
20. Bagshaw, C.R., Trentham, D.R., Wolcott, R.G., & Boyer, P.D. (1975) Proc. Natl, Acad. Sci. USA 72, 2592-2596.
21. Perry, S.V. (1955) Methods in Enzymology (Colowick, S.T. & Kaplan, N.O., eds.) Vol.2, pp.582-588, Academic Press, New York
22. Weeds, A.G. & Taylor, R.S. (1975) Nature 257, 229-231
23. Spudich, J.A. & Watt, S (1971) J. Biol. Chem. 246, 4866-4871
24. Tietz, A. & Ochoa, S. (1962) in Methods in Enzymology Colowick,S.P. and Kaplan,N.O.,eds.) Vol.5, pp.365-369, Academic Press, New York
25. Martin, J.B. & Doty, D.M. (1949) Anal. Chem. 21, 964-967
26. Glynn, I.M. & Chappel, J.B. (1964) Biochem. J. 90, 147-149
27. Reynard, A.M., Hass, L.E., jacobsen, D.D., & Boyer, P.D. (1961) J. Biol. Chem. 236, 2277-2288
28. Nakamura, H. & Tonomura, Y. (1968) J. Biochem. 63, 279-294
29. Hackney, D.D., Stempel, E.E., & Boyer, P.D.(1980) Methods in Enzymology (Purich, D.L., ed.) part B. pp.60-83 Academic Presss, New York.
30. Ikeuchi, Y., & Midelfort, C.F. (1986) Biochemistry 25,

411-419

31. Statman, E.R. (1957) in Methods in Enzymology (Colowick, S.P. & Kaplan, N.D. eds.) Vol. 3, pp. 228-231

32. Werhrli, W.E., Verheyder, D.L.M., & Moffatt, J.G. (1965) J. Am. Chem. Soc. 87, 2265-2277

33. Randerath, K. $ Randerrath, E. (1967) in Methods in Enzymology (Grossman, L. & Moldave, K. eds.) Vol. 12, pp. 323-347

34. Hackney, D.D., & Boyer, P.D. (1978) Proc. Natl. Acad. Sci U.S.A.

35. Levy, H.M., Sharon, N., Lindman, E., & Koshland, D.E.Jr. (1960) J. Biol. Chem. 235, 2628-2632

36. Midelfort, C.F. (1981) Proc. Natl. Acad. Sci. USA 78, 2067-2071.

37. Inoue, A., Shibata-Sekiya, K., and Tonomura, Y. (1972) J. Biochem. 71, 115-124

38. Hibberd, M.G., Dantzig, J.A., Trentham, D.R., & Goldman, Y.E. (1985) Science 228, 1317-1319

39. Dantzig, J.A., & Goldman, Y.E. (1985) J. Gen. Physiol. 86, 305-327

40. Sleep, J.A. & Hutton, R.L. (1978) Biochemistry 17, 5423-5430

41. Onishi, H., Nakamura, Y., and Tonomura, Y. (1968) J. Biochem 64, 769-784

Part 3

Energy Level of the Elementary Steps of Actomyosin ATPase Reaction

SUMMARY

The thermodynamic parameters in the elementary steps of non-dissociating pathway of the acto-S-1 ATPase reaction were calculated based on those of the elementary steps in the myosin ATPase reaction (Arata et al. (1975) J. Biochem. 77, 895-900), and the binding of S-1 with F-actin in the absence of nucleotide (Yasui et al. (1985) J. Biochem. 96, 1673-1680). The binding of S-1 with F-actin in the presence of AMPPNP and ADP at 0.1 M KCl and pH 7.8 was measured as a function of temperature, by using a centrifugal and a light scattering techniques. The dissociation constant, K_d (M), ΔG° (Kcal/mol), ΔH° (Kcal/mol), and ΔS° (cal/deg·mol) of the binding of S-1-AMPPNP and S-1-ADP with F-actin were: $K_d = 2.0 \times 10^{-5}$, $\Delta G^\circ = -6.3$, $\Delta H^\circ = +1.4$, $\Delta S^\circ = +27$. and $K_d = 1.2 \times 10^{-6}$, $\Delta G^\circ = -7.9$, $\Delta H^\circ = +11.1$, $\Delta S^\circ = +65$, respectively. Thus, the binding reactions are endothermic and entropy driven. The equilibrium constant of the step from Actomyosin-ATP complex, AM^*ATP to actomyosin-P-ADP complex, AM_P^{ADP}, was calculated from the rate constant of forward and backward reaction. The values of ΔG°, ΔH°, and ΔS° of this step were calculated to be +0.2 Kcal/mol, +1.8 Kcal/mol, and +5 cal/deg·mol, respectively.

The results were adjusted to the following scheme:

$$AM \underset{(1)}{\rightleftharpoons} AMATP \text{ (or } AMAMPPNP) \underset{(2)}{\rightleftharpoons} AM_P^{ADP} \underset{(3)}{\rightleftharpoons} AMADP \underset{(4)}{\rightleftharpoons} AM$$

The thermodynamic properties of the steps (1), (2), (3), and (4) were: ΔG° (Kcal/mol), -7.1, +0.2, -4.7, +3.9; ΔH° (Kcal/mol), +15.1, +1.8, -26.8, +5.2; ΔS° (cal/deg·mol), +72, +5, -73, +5, respectively. The basic free energy change (Kcal/mol in the

elementary steps of acto-S-1 ATPase were calculated for the physiological concentrations of ATP, ADP, and Pi to be -4.1, +0.2, -8.7 and -1.5 Kcal/mol, respectively, for steps (1) to (4). Thus, most of the energy obtained by ATP hydrolysis was liberated at the step from AM^*ATP to AM_P^{ADP}, and this step is considered to be coupled with force development in muscle.

INTRODUCTION

Muscle contraction occurs as a result of cyclic interaction of myosin head (S-1) with F-actin. This reaction is driven by ATP hydrolysis. Numerous studies (1-4) using soluble S-1 and F-actin have reached the mechanism of actomyosin ATPase reaction shown schematically in Figure 1. The right-side pathway (steps 1-4) is the ATPase cycle of S-1 dissociated from F-actin. The left-side pathway (steps 1'-4') is the direct ATP hydrolysis catalyzed by S-1 bound with F-actin. Step 3 in the right side pathway is extremely slow, so M_P^{ADP} with F-actin before it is converted into MADP and return to the original state. The rate of decomposition of AM_P^{ADP} into AMADP (step 3') is much faster than the rate of dissociation of AM_P^{ADP} into A + M_P^{ADP}. Thus, ATP is hydrolyzed via two pathways one via left side pathway of Fig.1 and the other *via* A + M^*ATP and A + M_P^{ADP} (2). It was also suggested that force generation is coupled with some step(s) of the direct hydrolysis pathway (2, 5, 6).

Since the basic free energy change refers to the free energy difference between the states of a single acto-S-1 molecule which undergoes transition stochastically, it provides a fundamental basis for determining the driving step in the direct hydrolysis pathway (7, 8). Arata *et al.* (9) have estimated the standard free energy changes for elementary steps 1-4 in myosin ATPase reaction. The standard free energy change for the binding of S-1 with F-actin in the absence of ATP (equilibrium a) was calculated by Yasui et al. (10). In this study, the standard free energy changes for the binding of S-1-AMPPNP and S-1-ADP with F-actin

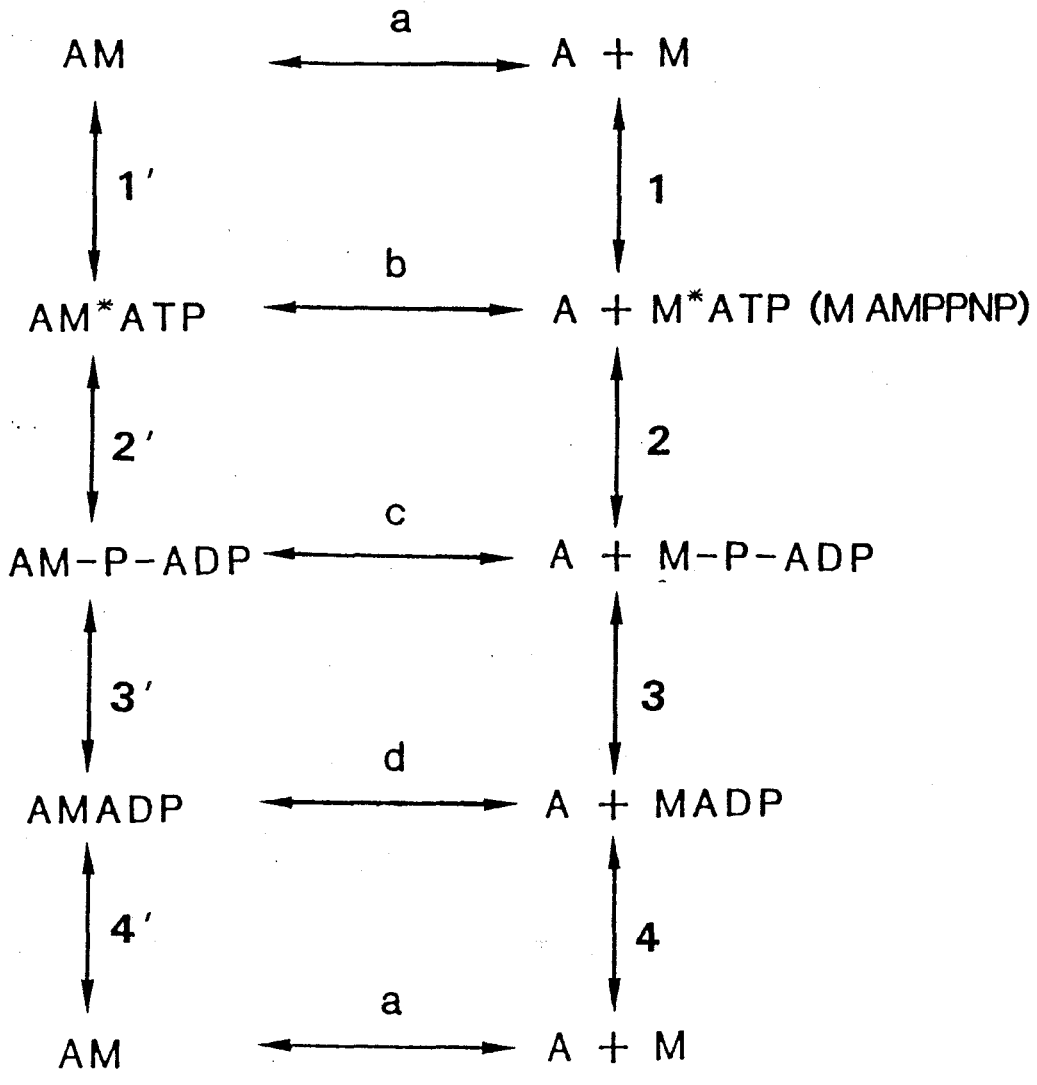

Figure 1. Schematic diagram for the mechanism of actomyosin ATPase reaction. See text for details.

(equilibrium b and d) were estimated from the dissociation constants for these binding reactions. The standard free energy changes for elementary steps 1'-4' were determined from those for the steps 1 and 4 and those for the equilibria a, b and d. The standard free energy change for step 2' was calculated from the rate constant of the forward and backward reaction of this step. The standard free energy change of the step 3' was calculated from the standard free energy change of ATP hydrolysis and those of the steps 1',2' and 4'. The basic free energy changes were finally calculated for physiological concentrations of ATP, ADP, and Pi. It is concluded that more than 60 % of the energy of ATP hydrolysis is available in the transition from AM_P^{ADP} to AMADP.

EXPERIMENTAL PROCEDURE

Materials—Myosin was prepared from rabbit white skeletal muscle by the method of Perry (11). S-1 was prepared by chymotryptic digestion of myosin, as described by Weeds and Taylor (12). G-actin was prepared from an acetone powder of rabbit white skeletal muscle by the method of Spudich and Watt (13). The concentration of free ATP in G-actin solution was reduced to 2 μM by dialysis against 2 mM Tris-HCl at pH 7.8. Therefore, the molar concentration of nucleotide in the reaction mixture was less than 1/60 that of S-1. G-actin was polymerized into F-actin by adding KCl with buffer. Pyruvate kinase was prepared from rabbit skeletal muscle as described by Tiez and Ochoa (14). Acetate kinase and myokinase were purchased from

Boehringer Mannheim, GMBH. The proteins were analyzed by SDS gel electrophoresis (15). Protein concentrations were determined by means of the Biuret reaction calibrated by nitrogen determination. The molecular weight of S-1 and actin monomer were adopted to be 1.2×10^5 and 4.2×10^4, respectively (16).

Reagents—EDC (1-ethyl-3-(3-dimethyl aminopropyl) carbodiimide) was purchased from Nakarai Chemical Co. Ltd, Kyoto. ATP and ADP were purchased from Kohjin Co. Ltd, Tokyo. AMP was purchased from Yamasa Co. Ltd. PEP was purchased from Sigma Co. ($^{18}O)H_2O$ (98 atom % of ^{18}O) was purchased from Amersham International plc. or CEA oris. (γ-^{32}P)ATP was synthesized enzymatically by the method of Glynn and Chappel (17). All other reagents were of analytical grade.

Binding of S-1 to F-actin —— The extent of binding of S-1 with F-actin was measured by the following two methods. (1) The extent of binding of S-1 with F-actin in the presence of ATP was measured from the change in the light scattering intensity at 360 nm by a stopped flow apparatus, using a Hitachi-Perkin Elmer MPF-2A fluorescent spectrophotometer with a Visigraph recorder (San-ei, FR-301) (3). (2) The extent of binding of S-1 with F-actin in the presence of AMPPNP or ADP by a ultracentrifugal separation (14). The reaction mixture (0.2 ml) was centrifuged at 1.3×10^5 g for 30 min. The concentration of S-1 in the supernatant was estimated by means of Bradford assay (19).

Crosslinking of acto-S-1—Acto-S-1 was crosslinked as described by Mornet et al. (20) and Arata (21) with slight modifications (Yasui et al. part 2 of this thesis). Amount of non-crosslinked S-1 in the preparation was determined by

SDS/polyacrylamide gel electrophoresis to be less than 5 % of total S-1.

ATPase activity—The rate of acto-S-1 ATPase reaction in the steady state was measured by coupling ATPase reaction with pyruvate kinase system. The reaction mixture contained 0.5 mg/ml pyruvate kinase, 0.1 mM ATP, 2 mM PEP, 0.1 M KCl, 2 mM $MgCl_2$, and 10 mM Imidazole at pH 7.0 and 0-20 °C. The amount of pyruvate liberated was determined as described by Reynard et al. (22). The initial phase of ATP hydrolysis was measured from ^{32}Pi liberation from (γ-^{32}P)ATP by employing Durrum rapid-flow apparatus. The reaction was started by mixing crosslinked acto-S-1 (5 μM S-1) with 100 uM (γ-^{32}P)ATP in 0.1 M KCl, 2 mM $MgCl_2$, and 10 mM Imidazole at pH 7.0 and 0-20 °C, and the reaction was terminated with 0.1 N HCl containing 0.1 mM Pi as a carrier. After adding 1 ml of 10 % TCA the denatured proteins were removed by centrifugation at 1 x 10^3 g for 10 min. The amount of ^{32}Pi liberated was measured as described previously (23).

Oxygen Exchange—(γ-^{18}O)ATP was synthesized based on the methods of Hackney et al. (24) and Ikeuchi and Miderfort (25) with slight modifications (Yasui et al. part 2 of this thesis). The ATPase reaction was carried out using (^{18}O)ATP as substrate, and the distribution of Pi with 3, 2, 1, and 0 ^{18}O atoms were analyzed as described in part 2. The amount of ^{18}O in the γ-position of ATP was determined from the distribution of Pi which is produced by the myosin EDTA ATPase reaction (26). The distribution of Pi produced by ATPase reaction was calculated from the given value of R (= k_{-3}/k_4) and the distribution of Pi produced by the EDTA-ATPase reaction, as described by Miderfort

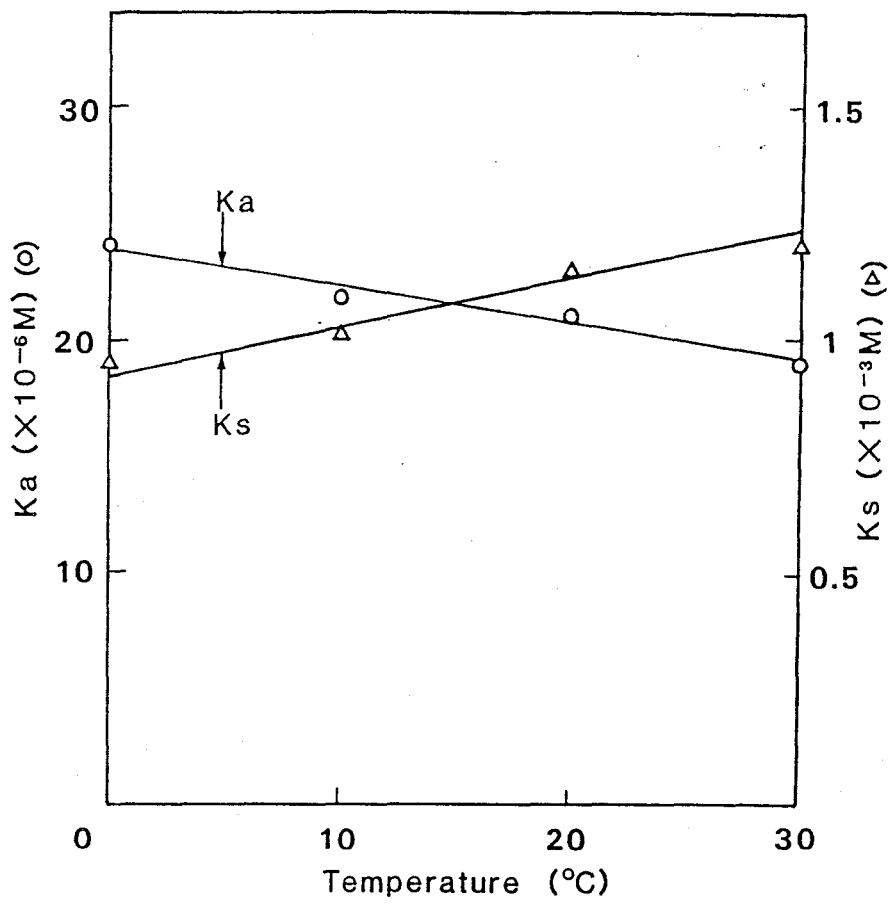

Figure 2. Dependence on temperature of the dissociation constants for the interaction of F-actin, S-1, and AMPPNP. 1.5 mg/ml S-1, 0-4 mg/ml F-actin, 0-1 mM AMPPNP, 0.1 M KCl, 4 mM $MgCl_2$, and 20 mM Tris-HCl at pH 7.8. The dissociation constant of F-actin to S-1-AMPPNP complex (Ka,○) and the dissociation constant of AMPPNP from acto-S-1 (Ks,△) were obtained by measuring the extent, α, of dissociation of S-1 from F-actin as a function of free concentration of F-actin and AMPPNP; $\alpha^{-1} = 1 + (1 + Ks(AMPPNP)^{-1})(F\text{-actin})Ka^{-1}$. The value of determined by centrifugal separation method. See text for details.

(36) and in part 2 of this thesis.

Calculation of ΔG°, $\Delta G'$, ΔH°, and ΔS° ——The value of standard free energy change, ΔG°, was calculated from the equilibrium constant of the step. The enthalpy change, ΔH°, and entropy change, ΔS° were calculated from the dependence of ΔG° on the temperature. The basic free energy change, $\Delta G'$ was calculated from ΔG° and actual concentration of ligand (ATP, ADP, or Pi) according to the following equations (8); $M + L \rightleftarrows ML$ (or $AM + \rightleftarrows AML$), $\Delta G' = \Delta G^\circ - RT\ln(L)$ and $ML \rightleftarrows ML'$ (or $AML - AML'$), $\Delta G' = \Delta G^\circ$, where M, A, and L (L') show S-1, F-actin, and ligand, respectively.

RESULTS

Binding of S-1 with F-actin in the Presence of AMPPNP —— The extent of dissociation of S-1 from acto-S-1, α, was measured in 1.5 mg/ml S-1, various concentrations of AMPPNP (0.2-2 mM), and F-actin (1-4 mg/ml), 4 mM $MgCl_2$, 20 mM Tris-HCl at pH 7.8. After incubation for 1 h, the reaction mixtures were centrifuged at 1.3 x 10^5 g for 30 min. The concentration of free S-1 in the supernatant (f) was measured and then the concentration of bound S-1 (b) was calculated as c-f where c is total concentration of S-1 added. The concentration of free F-actin (A) was calculated as d-b, where d is total concentration of F-actin. α (= f/c) was found to be given by $\alpha^{-1} = 1 + (1 + Ks(AMPPNP)^{-1})(A)Ka^{-1}$, where Ks and Ka were dissociation constants of the following steps;

$$\text{acto-S-1} + \text{AMPPNP} \overset{Ks}{\longleftrightarrow} \text{acto-S-1-AMPPNP} \overset{Ka}{\longleftrightarrow} \text{actin} + \text{S-1-AMPPNP}$$

(18). A linear relationship was observed in (α^{-1} - 1) vs. (A) plot and Ka' was determined from the slope of this plot; $\alpha^{-1} = 1 + (A)Ka^{-1}$. A linear plot of Ka'^{-1} vs. $(AMPPNP)^{-1}$ provided Ks and Ka; $Ka'^{-1} = Ka'^{-1}(1 + Ks(AMPPNP)^{-1})$. The Ka and Ks value of the acto-S-1-AMPPNP system were found to be 2.0×10^{-5} and 1.1×10^{-3} M, respectively. Figure 2 shows the temperature dependence of Ka and Ks. On raising temperature from 0 to 30 °C, the value of Ka decreased 2.4 to 1.9×10^{-5} M whereas the value of Ks increased from 0.95 to 1.2×10^{-3} M. the thermodynamic parameters of the binding of F-actin with S-1-AMPPNP were obtained from the plot of ΔG° (= RTlnKa) against absolute temperature (T) (cf. Fig. 5 in Part 1). The value of ΔG° at 20 °C, ΔH°, and ΔS° were also determined from Ks for the binding of AMPPNP with acto-S-1 complex to be -3.9 Kcal/mol, -1.3 Kcal/mol, and -9 cal/deg·mol, respectively.

Binding of S-1 with F-actin in the Presence of ATP —— The dissociation constant of acto-S-1 in the presence of ATP, was measured by a light-scattering method in 0.012 mg/ml S-1, 2, 4, and 6 mg/ml F-actin, 3 mM ATP, 4 mM $MgCl_2$, and 20 mM Tris-HCl at pH 7.8. The dissociation constants were obtained from the slope of (α^{-1} - 1) against free F-actin concentration,(A). As in the case of AMPPNP; $\alpha^{-1} = 1 + (A)/Kd$ (3). Figure 3 shows the dependence on temperature of the apparent dissociation constant, Kd, of acto-S-1 in the presence of ATP. On raising temperature from 10 to 30 °C.

Binding of S-1 with F-actin in the presence of ADP —— The

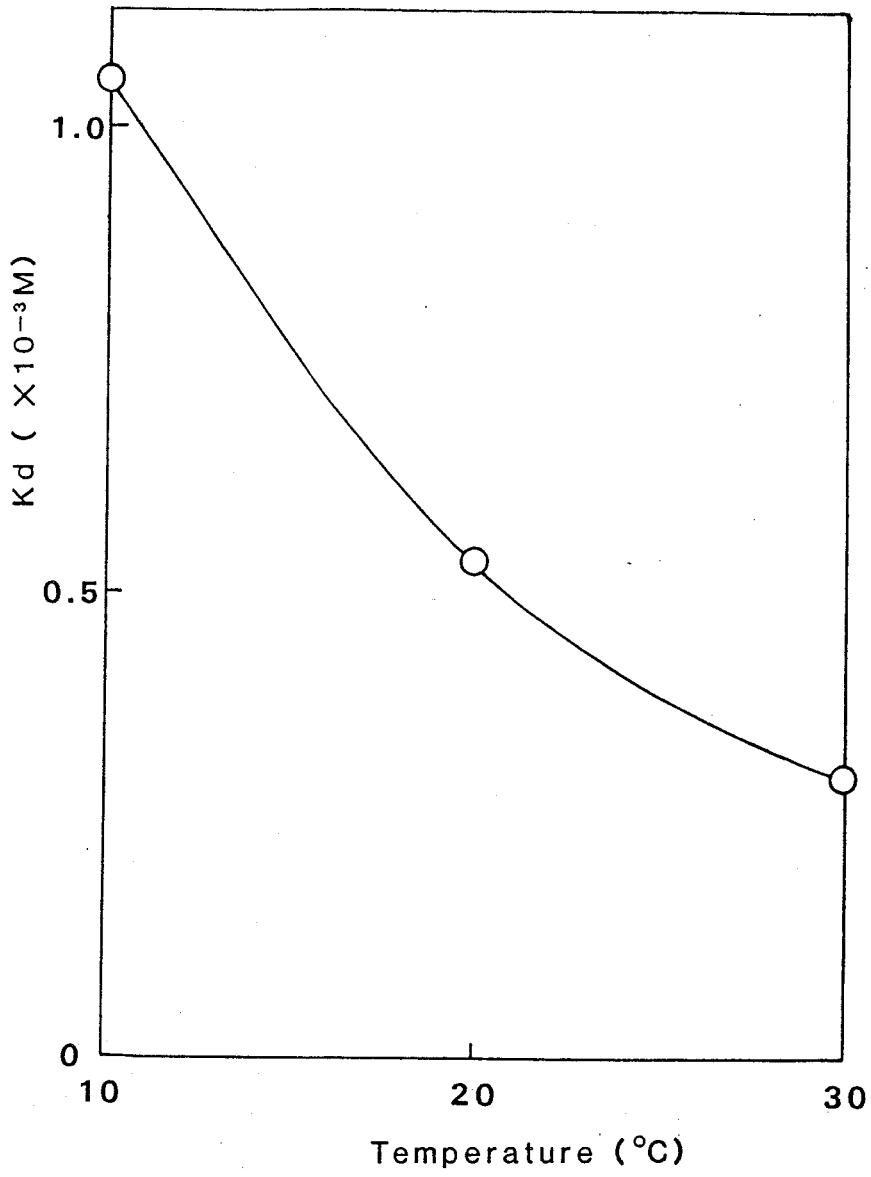

Figure 3. Dependence on temperature of the dissociation constants for the binding of S-1 with F-actin in the presence of ATP. 0.012 mg/ml S-1, 2-6 mg/ml F-actin, 3 mM ATP, 0.1 M KCl, 4 mM $MgCl_2$, and 20 mM Tris-HCl at pH 7.8. The extent of dissociation of S-1 from F-actin was determined as a function of free F-actin concentration by measuring the change in light scattering intensity. The dissociation constant (Kd) was obtained from the plot of $\alpha^{-1} - 1$ against free F-actin concentration; $\alpha^{-1} = 1 + Kd^{-1}$(F-actin). Other conditions were as described for Fig. 2.

Table I. Dissociation constants and thermodynamic parameters for elementary steps of the formation of acto-S-1-ADP complex.

	STEP 1	STEP 2	STEP 3	STEP 4
Kd (M)	3.3×10^{-9}	3.3×10^{-6}	1.2×10^{-6}	1.2×10^{-3}
ΔG° (Kcal/mol)	-11.3	-7.3	-7.9	-3.9
ΔH° (Kcal/mol)	+2.5	-13.8	+11.1	-5.2
ΔS° (cal/deg·mol)	+47	-23	+65	-5

0.5 μM S-1, 0-4 μM F-actin and 0.2-2 mM ADP. Thermodynamic properties of the following steps were measured:

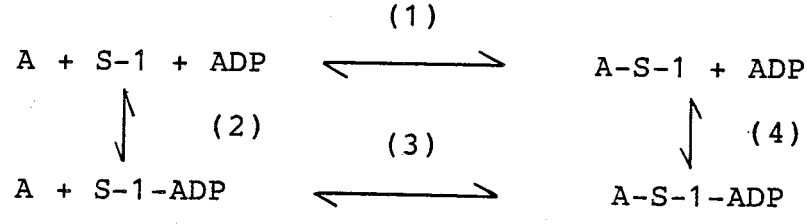

where A indicates F-actin. Kds for step 3 and 4 were determined by measuring the extent of dissociation as a function of ADP and F-actin concentration, as described for Fig. 2. Kd for step 1 was obtained in Part 1. Kd for step 2 was calculated from Kds for step 1, 3, and 4 (see the text for details). ΔG° (= RTlnKd) was calculated from the value of Kd and ΔH° and ΔS° were determined from the temperature dependence of ΔG°, as described for fig. 5 (Part 1).

binding of S-1 with F-actin in the presence of ADP was measured in 0.5 μM S-1 and 0, 1, 2, or 4 μM F-actin, 0.1 M KCl, 4 mM $MgCl_2$, and 20 mM Tris-HCl at pH 7.8. The mixture was centrifuged at 1.3×10^5 g for 30 min in the presence of various concentration of ADP. The values of Ka and Ks were determined as in the case of AMPPNP (see Fig. 2) and were found to be 1.2×10^{-6} M and 1.2×10^{-3} M at 20°C, respectively. It is likely that nucleotide (ADP) and F-actin bind with S-1 in accordance with the following mechanism (14, 16).

$$\begin{array}{ccc} & \overset{1}{\rightleftharpoons} & \\ A + M + ADP & & A\text{-}M + ADP \\ \Big\uparrow\Big\downarrow 2 & \overset{3}{\rightleftharpoons} & \Big\uparrow\Big\downarrow 4 \\ A + M\text{-}ADP & & A\text{-}M\text{-}ADP \end{array}$$

where A and M are F-actin and S-1, respectively. The dissociation constant (Kd) for steps 3 and 4 correspond to Ka (1.2×10^{-6} M) and Ks (1.2×10^{-3} M). Kd for step 1 corresponds to the dissociation constant of acto-S-1 in the absence of nucleotide and was obtained in Part 1 (3.3×10^{-9} M). Kd for step 2 (Kd(step 1) x Kd(step 4))/Kd(step 3) was calculated to be 3.4×10^{-6} M. These values for Kd were listed in the first row of Table I. The thermodynamic parameters were calculated from RTlnKd *vs.* T plot and listed in the rest of Table I. The values of ΔG°, ΔH°, and ΔS° for the binding of F-actin with S-1-ADP (step 3) were -7.9 Kcal/mol (at 20°C), +11.1 Kcal/mol, and +65 cal/deg·mol, respectively.

Initial Stage of Crosslinked Acto-S-1 ATPase Reaction——The rate constant of the elementary steps of actomyosin ATPase

TABLE II. Kinetic constants of the steps between actomyosin-ATP and actomyosin-P-ADP complexes. 0.1 M KCl, 2 mM $MgCl_2$, 10 mM Imidazole-HCl at pH 7.8, 0 or 20°C.

temp. (°C)	burst size (mol/mol)	R	v (ATPase) (s^{-1})	k_4 a) (s^{-1})	k_{-3} b) (s^{-1}) free site	k_3 c) (s^{-1})	K_3 d) (s^{-1})
20	0.1	0.52	13	130	68	49.5	0.73
0	0.09	0.65	0.5	5.5	3.6	2.1	0.58

a) k_4 = v/(burst size)

b) $k_{-3} = k_4 \times R$

c) k_3 = (v + k_{-3}(burst size))/((total site) - burst size)

d) $K_3 = k_3/k_{-3}$

reaction without accompanying the dissociation of actomyosin was measured using crosslinked acto-S-1. The rate of crosslinked acto-S-1 ATPase reaction was measured in crosslinked acto-S-1 (0.1 μM S-1) 0.5 mg/ml pyruvate kinase, 0.1 mM ATP, 2 mM ATP, 0.1 mM KCl, 2 mM $MgCl_2$, and 10 mM Imidazole-HCl at pH 7.0, 0 and 20 °C. The rate of acto-S-1 ATPase reaction was found to be 0.5 and 13 s^{-1}, respectively.

The time course of Pi-liberation was measured after mixing (γ-^{32}P)-labelled ATP (100 μM) with crosslinked acto-s-1 (5 μM S-1) in 0 or 0.1 M KCl, 2 mM $MgCl_2$, and 10 mM Imidazole at pH 7.0, 0 and 20 °C. The Pi burst size of crosslinked acto-S-1 was 0.09 and 0.1 mole/mole·S-1, respectively, at 0 and 20 °C. The amount of initial rapid Pi liberation after ATP quenching was found to be 0.5 mole/mole·S-1 (part 2 of this thesis).

Oxygen Exchange during Acto-S-1 ATPase——Oxygen exchange reaction in the crosslinked acto-S-1 ATPase was analyzed using (γ-^{18}O)ATP as substrate. Distribution of Oxygen in γ-P position of ATP was measured from the distribution of Pi produced by S-1 EDTA-ATPase reaction. As shown Table II, about 72 % of total Pi contained 3 ^{18}O atoms. The amount of Pi with 0, 1, 2, and 3 ^{18}O atoms were 16.8, 3.4, 8.2 and 72.0 %, respectively. The exchange ratio in the crosslinked acto-S-1 ATPase reaction was calculated using the distribution of Pi produced by the EDTA-ATPase reaction. When Pi was produced by the crosslinked acto-S-1 ATPase reaction at 20 °C, the number of Pi with three ^{18}O atoms decreased from 72 to 51 %. The number of Pi with 0, 1 and 2 ^{18}O atoms were 12.5, 13.5 and 23.0 %, respectively. The value of R was assumed to be 0.52. The calculated distribution Pi with 0, 1,

TABLE III. Distribution of ^{18}O-Pi produced by crosslinked acto-S-1 ATPase reaction at 0 and 20 °C.

Experiments	number of ^{18}O-atoms				R
	0	1	2	3	
Control[a]	16.8	3.4	8.2	72.0	
acto-S-1 (20 °C)	12.5 (11.7)	13.5 (8.2)	23.0 (22.4)	51.0 (51.5)	0.52
acto-S-1 (0 °C)	18.3 (18.0)	11.8 (9.5)	21.3 (24.0)	48.6 (48.5)	0.65

[a]Distribution pattern of Pi produced by EDTA-ATPase reaction. Values in parenthesis show the calculated values from R value and distribution of Pi produced by EDTA ATPase reaction.

2 and 3 atoms were 17.9, 8.2, 22.4, and 51,5 %, respectively. When the ATPase reaction was carried out at 0 °C, The number of Pi with 3 ^{18}O atoms was decreased to 48.6%. The number of Pi with 0, 1, 2, and 3 ^{18}O atoms were 18.3, 11.8, 21.3, and 48.6%, respectively. The value or R was estimated to be 0.65. The calculated distribution of Pi were 18.0, 9.5, 24.0, 48.5%, respectively.

DISCUSSION

The binding of S-1 with F-actin was measured in the presence of AMPPNP, ATP, and ADP in 0.1 M KCl at pH 7.8. Although it has been proposed that two heads of myosin are non-identical (2, 13), no heterogeneity was fortunately observed in the kinetical analysis under the condition used. Therefore, two species of S-1 appear to bind with F-actin similarly and all the results obtained here can be adequately explained by the simple scheme.

The binding of S-1 with F-actin in the presence of AMPPNP or ADP was assumed to fit the following scheme (18):

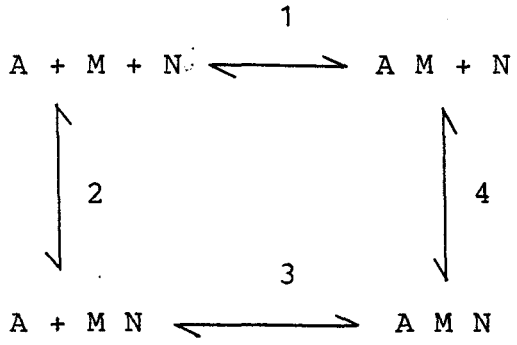

where A, M, and N mean F-actin, S-1, and nucleotide, respective-

ly. The validity of this scheme was examined by using independently measured values for ADP as nucleotide (Table I). The dissociation constant (Kd) for step 1 was determined to be 3.3×10^{-9} M (Part 1). Values of Kd for step 3 and 4 were found to be 1.2×10^{-6} and 1.2×10^{-3} M, respectively. The value for step 2, i.e., binding of S-1 with ADP was calculated as (Kd(step 2) = Kd(step 1) Kd(step 4)/Kd(step3)) to be 3.3×10^{-6} M which was close to be the value (5.32×10^{-6} M, $\Delta G^\circ = -7.1$ Kcal/mol in 0.5 M KCl at pH 7.8 and 20°C) reported by Arata et al. with HMM (26). Therefore, the scheme appears to be valid for ADP.

In the presence of ATP, S-1 exists as S-1-P-ADP complex, however, in the presence of F-actin acto-S-1 exists as acto-S-1*ATP complex (part 2 of this thesis), and there is no rapid equilibrium between acto-S-1-P-ADP and S-1-P-ADP complexes. The apparent dissociation comstant, 5.3×10^{-4} M at 20°C (Fig. 3) would be a complicated function of the decomposition rate constant of steps 3' and 3 (Fig. 1).

The value of ΔG° (Kcal/mol), ΔH° (Kcal/mol), and ΔS° (cal/deg·mol) were calculated from the temperature dependence of Kd for the binding of S-1-AMPPNP (b) and S-1-ADP (d) with F-actin. The values at 20 °C were as follows: (b) $\Delta G^\circ = -6.3$, $\Delta H^\circ = +1.4$, $\Delta S^\circ = +27$); (d) $\Delta G^\circ = -7.9$, $\Delta H^\circ = +11.1$, $\Delta S^\circ = +65$. Positive H and large negative ΔS° indicate that all the binding reactions are endothermic and are entropy driven. These characteristics are apparently similar to those for the binding of acto-S-1 complex in the absence of nucleotide, and may be explained by similar structural change as discussed previously (10, part 1).

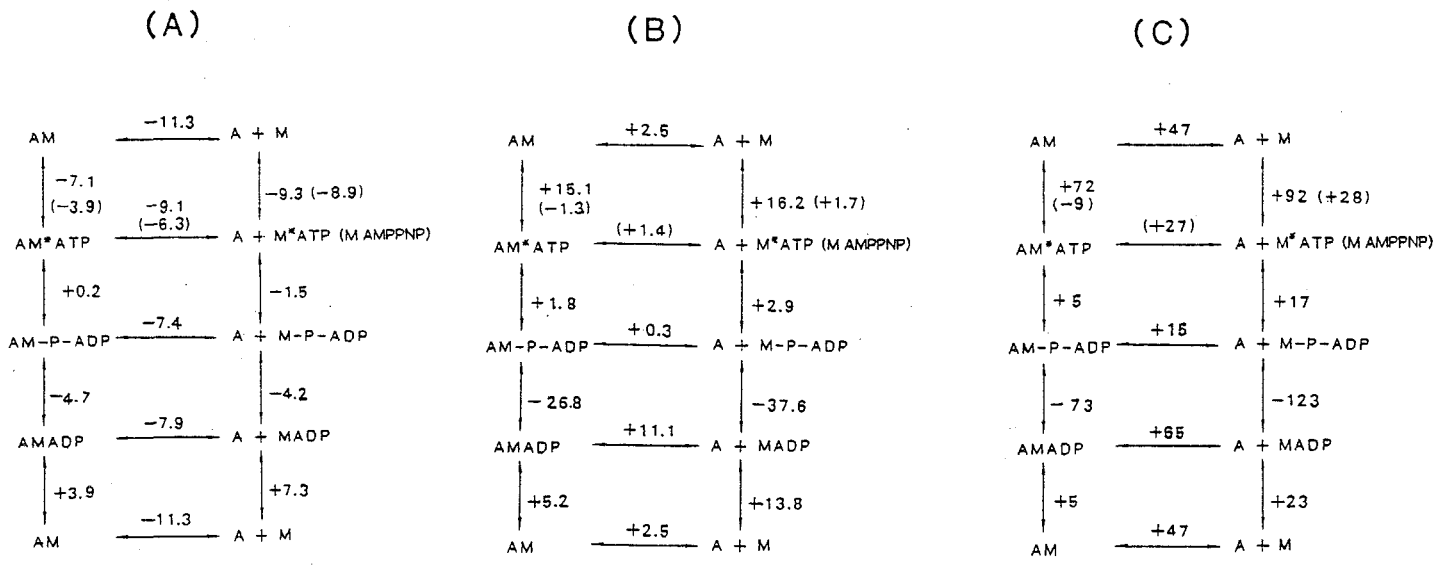

Figure 4. Changes in standard free energy (A), enthalpy (B), and entropy (C) for elementary steps of actomyosin ATPase reaction. ΔG°, ΔH°, and ΔS° are defined for the steps toward the left and downward, and are expressed as Kcal/mol, Kcal/mol, and cal/deg·mol, respectively. Thermodynamic parameters for the elementary steps in dissociating pathway (the right-hand) were taken from those of myosin ATPase reported in ref. 9. Based on the parameters for myosin ATPase reaction, the parameters for the elementary steps of nondissociating pathway (the left-hand) were calculated from those for the binding of F-actin to S-1 (Part 1), S-1-AMPPNP (Fig. 2) and S-1-ADP (Table I) and the equilibrium constant between AM^*ATP and AM_P^{ADP}. The numbers in parenthesis are the values obtained with AMPPNP. See the text for details.

The equilibrium constant of AM^*ATP and AM_P^{ADP} was estimated from the kinetic analysis of actomyosin ATPase (see part 2 for detail). The rate constant of the decomposition of AM_P^{ADP} into AM + ADP + Pi, k_4, is given as $Vmax/(AM_P^{ADP})$. The amount of AM_P^{ADP} can be estimated from the size of initial Pi-burst (3). The ratio of the rate constants, k_{-3} and k_4, can be estimated as $R = k_{-3}/k_4$. Furthermore, the net rate of step (3), $(AM^*ATP)k_3 - (AM_P^{ADP})k_{-3}$ is equal to Vmax the rate of k_3 can be calculated. Then, the equilibrium constant of the step (3), K_3 was calculated as k_{-3}/k_3 As summarized in Table II, the equilibrium constant was found to be 0.73 and 0.58, respectively at 20 and 0 °C. Therefore the value of ΔG°, ΔH°, and ΔS° were calculated to be +0.2 Kcal/mol, +1.8 Kcal/mol and +5 cal/deg·mol. K1, k_2 and k_{-2} were found to be 1 mM, 1000 s^{-1} and 5 s^{-1}, respectively (Part 2). Then the ΔG° of these two steps were calculated to be -4.0 and -3.1 Kcal/mol, respectively.

The values of ΔG°, ΔH°, and ΔS° for elementary steps in non-dissociating pathway (1'-4') of actomyosin ATPase reaction were calculated from those for the binding of S-1-nucleotide intermediate and F-actin (a, b, and d) (see Fig. 1) and the equilibrium constant of steps 1', 2' and 3'. Figure 4 summarized thermodynamic parameters ΔG°(A), ΔH°(B), and ΔS°(C) for elementary steps of actomyosin ATPase. ΔG° for $AM \rightleftharpoons A + M$ was taken as -11.3 Kcal/mol (Part 1) and ΔG° for AM-ADP $\rightleftharpoons$ A + M-ADP were taken as -7.9 Kcal/mol. ΔG°s for elementary steps of myosin ATPase reaction were taken from those obtained by Arata et al. (9). The values of ΔH° and ΔS° for the step from M + AMPPNP to MAMPPNP (+1.7 Kcal/mol and +28 cal/deg·mol) were different

from those estimated kinetically (+16.2 Kcal/mol and +92 cal/deg·mol). The value (-7.1 Kcal/mol) of ΔG° for step from AM to AM^*ATP obtained from K1, k_2 and k_{-2} was larger than that (-3.9 Kcal/mol) using AMPPNP (see Fig. 5). The ΔG° for formation of AM^*ATP was estimated from the equilibrium constant of AMATP formation, K1, and the values of k_2 and k_{-2} for the step AMATP to AM^*ATP. By analogy with ΔG°, the values for ΔH° and ΔS° were calculated and shown in B and C of Fig. 4. Profile for ΔH° shows no significant difference between nondissociating and dissociating pathway; formation of (A)M-P-ADP from (A)M was associated with large increase in enthalpy (about 20 Kcal/mol) whereas its decomposition into (A)M-ADP associated with large decrease in enthalpy (-35 Kcal/mol). Profile for ΔS° also show no significant difference between two pathways. However, formation of $(A)M_P^{ADP}$ from (A)M was associated with large increase in entropy ((-77) -109 cal/deg·mol). Therefore, it is suggested that conformation change in acto-S-1 complex may occur during ATP hydrolysis and AM_P^{ADP} complex may be a key intermediate for energy transduction.

The basic free energy changes, $\Delta G'$ for actomyosin ATPase reaction were finally calculated from ΔG° profile (Fig. 5) by the method described in "EXPERIMENTAL PROCEDURE". The concentrations of ATP, ADP and Pi were 5 mM 0.1 mM and 1 mM, respectively, as a rough approximation to the physiological concentration in muscle. In the absence of F-actin (right-side pathway), $\Delta G'$ for formation of M_P^{ADP} was 55% (-7.8 Kcal/mol) and the remaining 45% (-6.3 Kcal/mol) was for decomposition of M_P^{ADP} to M. In the presence of bound F-actin (left-side pathway) $\Delta G'$ for formation of AM_P^{ADP} was

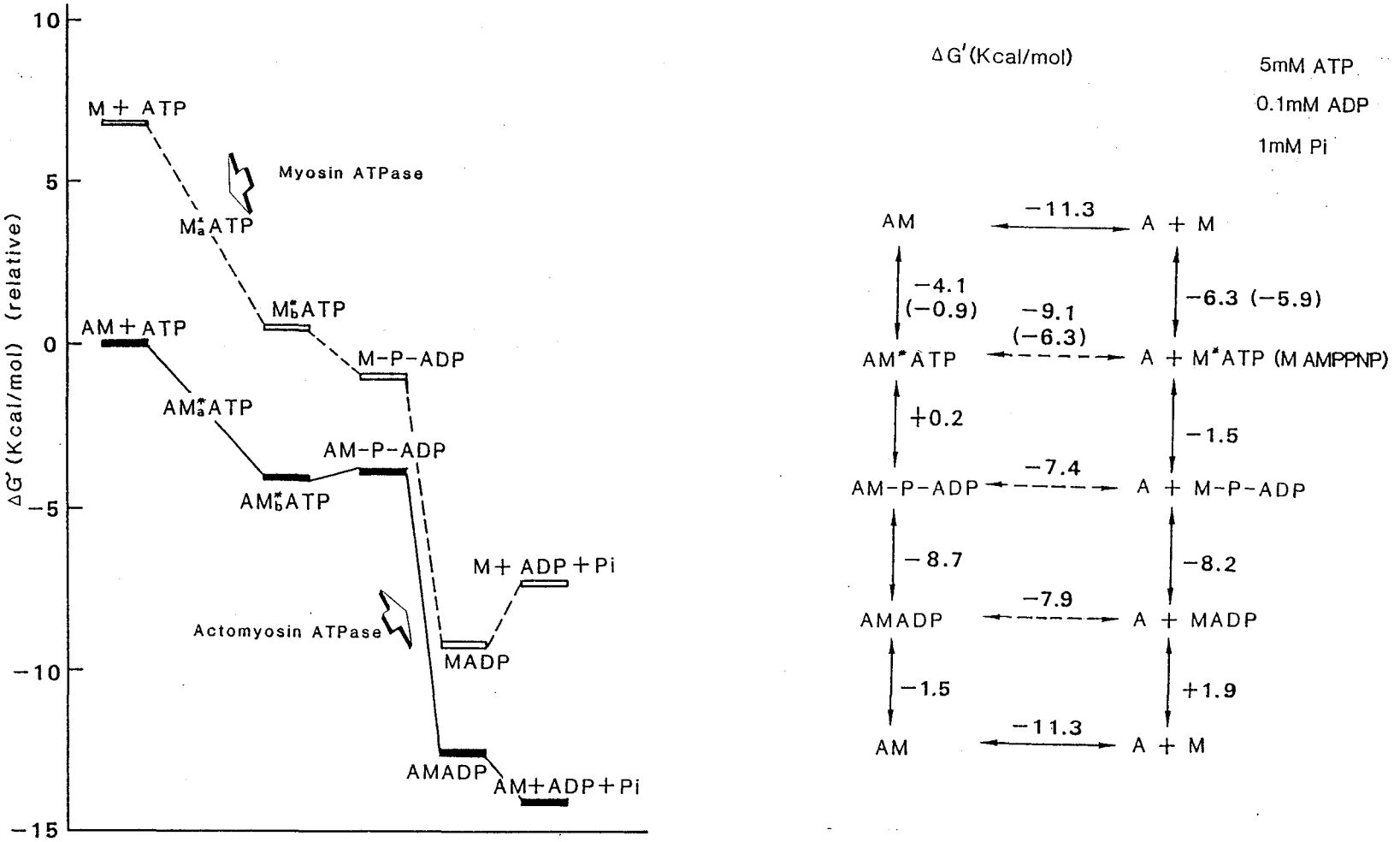

Figure 5. Basic free energy changes for elementary steps of actomyosin ATPase reaction. Basic free energy changes ($\Delta G'$) were calculated from the standard free energy changes (ΔG°) shown in fig 4.A. The concentrations of ATP, ADP, and Pi were taken as 5, 0.1, and 1 mM, respectively.

-3.9(-0.7) Kcal/mol, whereas -10.2 Kcal/mol was for decomposition of AM_P^{ADP} to AM. About 30 % of the energy of ATP hydrolysis was lost in the step from AM to AM_P^{ADP}, and thus AM_P^{ADP} state can assigned as "high energy" state. It is likely that force development and of muscle are coupled with the chemical step with a major drop in basic free energy (7,8). In the transition from AM_P^{ADP}, a maximum of 62 % (-8.7 Kcal/mol) of free energy drop is available for force generation in muscle.

REFERENCES

1. Inoue, A., Shigekawa, M., & Tonomura, Y. (1973) J. Biochem. 74, 923-934
2. Inoue, A., Takenaka, H., Arata, T., & Tonomura, Y. (1979) in Advances in Biophysics (Kotani, M. ed.) vol. 13, pp 1-194, Japan Scientific Societies Press and Univ. Park Press, Tokyo and Baltimore
3. Inoue, A., Ikebe, M., & Tonomura, Y. (1980) J. Biochem. 87, 219-226
4. Stein, L.A., Schwartz, R.P., Chock, P.B., & Eisenberg, E. (1979) Biochemistry 18, 3895-3909
5. Arata, T., Shimidzu, H. (1981) J. Mol. Biol. 151, 411-437
6. Yanagida, T., Kuranaga, I., & Inoue, A. (1982) J. Biochem. 92, 407-412
7. Simmons, R.M. & Hill, T.L. (1976) Nature 263, 615-617
8. Hill, T.L. (1977) Free Energy Transduction in Biology, Academic Press, New York, San Francisco and London
9. Arata, T., Inoue, A., & Tonomura, Y. (1975) J. Biochem. 77, 895-900
10. Yasui, M., Arata, T., and Inoue, A. (1985) J. Biochem. 96, 1673-1680
11. Perry, S.V. (1952) in Methods in Enzymology (Colowick, S.P. & Kaplan, N.O., eds.) Vol. 2, pp.582-588, Academic Press, New York
12. Weeds, A.V. & Taylor, R.S. (1975) Nature 257, 54-56
13. Spudich, J.A. & Watt, S. (1971) J. Biol. Chem. 246, 4866-4871

14. Tietz, A. & Ochoa, S. (1962) in Methods in Enzymology Colowick,S.P. and Kaplan,N.O.,eds.) Vol.5, pp.365-369, Academic Press, New York
15. Laemmli, V.K. (1970) Nature 277, 680-685
16. Tonomura, Y. (1972) Muscle Proteins, Muscle Contraction and Cation Transport, Univ. Tokyo Press and Univ. Park Press, Tokyo and Baltimore
17. Glynn, I.M. & Chappel, J.B. (1964) Biochem. J. 90, 147-149
18. Inoue, A. & Tonomura, Y. (1980) J. Biochem. 88, 1643-1651
19. Bradford, M.M. (1976) Anal. Biochem. 72, 248-254
20. Mornet, D., Bertland, R., Pantel, P., Audemard, E., & Kassab, R. (1981) Nature 292, 301-306
21. Arata, T. (1984) J. Biochem. 96, 337-347
22. Reynard, A.M., Hass, L.E., Jacobsen, D.D., & Boyer, P.D. (1961) J. Biol. Chem. 236, 2277-2288
23. Nakamura, H. & Tonomura, Y. (1968) J. Biochem. 63, 279-294
24. Hackney, D.D., Stempel, E.E., & Boyer, P.D.(1980) Methods in Enzymology (Purich, D.L., eds.) part B. pp.60-83 Academic Press, New York.
25. Miderfort, C.F. (1981) Proc. Natl. Acad. Sci. USA 78, 2067-2071.
26. Arata, T., Inoue, A., & Tonomura, Y. (1974) J. Biochem. 76, 1211-1216

Part 4

Two Routes of Acto-Subfragment-1 ATPase Reaction Analyzed by Oxygen Exchange

SUMMARY

We analyzed an oxygen exchange during the acto-S-1 ATPase reaction from the distribution of ^{18}O labeled species using (γ-^{18}O)ATP as substrate. The results obtained can be explained by the two route mechanism in which ATP is hydrolyzed by two routes one with the dissociation of acto-S-1 into F-actin anf S-1-phosphate-ADP complex, S-1$_P^{ADP}$, and the other without accompanying the dissociation of acto-S-1. (Inoue, A., Shigekawa, M. & Tonomura, Y. (1973) J. Biochem. 74, 923-934; Inoue, A., Ikebe, M. & Tonomura, Y. (1980) J. Biochem. 88, 1663-1677). Under the condition where ATP is mainly hydrolyzed by a route without accompanying the dissociation of acto-S-1 the extent of oxygen exchange was low. While under the condition where ATP is hydrolyzed by two routes, the distribution of product Pi with 3, 2, 1, and 0 ^{18}O atoms showed the mixture of low and high oxygen exchange. The ratio of ATP hydrolysis via two pathways calculated from the distribution of Pi species was equal to that determined from the rate of overall reaction and that of recombination of F-actin with S-1$_P^{ADP}$. This results suggested that the rate of binding and dissociation of acto-S-1$_P^{ADP}$ into F-actin and S-1$_P^{ADP}$ was lower than the rate of decomposition of acto-S-1-P-ADP complex.

INTRODUCTION

Muscle contraction occurs by a cyclic interaction of myosin head with F-actin coupled with ATP hydrolysis. Then, it is important to clarify the mechanism of actomyosin ATP reaction for elucidation of the molecular mechanism of muscle contraction. There is diversity of opinions among workers on the mechanism of actomyosin ATPase (see ref. 1-4). Lymn and Taylor (5) proposed that ATP is hydrolyzed via the dissociation-recombination cycle of actomyosin:

$$AM + ATP \rightleftharpoons A + MATP \rightleftharpoons A + M_P^{ADP} \longrightarrow AM + ADP + Pi.$$

On the other hand, we (6, 7) showed ATP is hydrolyzed via two routes one with and the other without accompanying the dissociation of actomyosin:

$$M + ATP \rightleftharpoons AMATP \rightleftharpoons AM_P^{ADP} \longrightarrow AM + ADP + Pi$$

$$A + MATP \rightleftharpoons A + M_P^{ADP}$$

where AMATP is in rapid equilibrium with A + MATP. Eisenberg et al. (8) later confirmed the existence of ATP hydrolysis without accompanying the dissociation of actomyosin. However, they proposed that AM_P^{ADP} is also in rapid equilibrium with $A + M_P^{ADP}$.

In this paper, we analyzed the mechanism of acto-S-1 ATPase reaction by an oxygen exchange reaction. In the preceding paper (9), we showed that the extent of oxygen exchange is low when ATP is hydrolyzed via route without accompanying the dissociation of acto-S-1. On the other hand, oxygen exchange during ATP hydrolysis via dissociation-recombination cycle is considered to

be very high, since S-1$_P^{ADP}$ is stable, i. e. , the rate of ATP hydrolysis via dissociation-recombination cycle is determined by the transition from M_P^{ADP} in refractory state to that in non-refractory state (10, 11, 7) and M_P^{ADP} is in rapid equilibrium with MATP (7). However, if M_P^{ADP} is in rapid equilibrium with AM_P^{ADP}, Pi with low oxygen exchange may not be observed. The heterogeneity in oxygen exchange during actomyosin type ATPase reaction has been reported by Miderfort (12, 13), Shukla et al. (14, 16), Hackney (17) and Hibbert et al. (18). However, the relationship of two Pi species with mechanism of ATP hydrolysis has not been analyzed.

In the present paper, we found that ATP hydrolysis with high and low extent of oxygen exchange, respectively, are those with and without accompanying the dissociation of actomyosin.

EXPERIMENTAL PROCEDURES

Materials—Myosin was prepared from rabbit white skeletal muscle by the method of Perry (19). S-1 was prepared by chymotryptic digestion of myosin, as described by Weeds and Taylor (20). G-actin was prepared from an acetone powder of rabbit white skeletal muscle by the method of Spudich and Watt (21). The concentration of free ATP in G-actin solution was reduced to 2 μM by a dialysis against 2mM Tris-HCl at pH 7.8. G-actin was polymerized into F-actin by adding KCl to 50 mM, and after the mixture was ultracentrifuged at 1 x 10^5g for 90 min the pellet was homogenized in the buffer. The molecular weight

of S-1 and actin monomer were adopted to be 1.2×10^5 and 4.2×10^4, respectively (22). Crosslinked acto-S-1 was obtained as described previously (9). Pyruvate kinase was prepared from rabbit skeletal muscle as described by Tietz and Ochoa (23). Acetate kinase and myokinase were purchased from Boehringer Mannheim, GmbH. Protein concentrations were determined by means of the Biuret reaction calibrated by nitrogen determination.

ATP and ADP were purchased from Kohjin Co. Ltd, Tokyo. AMP was purchased from Yamasa Co. Ltd. PEP was purchased from Boehringer Mannheim, GmbH. (^{18}O)water(98 atom % of ^{18}O) was purchased from Amersham International plc. or CEA oris. (γ-^{18}O)ATP was synthesized using acetate kinase system by the method of Ikeuchi and Miderfort (13) with slight modification (9). All other reagents were of analytical grade.

Methods—The rate of acto-S-1 ATPase reaction in the steady state was measured by coupling ATPase reaction with pyruvate kinase system. The reaction was started by mixing 0.1 mM ATP and 2 mM PEP with acto-S-1 containing 0.5 mg/ml pyuvate kinase in 0.1 M KCl, 2 mM $MgCl_2$, and 10 mM Imidazole at pH 7.0 and 20 °C. The ATPase activity was determined by measuring the pyruvate liberation. The amount of pyruvate liberated was determined as described by Reynard et al. (24).

The rate of binding of $S\text{-}1_P^{ADP}$ with F-actin was measured from the change in the light scattering intensity of acto-S-1 at 400 nm using a stopped apparatus combined with a Hitachi MPF-2A fluorescence spectrophotometer as described previously (6, 25).

The extent of oxygen exchange was measured using (γ-^{18}O)ATP as substrate (part 2 of this thesis). ATPase reaction was performed

usually in 10 uM S-1, 0.6-5.8 mg/ml F-actin, 1 mM (γ-^{18}O)ATP, 50 mM KCl, 2 mM $MgCl_2$, 20 mM Tris-HCl at pH 7.8 and 20 °C. ATPase reaction was stopped with 10 % of PCA after about 50 % of labeled ATP was hydrolyzed by the ATPase reaction and the product Pi was separated on Dowex 1X2 (H^+) column chromatography. The fraction was lyophilized and converted into trimethylsilyl phosphate. The fraction of each labeled Pi species were determined by a gas chromatography that is directly coupled to the mass spectrometer (Shimadzu-LKB 9000 or Shimadzu QP-1000). The amount of Pi which contained 0, 1, 2 and 3 ^{18}O atoms were determined from the signal intensities at m/e = 314, 316, 318 and 320, respectively. The natural abundance of ^{29}Si and ^{30}Si was corrected as described Hackney and Boyer (26). The distribution of Pi which is produced by the myosin EDTA ATPase reaction, since Levy et al.(27) reported that there was no oxygen exchange reaction in the myosin EDTA ATPase reaction.

RESULTS

Oxygen Exchange during Acto-S-1 ATPase Reaction—— Oxygen exchange between water and phosphate during acto-S-1 ATPase reaction (intermediate exchange) was measured in 10 μM S-1, 0.6-6 mg/ml F-actin, 1 mM (γ-^{18}O)ATP, 50 mM KCl, 2 mM $MgCl_2$, 20 mM Tris-HCl at pH 7.8 and 20 °C (Table 1). The isotopic distribution in the original (γ-^{18}O)ATP was measured from the distribution of ($^{18}O_n$)Pi species in the Pi produced by EDTA-ATPase. The distribution ratio of ($^{18}O_0$)Pi:($^{18}O_1$)Pi:($^{18}O_2$)Pi:($^{18}O_3$)Pi in

TABLE I. Oxygen exchange during acto-S-1 ATPase reaction. 0.6-3.0 mg/ml F-actin, 10 μM S-1, 50 mM KCl, 1 mM ^{18}O-ATP, 2mM $MgCl_2$ and 50 mM Tris-HCl at pH 7.8 and 20°C. The ratio of ATP hydrolysis *via* two routes was estimated using the values of exchange ratio, R, of the inner and outer cycle as 0.6 and 18, respectively. Theoretical distribution of Pi from the ratio of ATP hydrolysis and the values of R are shown in parentheses.

Conc. of F-actin (mg/ml)	^{18}O / Pi 0	1	2	3	Ratio of ATPase[a] F (%)
Control[b]	16.8	3.4	8.2	71.6	
0.6	61.1(60.6)	9.1(11.9)	8.9(11.5)	20.9(16.0)	25
1.5	57.9(54.9)	8.3(11.5)	10.7(13.1)	23.1(20.5)	35
2.0	50.7(52.1)	13.8(11.3)	13.8(13.9)	21.7(22.7)	40
3.0	36.9(40.8)	15.0(10.6)	19.1(17.0)	29.0(31.6)	60

[a], The fraction of ATPase without accompanying dissociation of acto-S-1, F, estimated from the distribution of (^{18}O)Pi.

[b], Distribution of Pi produced by S-1 EDTA(K^+)-ATPase reaction.

percent was 16.8:3.4:8.2:71.6 (Fig. 1A). At 0.6 mg/ml F-actin amount of ($^{18}O_0$)Pi increased from 16.8 to 61.1 %, while that of ($^{18}O_3$)Pi decreased from 71.6 to 20.9 %. The content of ($^{18}O_1$)Pi increase slightly from 3.4 to 9.1 %. The content of ($^{18}O_2$)Pi was the same as that of control Pi. When the concentration of F-actin was increased from 0.6 to 3.0 mg/ml, the amount of ($^{18}O_0$)Pi was decreased from 61.1 to 36.9 % while that of ($^{18}O_3$)Pi increased from 20.9 to 29.0 %. The amounts of ($^{18}O_1$)Pi and ($^{18}O_2$)Pi increased to 15.0 and 19.1 %, respectively.

The distribution of (^{18}O)Pi can be explained if there are two kinds of ATPases with different exchange ratio. Then, we measured the oxygen exchange reaction at extreme conditions. Figure 1b shows the distribution of Pi species produced by the ATPase reaction of S-1 alone. Figure 1cand 1d are the distribution of Pi produced by crosslinked acto-S-1 and acto-S-1 in the presence of 5.8 mg/ml F-actin and in the absence of KCl. When Pi was produced by the S-1 ATPase reaction, ^{18}O in the -P position was almost completely displaced by ^{16}O and the distribution of Pi with 3, 2, 1, and 0 ^{18}O atoms were 82.0, 6.0, 4.0, 8.0, respectively). On the other hand, when ATP is hydrolyzed by crosslinked acto-S-1 (10 μM S-1 in acto-S-1), the percentage of ($^{18}O_3$)Pi decreased only slightly (($^{18}O_0$)Pi: ($^{18}O_1$)Pi:($^{18}O_2$)Pi:($^{18}O_3$)Pi = 22.5:3.8:15.0:58.7). It has been shown by Inoue et al.(7) that in the absence of KCl, in the presence of high concentration of F-actin and at room temperature ATP was hydrolyzed mainly *via* a route without accompanying the dissociation of acto-S-1. The distribution of Pi produced by the ATPase reaction in 5.8 mg/ml F-actin, 10 μM S-1, 2 mM $MgCl_2$, 20

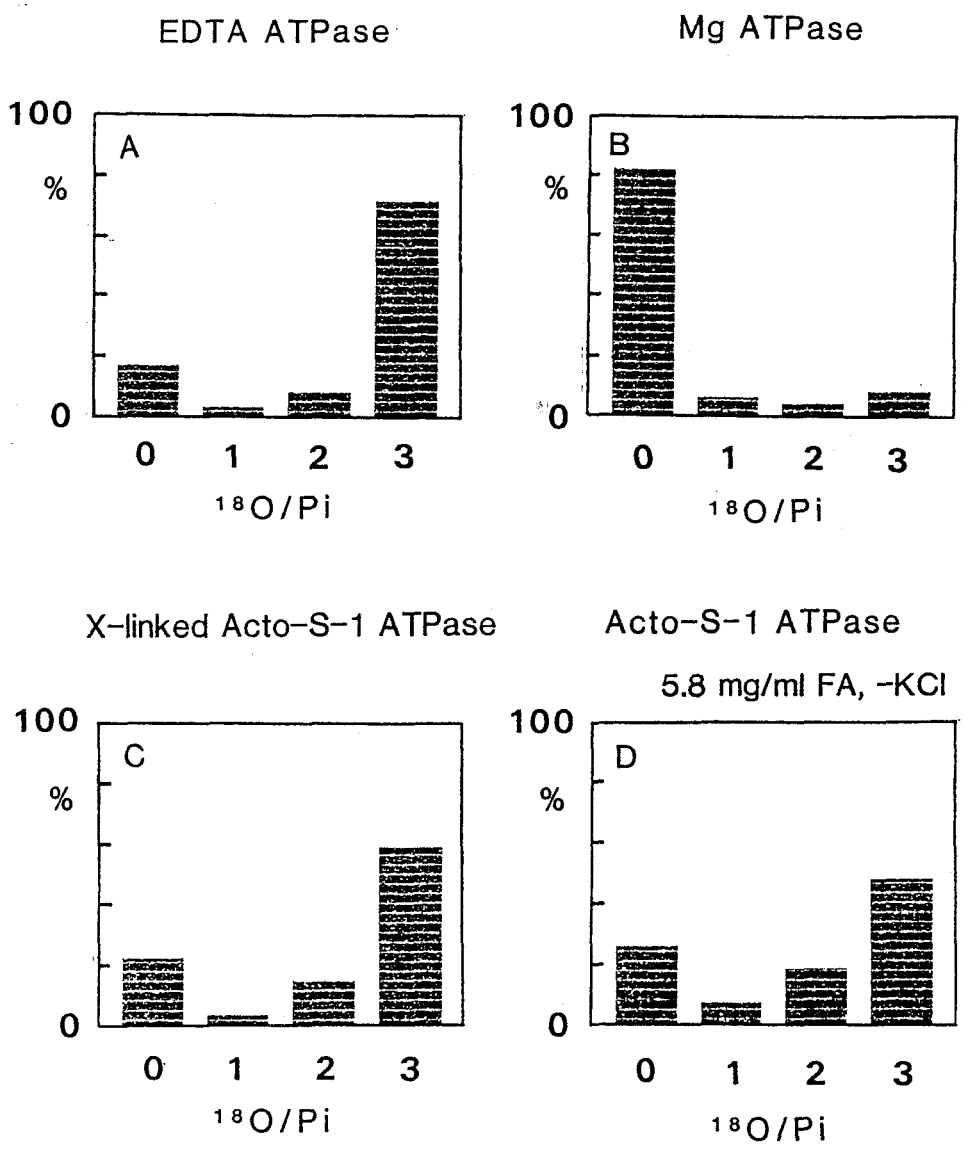

Figure 1. Distribution pattern of (^{18}O)Pi species from hydrolysis of (γ-^{18}O)ATP by S-1 ATPase in the presence of EDTA or Mg^{2+}, and by acto-S-1 ATPase without accompanying dissociation of acto-S-1. The conditions were a. 10 μM S-1, 1 mM (γ-^{18}O)ATP, 0.5 M KCl, 10 mM EDTA, 50 mM Tris-HCl at pH 7.8 and 20°C; b. 10 μM S-1, 1 mM (γ-^{18}O)ATP, 50 mM KCl, 2 mM $MgCl_2$, 20 mM Tris-HCl at pH 7.8 and 20°C; c. crosslinked acto-S-1(10 μM S-1), 1 mM (γ-^{18}O)ATP, 50 mM KCl, 2 mM $MgCl_2$, 20 mM Tris-HCl at pH 7.8 and 20°C; . d. 10 μM S-1, 5.8 mg/ml F-actin 1 mM (γ-^{18}O)ATP, 50 mM KCl, 2 mM $MgCl_2$, 20 mM Tris-HCl at pH 7.8 and 25°C.

mM Tris-HCl at pH 7.8 and 25 °C was $(^{18}O_0)Pi:(^{18}O_1)Pi:(^{18}O_2)Pi:(^{18}O_3)Pi = 26.1:7.2:18.5:48.2$, which was almost the same as that produced by crosslinked acto-S-1 ATPase. The extent of oxygen exchange was determined by the ratio of k_{-3} and k_4 in the scheme:

$$M + ATP + H_2{}^{18}O \rightarrow M\text{-}ATP + H_2{}^{18}O \underset{k_{-3}}{\overset{k_3}{\rightleftharpoons}} M\text{-}{}^{18}O\text{-}P\text{-}ADP \xrightarrow{k_4} M + ADP + {}^{18}O\text{-}P\text{-}{}^{18}O \quad (\text{with } {}^{18}O \text{ below})$$

If we denote $R = k_{-3}/k_4$, the distributions of $(^{18}O_3)Pi$, $(18O_2)Pi$, $(^{18}O_1)Pi$ and $(^{18}O_0)Pi$ (a, b, c, d, respectively) are given by

$$a = a_0 \frac{4}{3R + 4}$$

$$b = (a_0 + b_0 - a) \frac{2}{R + 2}$$

$$c = (a_0 + b_0 + c_0 - a - b) \frac{4}{R + 4}$$

$$d = 100 - (a + b + c)$$

Where a_0, b_0, c_0 and d_0 are the distribution of Pi produced from $(\gamma\text{-}^{18}O)ATP$ with no oxygen exchange. The value of R in the S-1 Mg-ATPase reaction was very high. If R=25 the calculated

distribution of Pi is 80.5:10.2:5.7:3.6. In the crosslinked acto-S-1 ATPase reaction the value of R was 0.3-0.5. The calculated distribution of Pi at R=0.4 is 17.5:6.8:20.6:55.1. On the other hand, the values of R in acto-S-1 ATPase reaction at high concentrations of F-actin in the absence of KCl was about 0.6 (if R = 0.6, distribution of Pi was 18.1:9.1:23.4:49.4). We calculated the ratio of two kinds of ATPase reaction from the distribution of (^{18}O)Pi produced by the ATPase reaction. Since the rate of recombination of M_P^{ADP} with F-actin , k_4, at F-actin concentration higher than 1 mg/ml was 0.55 s^{-1} (6) and the rate of backward reaction of M_P^{ADP} to MATP, k_{-3} was 10 s^{-1} (1, 3), the value of R in the ATPase reaction *via* the dissociation of acto-S-1 was taken as 18. Whereas, the value of R in the ATPase reaction route without accompanying the dissociation of acto-S-1 was taken as 0.6. As shown in Table I, the fraction of ATPase reaction without accompanying the dissociation of acto-S-1, F, at 0.6 mg/ml F-actin was 25%. The calculated distribution of Pi was $(^{18}O_0)$Pi:$(^{18}O_1)$Pi:$(^{18}O_2)$Pi:$(^{18}O_3)$Pi = 60.6:11.9:11.5:16.0, which was almost the same as that measured 61.1:9.1:8.9:20.9. The value of F increased to 35, 40 and 60 %, respectively with increase in F-actin concentration to 1.5, 2.0 and 3.0 mg/ml.

Rate of Two Routes of Acto-S-1 ATPase Reaction —— It was shown by Inoue et al. (6, 7) that the rate of acto-S-1 ATPase reaction, v, is given by $v = (1-\alpha)k_v + \alpha k_r$ where α, k_v and k_r are the extent of dissociation of acto-S-1 during the ATPase, the rate of ATPase at infinite concentration of F-actin and the rate of recombination of $S\text{-}1_P^{ADP}$ with F-actin, respectively. They (6, 7) assumed that $(1-\alpha)k_v$ and αk_r were the rate of ATPase reactions

TABLE II. The kinetic constants of acto-S-1 ATPase reaction. The rate of acto-S-1 ATPase reaction, v, was measured under the conditions described for Table I except that 0.5 mg/ml pyruvate kinase and 2 mM PEP were added. The extent of dissociation of acto-S-1 in the presence of ATP, α, was measured from the change in light-scattering intensity at 400 nm. The rate of recombination of $S\text{-}1_P^{ADP}$ with F-actin, k_r, was measured from the recovery in light-scattering intensity at 400 nm after adding 10 μM ATP to acto-S-1. Other conditions were the same as for Table I.

Conc. of FA (mg/ml)	v (s^{-1})	k_r (s^{-1})	α	αk_r (s^{-1})	$v - \alpha k_r$ (s^{-1})	$(v - \alpha k_r)/v$ (%)
0.6	0.47	0.30	0.95	0.29	0.18	38
1.5	0.90	0.55	0.90	0.50	0.40	45
3.0	1.30	0.70	0.70	0.49	0.81	62
4.5	1.80	0.90	0.55	0.50	1.30	72

without dissociation of acto-S-1 and that <u>via</u> dissociation and recombination of acto-S-1, respectively. Then, we measured values of k_r,α under the same condition using same preparations of S-1 and F-actin. The results were summarized in Table II. The rate of acto-S-1 ATPase, v, increased with increase in F-actin concentration, and was 1.8 s^{-1} at 4.5 mg/ml F-actin. The rate of recombination of $S\text{-}1_P^{ADP}$ with F-actin, k_r, increased to 0.9 s^{-1} at 4.5 mg/ml F-actin. On the other hand, the extent of dissociation,α, decreased to 0.55. The rate of acto-S-1 ATPase <u>via</u> dissociation and recombination of acto-S-1 was calculated as αk_r while that without accompanying the dissociation of acto-S-1 was obtained as $v - \alpha k_r$. Therefore, the fraction of ATPase without accompanying the dissociation of acto-S-1, F, was calculated as $(v - \alpha k_r)/v$. As shown in the right column in Table II, the fraction, F, increased from 38 to 72 % with increase in F-actin concentration from 0.6 to 4.5 mg/ml. Figure 2 compared the fraction of ATPase without accompanying the dissociation of acto-S-1 obtained from oxygen exchange (○) (Table I) and that obtained by the kinetic method (×)(Table II). The ratio of ATPase with and without accompanying the dissociation of acto-S-1 were the same both obtained by the oxygen exchange and kinetic method and it increased from 30 to 65 % with increase in F-actin concentration from 0.6 to 3.0 mg/ml.

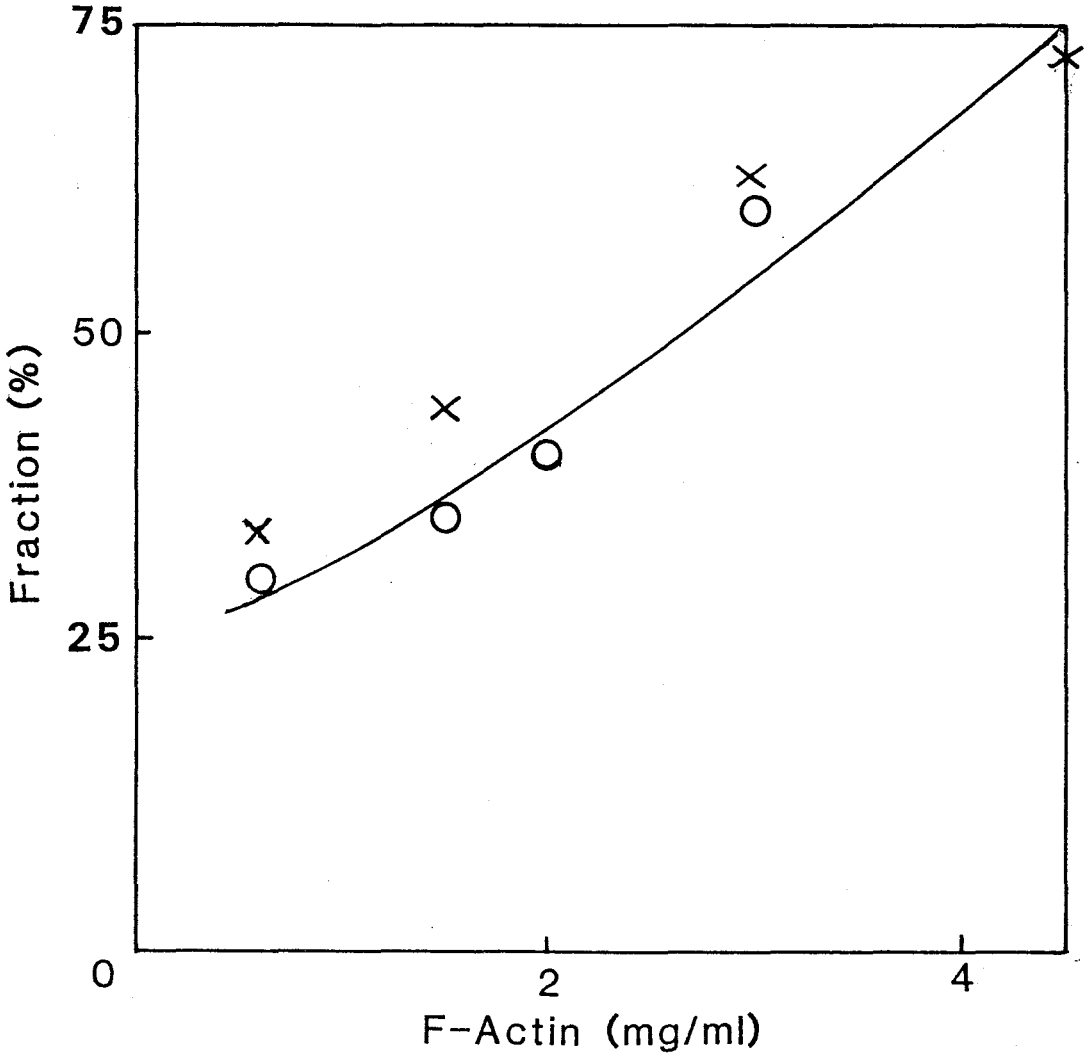

Figure 2. Dependence on F-actin concentration of the fraction of ATP hydrolysis without accompanying dissociation of acto-S-1. The fraction of ATP hydrolysis without accompanying dissociation of acto-S-1 was obtained by the oxygen exchange (O), by the kinetic method (×). The detail of the results were shown in Table I and II, respectively.

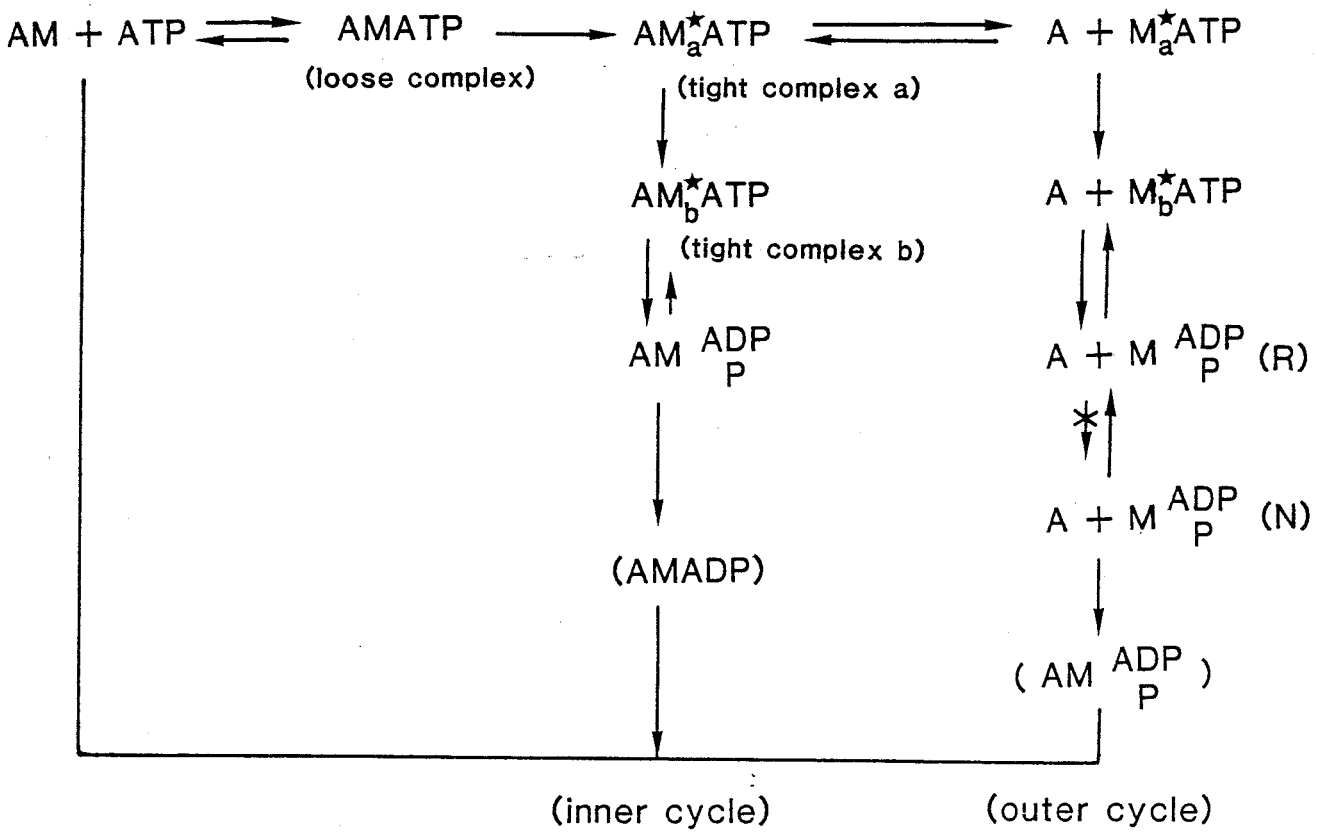

Figure 3. The mechanism of acto-s-1 ATPase reaction. See Text for detail.

DISCUSSIONS

In this paper the mechanism of actomyosin ATPase reaction was examined by oxygen exchange analysis. We (6, 7) showed that in the actomyosin type ATPase reaction, ATP was hydrolyzed *via* two routes one with (outer route) and the other (inner route) without accompanying dissociation of actomyosin (Fig. 3). The mechanism of ATP hydrolysis was studied in the preceding paper (9), and we found that the rate of ATPase reaction is determined by transition from AM^*ATP to AM_P^{ADP}. On the other hand, the outer cycle of the ATPase reaction is determined by transition from M_P^{ADP} in refractory state (R) to that in non-refractory state (N) (7, 8). We (6, 7) showed that the rate of overall ATPase reaction, v, is given by $v = (1-\alpha)k_v + \alpha k_r$ where α and k_r are the extent of dissociation of acto-S-1 and the rate of recombination of $S\text{-}1_P^{ADP}$ with F-actin. This result suggests that AM_P^{ADP} and $A + M_P^{ADP}$ are not in the rapid equilibrium.

In the preceding paper (part 2 of this thesis) We found that when ATP was hydrolyzed without accompanying dissociation of acto-S-1, the extent of oxygen exchange was very low (Fig. 1). Under the conditions where ATP was hydrolyzed *via* two routes, the distribution of $(^{18}O)Pi$ was explained as there were two kinds of ATPases with different R values. The ratio of two kinds of ATPases agreed well with that of ATPases with and without accompanying dissociation of acto-S-1 measured by the kinetic method (Fig.2).

We have examined whether the distribution of $(^{18}O)Pi$ produced by acto-S-1 ATPase reaction can be explained by single R value.

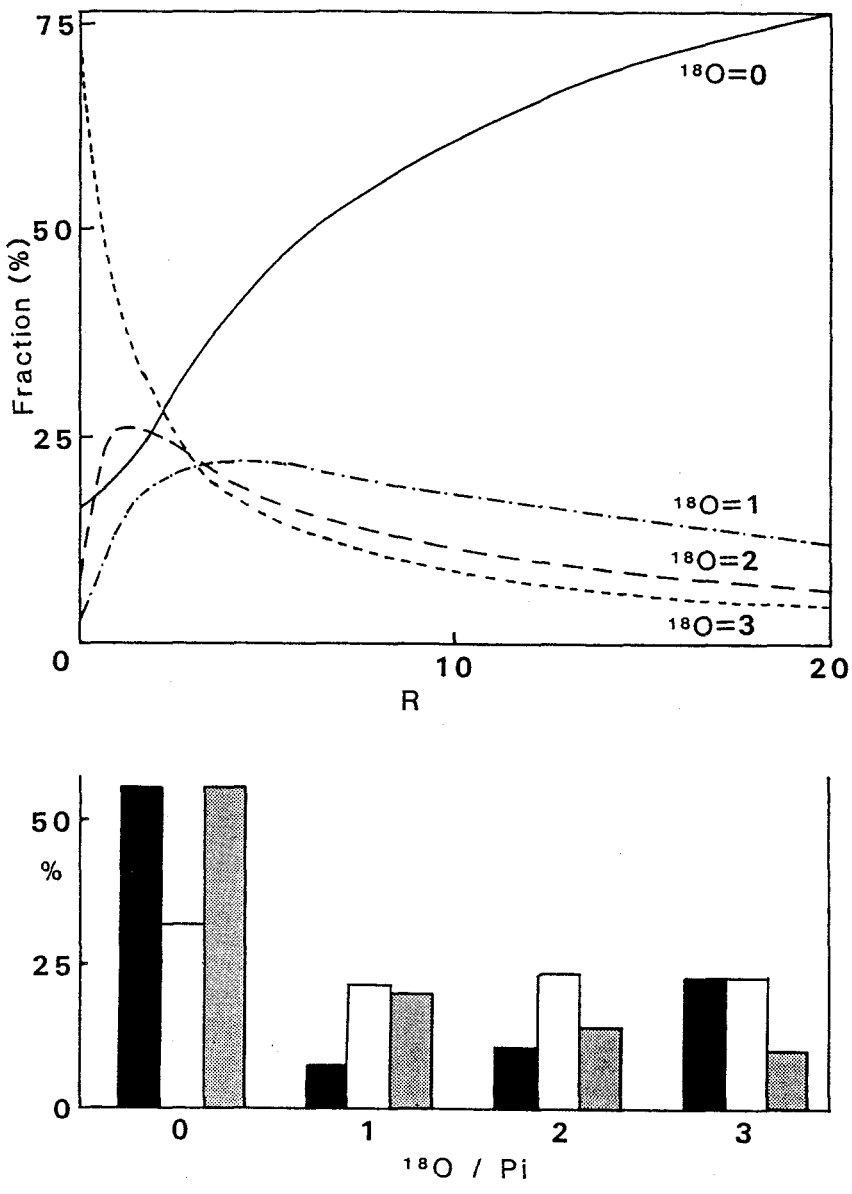

Figure 4. Upper: Theoretical distribution pattern of (^{18}O)Pi species at various the value of R. Initial distribution of ^{18}O in γ-position of ATP was $^{18}O_0$:$^{18}O_1$:$^{18}O_2$:$^{18}O_3$ = 16.8:3.4:8.2:71.6. ——, $^{18}O_0$;-·-·-,$^{18}O_1$;– – –, $^{18}O_2$;-----, $^{18}O_3$. The distribution of (^{18}O)Pi at various value of R was calculated using the equation shown in RESULTS. Lower: Observed and theoretical distribution of (^{18}O)Pi species for acto-S-1 ATPase reaction. ■ , (^{18}O)Pi produced by acto-S-1 ATPase (Table I, 1.5 mg/ml F-actin). □ and ▒ are the distribution of (^{18}O)Pi if R = 2.8 or 8, respectively.

Figure 3 shows the dependence of (^{18}O)Pi on the value of R. The initial distribution of (^{18}O)Pi was used as ($^{18}O_0$)Pi:($^{18}O_1$)Pi:($^{18}O_2$)Pi:($^{18}O_3$)Pi = 16.8:3.4:8.2:71.6. The extent of (^{18}O)Pi increased with increasing R value while that of ($^{18}O_3$)Pi decreased with increasing R value. The extent of ($^{18}O_1$)Pi and ($^{18}O_2$)Pi increased to around 25 % when R is between 1 to 5. When R is 2-2.5 the extents of ($^{18}O_0$)Pi, ($^{18}O_1$)Pi, ($^{18}O_2$)Pi and ($^{18}O_3$)Pi were almost the same. The lower figure of Fig. 3 compares the ^{18}O distribution produced by acto-S-1 ATPase reaction and those calculated as R = 2.8 or 8. The extents of ($^{18}O_1$)Pi and ($^{18}O_2$)Pi become much less than those calculated by the single R value.

The existence of two R values has been reported by several workers. Miderfort (12) and Ikeuchi & Miderfort (13) reported the existence of ATPases with two R values. Shukla et al. (14-16), Hackney (17) and Hibbert et al. (18) also reported the existence of two ATPases with different R values. However, the cause of these two ATPases has not been analyzed. It is not due to the heterogeneity in the system since two R values were observed not only in actomyosin but also in acto-HMM and acto-S-1. Shukla et al. (15) considered that ATPases with two R values are catalyzed by different head, however as shown in Fig. 2 the ratio of two ATPases depend on F-actin concentration and under extreme condition ATP was hydrolyzed only by ATPase with low R value. These two ATPases are not due to the contamination of ATPase since the ratio of two ATPases obtained by oxygen exchange agreed well to the kinetic method.

In Table I and Fig. 2, the ratio of two ATPases is estimated

by one set of R value. However, it should be noted that the ratio of two ATPases does not depend greatly on the change in R value. The value of R in the outer cycle is considered to be changed by F-actin concentration and the value of R in the inner cycle is that estimated in the different conditions (-KCl, 25 °C). The distribution of (^{18}O)Pi produced by crosslinked acto-S-1 and acto-S-1 at high concentration of F-actin in the absence of KCl were not explained exactly by a single R value. This is considered too be due to the contamination of S-1

The existence of two R values indicates that AM_P^{ADP} in the inner cycle is not in rapid equilibrium with A + M_P^{ADP}. Since the rate constant of AM_P^{ADP} decomposition is more than 100 s^{-1} (9), the rate constant of transition from AM_P^{ADP} to A + M_P^{ADP} might be less than 10 s^{-1}. It was shown that M_P^{ADP} is in rapid equilibrium with M_b^*ATP (28, 29). AM_P^{ADP} is also in rapid equilibrium with AM_b^*ATP (9). AM_b^*ATP is in rapid equilibrium with A + M_a^*ATP (1, 3). Therefore, AM_b^*ATP is not in rapid equilibrium with A + M_b^*ATP and the transition from AM_b^*ATP to AM_a^*ATP may be slow.

The analysis of ATPase reaction by oxygen exchange is useful for study of mechanism of ATPase reaction during muscle contraction since the diffusion of ligand in muscle fiber is low. The analysis of ATPase reaction by myofibrils and muscle fibers will be reported in the forthcoming paper.

REFERENCES

1. Inoue, A., Takenaka, H., Arata, T. & Tonomura, Y. (1979) Adv. Biophys. 13, 1-194.
2. Inoue, A., & Tonomura, Y. (1974) Mol. Cel. Biochem. 5, 127-143.
3. Taylor, E.W. (1979) CRC Crit. Rev. Biochem. 6, 103-164
4. Eisenberg, E. & Green, E. (1980) Ann. Rev. Physiol. 42, 293-309
5. Lymn, R.W. & Taylor, E.W. (1971) Biochemistry 10, 4617-4624
6. Inoue, A., Shigekawa, M., & Tonomura, Y. (1973) J. Biochem. 74, 923-934
7. Inoue, A., Ikebe, M., & Tonomura, Y. (1980) J. Biochem. 88, 1663-1677
8. Stein, L.A., schwartz, R.R., Chock, P.B. & Eisenberg, E. (1979) Biochemistry 18, 3895-3909.
9. Yasui, M., Ohe, M., Kajita, A., Nakamura, T., Arata, T. & Inoue, A. J. Biochem. submitted
10. Eisenberg, E. & Kielley, W.W. (1973) Cold Spring Harver Symp. Quant. Biol. 37, 145-152
11. Chock, S.P., Chock, P.B., & Eisenberg, E. (1976) Biochemistry 15, 3244-3253
12. Midelfort, C.F. (1981) Proc. Natl. Acad. Sci. USA 78, 2067-2071.
13. Ikeuchi, Y. & Miderfort, C.F. (1987) Biochemistry 25, 411-419
14. Shukla, K.K., Levy, H.M., Ramirez. F., Marecek, J.F., Meyerson, S., & Kuhn, E.S. (1980) J. Biol. Chem. 255, 11344-11350.

15. Shukla, K.K., Levy, H.M., Ramirez, F., & Marecek, J.F. (1984) J. Biol. Chem. 259, 5423-5429.

16. Shukla, K.K., Levy, H.M., Ramirez, F., Marecek, J.F., McKeever, B., & Margossian, S.S. (1983) Biochemistry 22, 4822-4830.

17. Hackney, D.D. (1982) J. Biol. Chem. 257, 9494-9500

18. Hibberd, M.G., Webb, M.R., Goldman, Y.E., & Trentham, D.R. (1985) J. Biol. Chem. 260, 3496-3500.

19. Perry, S.V. (1955) Methods in Enzymology (Colowick, S.P. & Kaplan, N.O., eds.) Vol.2, pp.582-588, Academic Press, New York

20. Weeds, A.V. & Taylor, R.S. (1975) Nature 257, 54-56

21. Spudich, J.A. & Watt, S. (1971) J. Biol. Chem. 246, 4866-4871.

22. Tonomura, Y. (1972) Muscle Protein, Muscle Contraction and Cation Transport, Univ. Tokyo Press and Univ. Park Press, Tokyo and Baltimore

23. Tietz, A. & Ochoa, S. (1958) Arch. Biochem. Biophys. 78, 477-496

24. Reynard, A.M., Hass, L.E., Jacobsen, D.D. & Boyer, P.D. (1961) J. Biol. Chem. 236, 2277-2288

25. Takemori, S., Nakamura, M., Suzuki, K., Katagiri, M., & Nakamura, T. (1972) Biochem. Biophys. Acta 284, 382-393.

26. Hackney, D.D. & Boyer, P.D. (1978) Proc. Natl. Acad. Sci. U.S.A. 75, 3133-3177

27. Levy, H.M., Sharon, N., Lindemann, E., & Koshland, D.E., Jr. (1960) J. Biol. Chem. 235, 2628-2632

28. Bagshaw, C.R. & Trentham, D.R. (1973) Biochem. J. 133,

323-328

29. Bagshaw, C.R., Trentham, D.R., Wolcott, R.G., & Boyer, P.D. (1975) Proc. Natl. Acad. Sci. U.S.A.72, 2592-2596

Part 5

Mechanism of ATP Hydrolysis by Glycerol-Treated Muscle Fibers, Myofibrils and Synthetic Actomyosin Filaments Studied by Oxygen Exchange

SUMMARY

The mechanism of ATP hydrolysis was studied using oxygen exchange analysis on glycerinated muscle fibers, myofibrils, and synthetic actomyosin filaments. We (part 4 of this thesis) showed that in acto-S-1 ATPase reaction ATP was hydrolyzed via two routes: one with and the other without accompanying the dissocistion of actomyosin into F-actin + myosin-phosphate-ADP complex, M_P^{ADP}, and that oxygen exchange between γ-position of Pi and water during ATPase reaction is low in the former route and high in the latter route of ATP hydrolysis. Then, the fraction of ATP hydrolysis by the above two routes was estimated from the distribution of Pi with 3, 2, 1, and 0 ^{18}O atoms using (γ-^{18}O)ATP as substrate. In glycerinated muscle fibers during isometric contraction ATP was hydrolyzed mainly via a route without accompanying the dissociation of actomyosin. The extent of ATP hydrolysis by this route was 0.82 or 0.7, respectively, in 0 and 120 mM KCl at 20 °C. When ATP was hydrolyzed by myofibrils the fraction of ATP hydrolysis without accompanying the dissociation was 0.48 at 0 °C and 120 mM KCl. At 20 °C the extent of this route was 0.72-0.88 in 0-120 mM KCl. In synthetic actomyosin filament the extent of ATP hydrolysis via this route was 0.3-0.16 at 20 °C in 5-120 mM KCl. Thus, the fraction of ATP hydrolysis without accompanying the dissociation of actomyosin was high in low ionic strength where the tension development is large. Therefore, ATP hydrolysis via this route may coupled with muscle contraction. However, the fraction of ATP hydrolysis via the dissociation of actomyosin into FA + M_P^{ADP} was higher than that expected from the

results on acto-S-1.

INTRODUCTION

Muscle contraction occurs as a result of sliding of thin filament past the thick filament. This is driven by a cyclic interaction of myosin heads with F-actin coupled with ATP hydrolysis. Therefore it is important to elucidate the mechanism of ATPase reaction for understanding the mechanism of muscle contraction. The mechanism of ATPase reaction has been studied using acto-HMM and acto-S-1 (1-4). We (5,6) showed that in acto-S-1-ATP system ATP is hydrolyzed via two routes in: one is accompanied by a dissociation and a recombination of actomyosin into F-actin and myosin-phosphate-ADP complex and the other without dissociation of actomyosin and directly decomposes into actomyosin + ADP + Pi (1, 5, 6).

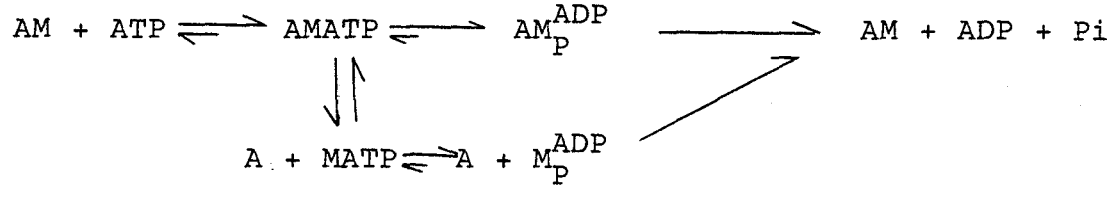

However, the mechanism of ATP hydrolysis in muscle fibers has not been studied sufficiently, since in the fiber myosin heads and actin are packed and highly ordered and the diffusion of ligands in the fiber is very low. However, the oxygen exchange is useful method in such a system (7). In the previous report (part 3 of this thesis), we showed that the fraction of two routes of ATPase can be determined by oxygen exchange. Therefore, in this paper we examined how ATP is hydrolyzed by actomyosin filament, myofibrils, and glycerinated muscle fibers during isometric contraction. The results obtained suggested

that ATP was mainly hydrolyzed via the direct decomposition of actomyosin$_P^{ADP}$.

EXPERIMENTAL PROCEDURES

Materials—Myosin was prepared from rabbit white skeletal muscle by the method of Perry (8). G-actin was prepared from an acetone powder of rabbit white skeletal muscle by the method of Spudich and Watt (9). The concentration of free ATP in G-actin solution was reduced to 2 μM by a dialysis against 2mM Tris-HCl at pH 7.8. G-actin was polymerized into F-actin by adding KCl to 50 mM and then the mixture was ultracentrifuged at 1 x 10^5g for 90 min. The pellet was homogenization in the buffer. Myofibrils were prepared from white rabbit skeletal muscle by the method of Perry & Corsi (10). Glycerinated muscle fibers were prepared from rabbit psoas muscle were prepared as described in Hanson & Huxley (11) and Arata et al. (12). The molecular weight of myosin and actin monomer were adopted to be 4.8 x 10^5 and 4.2 x 10^4, respectively (13). The contents of myosin in myofibrils and glycerinated muscle fibers were taken as 51 % (14). Pyruvate kinase was prepared from rabbit skeletal muscle as described by Tietz and Ochoa (15). Acetate kinase and myokinase were purchased from Boehringer Mannheim, GmbH. Protein concentrations were determined by means of the Biuret reaction calibrated by nitrogen determination.

ATP and ADP were purchased from Kohjin Co. Ltd. Tokyo. AMP was purchased from Yamasa Co. Ltd. PEP was purchased from

Boehringer Mannheim, GmbH. (^{18}O)water(98 atom % of ^{18}O) was purchased from Amersham International plc. or CEA oris. (γ-^{18}O)ATP was synthesized using acetate kinase system by the method of Ikeuchi and Miderfort (16) with slight modification (part 2 of this thesis). All other reagents were of analytical grade.

Methods—The extent of oxygen exchange was measured using (γ-^{18}O)ATP as substrate. Glycerinated muscle fibers with sarcomere length of 2-2.5 μm was mounted between two needle. One is connected to the manipulater for a control of sarcomere length and the other is connected to the strain gauge (Shinko, UL-2) for measurement of tension development. Sarcomere length was measured by means of optical diffraction of a He-Ne laser beam. The fibers were immersed in the buffer containing 0.1 mM $CaCl_2$, 0-120 mM KCl, 2 mM $MgCl_2$, 10 mM Imidazole-HCl at pH 7.0 and 20°C. The reaction was started by addition of 10 mM (γ-^{18}O)ATP with 10 mM $MgCl_2$. The ATPase activity of fibers was determined from the amount of Pi liberated to the solution. The amount of Pi was determined by Youngburg and Youngburg (17).

The ATP hydrolysis by myofibrils was performed in 2 mg/ml myofibrils, 1.5 mM (γ-^{18}O)ATP, 0-120 mM KCl, 5 mM $MgCl_2$, 10 mM imidazole-HCl at pH 7.0 and 0 or 20 °C. Actomyosin ATPase reaction was performed under the same condition except that 1 mg/ml F-actin, 1 mg/ml myosin were added in place of myofibrils. The reactions were stopped by removal of proteins by centrifugation at 10000 x g for 5 min, and then by addition of 10% PCA.

The distribution of Pi with 3, 2, 1, and 0 ^{18}O atoms were measured as described in part 2 of this thesis. The product Pi

was separated on Dowex 1X2 (H^+) column chromatography. The fraction was lyophilized and converted into trimethylsilyl phosphate. The fraction of each labeled Pi species were determined by a gas chromatography that is directly coupled to the mass spectrometer (Shimadzu-LKB 9000 or Shimadzu QP-1000). The amount of Pi which contained 0, 1, 2 and 3 ^{18}O atoms were determined from the signal intensities at m/e = 314, 316, 318 and 320, respectively. The natural abundance of ^{29}Si and ^{30}Si was corrected as described Hackney and Boyer (18). The distribution of Pi which is produced by the myosin EDTA ATPase reaction, since Levy et al.(19) reported that there was no oxygen exchange reaction in the myosin EDTA ATPase reaction. Distribution of Pi with 3, 2, 1, and 0 ^{18}O atoms were found to be 71.6, 8.2, 3.3, and 16.8%, respectively. The exchange ratio was calculated using the equation:

$$a = a_0 \frac{4}{3R + 4}$$

$$b = (a_0 + b_0 - a) \frac{2}{R + 2}$$

$$c = (a_0 + b_0 + c_0 - a - b) \frac{4}{R + 4}$$

$$d = 100 - (a + b + c)$$

Where a, b, c, and d were the distribution of Pi with 3, 2, 1, and 0 ^{18}O atoms produced by the ATPase reaction, whereas a_0, b_0, c_0 and d_0 are the distribution of Pi produced by (γ-^{18}O)ATP with no oxygen exchange (myosin EDTA-ATPase reaction).

In the preceding paper (part4 of this thesis) we showed that in the acto-S-1 ATPase reaction ATP is hydrolyzed via two routes one with (outer cycle) and the other (inner cycle) without accompanying the dissociation of actomyosin and that the extent of oxygen exchange in the former route (outer cycle) was high while that in the latter route (inner cycle) was low. In this paper we assumed the value of R of the inner and outer route of the ATPase reaction to be 0.3 and 10, respectively. Then, the distribution of Pi produced by the inner route of the ATPase reaction was calculated to be 61.5, 18.0, 12.0, and 8.5%, respectively. for 3, 2, 1, and 0 ^{18}O atoms. Whereas, Pi produced by the outer cycle of the ATPase reaction was estimated to be 16.9, 5.8, 18.7, and 59 %, respectively. The ratio of two route of the ATPase reaction was estimated by comparing the distribution of Pi measured with that calculated as Fa + (1 - F)b where, a, b, and F are the distribution of Pi produced by the inner cycle of the ATPase reaction, that in the outer cycle of the ATPase reaction, and the fraction of inner cycle of the ATPase reaction in the total ATPase.

The rate of ATPase hydrolysis by actomyosin and myofibrils in the steady state were measured by coupling ATPase reaction with pyruvate kinase system. The reaction mixture contained 0.5 mg/ml pyruvate kinase, 1.5 mM ATP and 2 mM PEP in the buffer, and the ATPase activity was determined by measuring the pyruvate

TABLE I. Distribution of ^{18}O-Pi produced by the ATPase reaction of glycerol-treated muscle fibers during isometric contraction. 10 mM (γ-^{18}O)ATP, 0.1 mM $CaCl_2$, 0 or 120 mM KCl, 12 mM $MgCl_2$, 20 mM imidazole-HCl at pH 7.0 and 20 °C.

KCl (mM)	number of ^{18}O atoms				Ratio of ATPase[a] (%)
	0	1	2	3	
0	24.8	7.4	17.2	50.6	83
	(24.7)	(7.8)	(17.5)	(50.0)	
120	32.6	6.4	4.4	56.7	70
	(30.6)	(9.4)	(16.6)	(43.5)	

a) The ratio of inner cycle of ATPase was given as (rate of inner cycle of ATPase)/(rate of total ATPase).

Parenthesis shows the calculated distribution of Pi.

Distribution of Pi produced by the EDTA-ATPase reaction was 71.6, 8.2, 3.3, and 16.8%, respectively, for Pi with 3, 2, 1, and 0 ^{18}O atoms. Distribution of Pi produced by the inner (1) and outer cycle of ATPase (2) were estimated as (1) R = 0.3, Pi with 3, 2, 1, and 0 ^{18}O atoms were 61.5, 18.0, 12.0, and 8.5%, respectively; (2) R = 10, Pi with 3, 2, 1, and 0 ^{18}O =16.9, 5,8, 18.7, 58.6%.

TABLE II. Distribution of ^{18}O-Pi produced by the ATPase reaction of myofibrils. 2 mg/ml myofibrils, 1.5 mM (γ-^{18}O)ATP, 0.1 mM $CaCl_2$, 0-120 mM KCl, 5 mM $MgCl_2$, 10 mM imidazole-HCl at pH 7.0 and 0 or 20 °C.

temperature (°C)	KCl (mM)	number of ^{18}O atoms 0	1	2	3	Ratio[a] (%)
0	120	41.0 (40.3)	12.1 (12.1)	13.2 (15.1)	33.7 (32.5)	48
20	0	18.6 (22.5)	9.3 (7.2)	18.6 (17.8)	53.5 (52.5)	88
20	50	27.9 (28.3)	9.3 (8.8)	15.3 (16.9)	47.5 (45.9)	75
20	120	25.4 (31.9)	12.6 (9.7)	19.9 (16.4)	42.1 (42.0)	67

a)The ratio of inner cycle of ATPase was given as (rate of inner cycle of ATPase)/(rate of total ATPase).
Parenthesis shows the calculated distribution of Pi from the ratio of two ATPase, F, as described for Table I.

TABLE III. Distribution of Pi produced by the ATPase reaction of synthetic actomyosin filaments. 1 mg/ml F-actin, 1 mg/ml myosin, 1.5 mM (γ-^{18}O)ATP, 5-120 mM KCl, 2 mM $MgCl_2$, 10 mM imidazole-HCl at pH 7.0 and 20 °C.

KCl (mM)	number of ^{18}O atoms				Ratio of ATPase (inner cycle/ total) (%)
	0	1	2	3	
5	46.8 (47.0)	10.4 (14.0)	15.5 (14.1)	22.3 (24.9)	33
50	63.2 (51.9)	9.3 (15.3)	7.4 (13.4)	20.1 (19.4)	22
120	58.4 (53.7)	16.4 (15.8)	9.6 (13.1)	15.6 (17.4)	18

Parenthesis shows the calculated distribution of Pi from the ratio of ATPase, F, as described for Table I.

liberation. The amount of pyruvate liberated was determined as described by Reynard et al. (20).

RESULTS

Oxygen Exchange by Glycerol Treated muscle Fibers—The oxygen exchange during isometric contraction of glycerinated muscle fibers was measured in 10 mM (γ-^{18}O)ATP, 0.1 mM $CaCl_2$, 0, or 120 mM KCl, 12 mM $MgCl_2$, and 20 mM imidazole-HCl at 7.8 and 20°C. The distribution of Pi with 3, 2, 1, and 0 ^{18}O atoms were found to be 50.6, 17.2, 7.4, and 24.8 %, respectively. The ratio of two routes of ATPase reaction was calculated as described in "EXPERIMENTAL". The fraction of inner route of ATPase reaction which does not accompany the dissociation of actomyosin into F-actin + M_P^{ADP} were assumed to be 83 and 70%, respectively in 0 and 120 mM KCl. The calculated distribution of Pi with 3, 2, 1, and0 ^{18}O atoms were 50.0, 17.5, 7.8, and 24.7, respectively, for 0 M KCl and 43.5, 16.6, 9.4, and 30.6, respectively for 120 mM KCl.

Oxygen Exchange by Myofibrils—The oxygen exchange during ATP hydrolysis by myofibrils was measured in 2 mg/ml myofibrils, 1.5 mM (γ-^{18}O)ATP, 0.1 mM $CaCl_2$, 0, 50, or 120 mM KCl, 5 mM $MgCl_2$, and 10 mM imidazole-HCl at 7.0 and 0 or 20°C. In 120 mM KCl and at 0°C, the distribution of Pi with 3, 2, 1, and 0 ^{18}O atoms were found to be 33.7, 13.2, 12.1, and 41.0, respectively. The fraction of inner route of ATPase reaction which does not accompany the dissociation of actomyosin was assumed to be 48%.

The calculated distribution of Pi with 3, 2, 1, and0 ^{18}O atoms were 32.5, 15.1, 12.1, and 40.3, respectively. At 20°C the distribution of Pi with 3, 2, 1, and 0 ^{18}O atoms were 53.5, 19.6, 9.3, and 18.6, respectively, in the absence of KCl. They were 47.5, 15.3, 9.3, and 27.9, respectively, in 50 mM KCl and 42.1, 19.9, 12.6, and 25.4, respectively, in 120 mM KCl. The fraction of inner route of ATPase reaction were assumed to be 88 75 and 67%, respectively in 0, 50 and 120 mM KCl. The calculated distribution of Pi with 3, 2, 1, and0 ^{18}O atoms were 52.5, 17.8, 7.2, and 22.5, respectively, for 0 M KCl, 45.9, 16.9, 8.8, and 28.3, respectively, for 50 mM KCl and 42.0, 16.4, 9.7, and 31.9, respectively for 120 mM KCl.

Oxygen Exchange by synthetic actomyosin filament— The oxygen exchange during the ATPase reaction of synthetic actomyosin filament was measured in 1 mg/ml myosin, 1 mg/ml actin, 1.5 mM (γ-^{18}O)ATP, 5, 50 or 120 mM KCl, 5 mM $MgCl_2$, and 10 mM imidazole-HCl at 7.0 and 20°C. The distribution of Pi with 3, 2, 1, and 0 ^{18}O atoms were found to be 22.3, 15.5, 10.4, and 46.8, respectively, for 5 mM KCl, 20.1, 7.4, 9.3, and 63.2 %, respectively, for 50 mM KCl, and 15.6, 9.6, 16.4, and 58.4 %, respectively, for 120 mM KCl. The fraction of inner route of ATPase reaction were assumed to be 33, 22, and 18 %, respectively in 0, 50, and 120 mM KCl. The calculated distribution of Pi with 3, 2, 1, and0 ^{18}O atoms were 24.9, 14.1, 14.0, and 47.0, respectively, for 5mM KCl, 19.5, 13.4, 15.3, and 51.9, respectively for 50 mM KCl, and 17.4, 13.1, 15.8, and 53.7, respectively, for 120 mM KCl.

Table IV. The rate of actomyosin-type ATPase reaction by actomyosin and muscle fibers via two routes one with and other without accompanying the dissociation of actomyosin.

Protein	Temp. (°C)	KCl (mM)	ATPase v (s^{-1})	Ratio of ATPase[a)]	ATPase (s^{-1}) inner	ATPase (s^{-1}) outer
glycerinated muscle fiber	20	0	11.0[b)]	83	9.1	1.9
	20	120	3.4[b)]	70	2.4	1.0
myofibrils[c)]	0	120	0.22	48	0.11	0.11
	20	0	12.5	88	11.0	1.5
	20	50	14.6	75	10.9	3.7
	20	120	12.2	67	8.2	4.0
actomyosin[c)]	20	5	1.8	30	0.54	1.26
	20	50	1.3	22	0.29	1.01
	20	120	2.1	18	0.38	1.72

a) The ratio of inner cycle of actomyosin-type ATP was estimated from distribution of Pi produced as described in Table I, II, and III. b) Ref (21). c) The ATPase activity was measured under the conditions described for Table II and III except that 0.5 mg/ml pyruvate kinase and 5 mM PEP were added.

ATPase Activity of Glycerol-Treated Muscle Fibers, Myofibrils and Synthetic Actomyosin Filament—Since the ratio of two route of the actomyosin ATPase reaction was determined we measured the rate of actomyosin-type ATPase reaction in glycerol-treated muscle fibers, myofibrils and synthetic actomyosin filament in the steady state (Fig. 4). The rate of ATP hydrolysis by glycerol treated muscle fibers was used those measured previously (21) using ATP generating system. They were 11 and 3.4 s^{-1}, respectively, in 5 and 120 mM KCl. In the absence of ATP regenerating system they were 4 and 2.5 s^{-1}, respectively. Using the ratio of inner cycle of ATPase reaction measured by oxygen exchange analysis, the rate of inner and outer route of ATP hydrolysis were estimated to be 9.1 and 1.9 s^{-1}, respectively in the absence of KCl and 2.4 and 1.0 s^{-1}, respectively in 120 mM KCl.

The rate of ATP hydrolysis by myofibrils was measured using pyruvate kinase system (0.5 mg/ml pyruvate kinase and 5 mM PEP). the rate of ATPase reaction was 0.22 s^{-1} in 120 mM KCl at 0 °C. The rate of ATP hydrolysis at 20 °C were 12.5, 14.6, and 12.2 s^{-1}, respectively. The rate of inner and outer cycle of the ATPase reaction were 0.11 s^{-1} at 0 °C and 120 mm KCl. The rate of ATP hydrolysis through inner route were 11.0, 10.9, 8,2 s^{-1}, respectively, at 0, 50, and 120 mM KCl, and those through outer cycle were 1.5, 3.7, and 4.0 s^{-1}.

The rate of ATP hydrolysis by synthetic actomyosin were measured as those described for myofibrils. The rate of ATPase hydrolysis at 20 °C were 1.8, 1.5, and 2.1 s^{-1} at 5, 50, and 120 mM KCl. The rate of inner cycle of ATPase reaction were

calculated to be 0.54, 0.28, and 0.38 s_{-1}, at 0, 50, and 120 mM KCl, whereas the rate of outer cycle of ATP hydrolysis were 1.26, 0.54, and 1.72 S^{-1}.

DISCUSSION

Muscle contraction occurs by a cyclic interaction of myosin head with F-actin coupled with ATP hydrolysis. The mechanism of ATP hydrolysis by actin-myosin system has mainly been studied using soluble acto-HMM or acto-S-1 system (1-4). We (1,5,6) have shown that in acto-S-1 ATPase reaction ATP was hydrolyzed *via* two routes one with (inner cycle) and the other (outer cycle) without accompanying the dissociation of acto-S-1:

$$AM + ATP = AMATP \rightleftharpoons AM_a^{*}ATP \rightleftharpoons AM_b^{*}ATP \rightleftharpoons AM_P^{ADP} \longrightarrow AM + ADP + Pi \quad \text{(inner cycle)}$$

$$AM_a^{*}ATP \rightleftharpoons A + M_a^{*}ATP \qquad AM + ADP + Pi \rightleftharpoons (AM_P^{ADP}) \rightleftharpoons A + M_P^{ADP}(N)$$

$$A + M_a^{*}ATP \rightleftharpoons A + M_b^{*}ATP \rightleftharpoons A + M_P^{ADP}(R) \rightleftharpoons A + M_P^{ADP}(N) \quad \text{(outer cycle)}$$

where $AM_a^{*}ATP$ is in rapid equilibrium with A + $M_a^{*}ATP$. The ATPase reaction of inner cycle is limited by the formation of AM_P^{ADP} (part 2), while the ATPase reaction of outer cycle is limited by the transition from A + M_P^{ADP} in refractory state (R) to that in non-refractory state (N). In preceding paper (Part 4 in this thesis) we showed that the extent of oxygen exchange is low in the inner cycle of the ATPase reaction, whereas it was high in the outer cycle of the ATPase reaction.

The mechanism of ATP hydrolysis in muscle fibers has not been well studied since myosin and actin are highly ordered and packed

in muscle fibers and the diffusion of ligand in the fiber is slow. The analysis of ATPase reaction by oxygen exchange is effective in such a system. In the present study we found that ATP was hydrolyzed by two routes even in glycerol treated muscle fibers, myofibrils, and synthetic actomyosin filaments (Table I-III).

We (1) proposed that muscle contraction is coupled with inner cycle of the ATPase reaction, since (1) development of tension by glycerol treated muscle fibers is high under the conditions where ATP is hydrolyzed mainly by an inner cycle of the ATPase reaction (21), and (2) the rate of outer cycle of the ATPase reaction which is limited by transition from M_P^{ADP} in refractory state to that in non-refractory state of (0.5 - 1.0 s^{-1}) was much lower than the rate of ATPase reaction of muscle fibers (6). This theory was supported by the present study, i.e., in low ionic strength and at room temperature the fraction of inner cycle of ATPase reaction is more than 80 % that of total ATPase both in glycerol treated muscle fibers (Table I) and myofibrils (Table II).

The distribution of Pi with 3, 2, 1, and 0 ^{18}O atoms produced by glycerole treated muscle fibers shows that there are two kinds of ATPase reaction one with low and the other with high extent of oxygen exchange reaction. This result agreed well with those of Shukla et al. (22) and Hibberd et al. (23). The results can be well explained if two ATPases have R value of 0.3 and 10 which are attributed to the ATPase reactions through inner and outer cycles. The value of R we adopted are slightly different from above authors (22, 23). The ratio of inner cycle of ATPase was

higher than 80 % in the absence of KCl. It decreased slightly (70%) by increasing KCl concentration to 120 mM. The rate of ATP hydrolysis by glycerol treated muscle fibers depended on the presence of ATP regenerating system, since the diffusion of ligand in the fiber is limited. We used the value of previous paper (21) measured in the presence of ATP regenerating system. We found that the rate of ATP hydrolysis through an inner cycle is about 9 s^{-1}. The rate of ATP hydrolysis by muscle fibers is stimulated by a shortening of fibers (12). Then, the rate of inner cycle of ATPase reaction during shortening is considered to be more than this value.

The result obtained by myofibrils was same as that on glycerole-treated muscle fibers, though it shortened quickly by the addition of ATP and it does not develop a tension. The rate of ATP hydrolysis at 20°C were more than 10 s^{-1} at KCl concentrations from 0 to 120 mM. Therefore, the state of myosin head after the contraction may be similar to that of muscle fiber during isometric contraction. The rate of outer cycle of ATPase reaction increased from 1 to 4 s^{-1} with increasing KCl concentration from 0 to 120 mM. This value (4 s^{-1}) was higher than that in acto-S-1 ATPase reaction. Therefore, the binding of M_P^{ADP} with F-actin takes place more rapidly in an organized systems.

The ratio of inner cycle of ATPase was low (18 - 30 %) in a synthetic actomyosin filaments (Table IV). When ATP is added to actomyosin the superprecipitation of actomyosin takes place. Therefore, the state of myosin head in contracted actomyosin filament is considered to be different from that in myofibrils and glycerol treated muscle fibers.

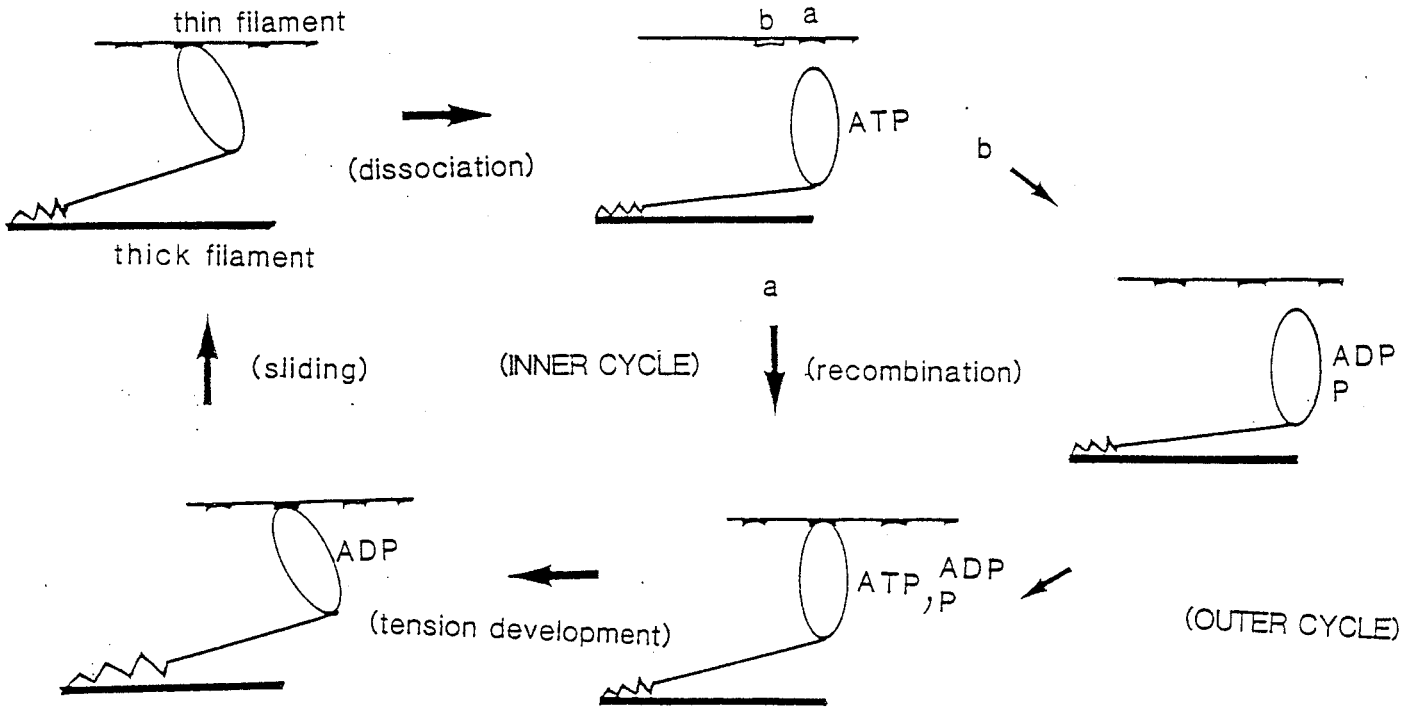

Figure 1. The mechanism of muscle contraction. See text for detail.

Next problem is how ATPase reaction is coupled with contraction. Muscle contraction occurs by a cycle of the following reaction: (1) binding of myosin head with F-actin (2) developement of tension induced by the movement of myosin head (crossbridges) and the following sliding of thick filament past thin filament (3) dissociation of actomyosin. In the inner cycle of the ATPase reaction only AM_a^*ATP is in rapid equilibrium with A + M_a^*ATP. Therefore, the dissociation and re-association of crossbridge may take place by this step. As shown in Part 3 in this thesis, most of energy obtained by ATP hydrolysis is liberated by the step from AM_P^{ADP} to AMADP. Therefore, this step is most probable to be coupled with movement of heads and thus development of tension. It was also supported by the results of Trayer & Trayer (24) and Arata (25) that structure of AMATP and AM_P^{ADP} are different from those of AMADP and AM.

Figure 1 shows the mechanism of muscle contraction based on the mechanism of actomyosin ATPase reaction. In the model, elastic component are considered to be located in the junction between S-2 and LMM (26). Tension is developed by decomposition of AM_P^{ADP} to AMADP. Dissociation of actomyosin and their recombination occurs by formation of AMATP. Myosin head which can not induced the tension may dissociate from actin (outer cycle) and it works after the recombination with actin.

REFERENCES

1. Inoue, A., Takenaka, H., Arata, T. & Tonomura, Y. (1979) Adv. Biophys. 13, 1-194.
2. Inoue, A., & Tonomura, Y. (1974) Mol. Cel. Biochem. 5, 127-143.
3. Taylor, E.W. (1979) CRC Crit. Rev. Biochem. 6, 103-164
4. Eisenberg, E. & Green, E. (1980) Ann. Rev. Physiol. 42, 293-309
5. Inoue, A., Shigekawa, M., & Tonomura, Y. (1973) J. Biochem. 74, 923-934
6. Inoue, A., Ikebe, M., & Tonomura, Y. (1980) J. Biochem. 88, 1663-1677
7. Hackney, D.D., Stempel, E.E., & Boyer, P.D.(1980) Methods in Enzymology (Purich, D.L., ed.) part B. pp.60-83 Academic Presss, New York.
8. Perry, S.V. (1955) Methods in Enzymology (Colowick, S.P. & Kaplan, N.O., eds.) Vol.2, pp.582-588, Academic Press, New York
9. Spudich, J.A. & Watt, S. (1971) J. Biol. Chem. 246, 4866-4871.
10. Perry, J.A. & Corsi, A. (1958) Biochem. J. 68, 5-12
11. Hanson, J. & Huxley, H.E. (1957) Biochim. Biophys. Acta 23, 250-260
12. Arata, T., Mukohata, Y., & Tonomura, Y. (1977) J. Biochem. 82, 801-812
13. Tonomura, Y. (1972) Muscle Protein, Muscle Contraction and Cation Transport, Univ. Tokyo Press and Univ. Park Press,

Tokyo and Baltimore

14. Arata, T. & Tonomura, Y. (19769 J. Biochem. 80, 1353-1358
15. Tietz, A. & Ochoa, S. (1958) Arch. Biochem. Biophys. 78, 477-496
16. Ikeuchi, Y. & Miderfort, C.F. (1987) Biochemistry 25, 411-419
17. Yougburg, G.E. & Yougburg, M.V. (1930) J. Lab. Clin. Med. 16, 158-166
18. Hackney, D.D. & Boyer, P. D. (1978) Proc. Natl. Acad. Sci. U.S.A. 75, 3133-3177
19. Levy, H.M., Sharon, N., Lindemann, E., & Koshland, D.E., Jr. (1960) J. Biol. Chem. 235, 2628-2632
20. Reynard, A.M., Hass, L.E., Jacobsen, D.D., & Boyer, P.D. (1961) J. Biol. Chem. 236, 2277-2288
21. Yanagida, T., Kuranaga, I., & Inoue, A. (1982) J. Biochem. 92, 407-412
22. Shukla, K.K., Levy, H.M., Ramirez, F., & Marecek, J.F. (1984) J. Biol. Chem. 259, 5423-5429.
23. Hibberd, M.G., Webb, M.R., Goldman, Y.E., & Trentham, D.R. (1985) J. Biol. Chem. 260, 3496-3500.
24. Trayer, H.R., & Trayer, R.S. (1983) Eur. J. Biochem. 135, 47-59
25. Arata, T. (1986) J. Mol. Biol. 191, 107-116
26. Huxley, H.E. (1969) Science 164, 1356-1366

ACKNOWLEDGEMENTS

I would like to express to migrate appreciation to Professor T. Nakamura, Faculty of Science, University of Osaka university for his kind guidance and continuous encouragement during the course of this work.

I am greatly indebted to Doctors A. Inoue and T. Arata who gave me excellent guidance and many valuable suggestions.

I would like to express migrate appreciation to Professor A. Kajita and Dr. M. Ooe, Dokkyo University, School of Medicine for their kind help in the operation of gas-chromato mass-spectrometer.

I would like to thank Professor T. Takeuchi and Professor Y. Takahashi for their warm encouragement during the preparation of this thesis.

I am also grateful to the member of Professor Nakamura's laboratory for their kind help during this study.

CONCLUSION

The mechanism of Actomyosin ATPase reaction was studied using acto-S-1 and glycerol-treated muscle fibers, and the following results were obtained.

1. The elementary steps of actomyosin ATPase reaction was studied using transient kinetics and oxygen exchange analysis. It was found that the rate of acto-S-1 ATPase reaction is limited by the formation of AM_P^{ADP} and that the rate of decomposition of M_P^{ADP} is accelerated about 2600 times by the binding of F-actin.

2. Most of the energy obtained by ATP hydrolysis is liberated at the step from AM_P^{ADP}.

3. Using the difference in the extent of oxygen exchange, we provide that in the acto-S-1 ATPase reaction, ATP is hydrolyzed by two routes: one with (outer cycle) and the other without (inner cycle) accompanying the dissociation of acto-S-1.

4. In glycerol treated muscle fibers during isometric contraction, ATP was mainly hydrolyzed <u>via</u> the inner cycle of ATPase reaction.

Therefore, we concluded that muscle contraction is induced by the inner route of ATPase reaction and that tension development is induced by the step from AM_P^{ADP} to AMADP.